

Universidade do Minho
Escola de Ciências



Vanessa de Sousa Vieira

Cardosins trafficking and sorting events in *Arabidopsis*
and Tobacco plants

Tese de Mestrado
Biologia Molecular, Biotecnologia e Bioempendedorismo em
Plantas

Trabalho efetuado sob a orientação da
Professora Doutora Susana Pereira
e
Doutora Cláudia Pereira

Outubro de 2013

DECLARAÇÃO

Nome: VANESSA DE SOUSA VIEIRA

Endereço eletrónico: vieira.aad@gmail.com

Telefone: 918229557

Nº do Bilhete de Identidade: 13184335

Título da Tese de Mestrado:

Cardosins trafficking and sorting events in *Arabidopsis* and Tobacco plants

Orientadoras:

Professora Doutora Maria Susana Pereira e Doutora Cláudia Pereira

Ano de conclusão: 2013

Designação do Mestrado:

Biologia Molecular, Biotecnologia e Bioempendedorismo em Plantas

É AUTORIZADA A REPRODUÇÃO INTEGRAL DESTA TESE/TRABALHO, APENAS PARA EFEITOS DE INVESTIGAÇÃO, MEDIANTE DECLARAÇÃO ESCRITA DO INTERESSADO, QUE A TAL SE COMPROMETE,

Universidade do Minho, / /

Assinatura: _____

Acknowledgements

À Doutora Cláudia Pereira por todo o apoio, pelo encorajamento, pela dedicação e sobretudo por acreditares na minha capacidade e competência para realizar este trabalho. Muito obrigada pela orientação e amizade.

À Professora Doutora Susana Pereira um agradecimento especial por toda a motivação, disponibilidade, e sobretudo por me receber no “lab 2.61”. Muito obrigada por toda a ajuda, discussão de ideias e orientação.

Ao Professor Doutor José Pissarra pelo apoio e motivação transmitidos através da sua orientação e exigência. Por estar sempre disponível para ouvir os nossos desabafos e preocupações. Obrigada por me integrar neste grupo que se tornou uma família.

Obrigada a todos os meus colegas por criarem esta família. Ao Bruno que partilhou comigo todos os “negativos e positivos” durante este ano de trabalho. À Marta pela amizade, motivação e por tantas conversas. Ao Alberto (proibo-te de comentares o teu aparecimento aqui!) obrigado por todo o apoio, preocupação, orientação, ajuda e por seres tu mesmo. Ao lab 2.60 por estarem sempre ali ao lado quando precisamos. Em especial à Ana Marta por todos os conselhos sobre as nossas ‘plantinhas’ e por reabasteceres os meus *stocks* de mel que sempre tornam a vida mais doce.

Aos “meus estagiários” que vão ser sempre os meus estagiários, desejo-vos um futuro de sucesso e muitas alegrias. Ao Luís, que também fez parte deste projeto, pela dedicação e empenho. Em especial, ao Rui pela amizade que ficou depois de tantas batalhas com o cardo.

Aos meus pais, que fizeram todo o esforço para eu chegar até aqui, por acreditaram em mim e por me amarem desde sempre. Adoro-vos e tenho muito orgulho em vocês.

À Pretinha, a minha pantera, pelos momentos de mimo e brincadeira que ajudam aliviar a má disposição que às vezes decorre deste trabalho.

Ao meu Joel por todo o amor, compreensão e tudo mais que só nós sabemos.

Cardosins trafficking and sorting events in *Arabidopsis* and Tobacco plants

Summary

Cardosin A and B are aspartic proteinases from *Cynara cardunculus* L. and a role during several important developmental stages of the plant have been suggested for cardosins namely during plant reproduction and seed germination. In order to participate in these events, cardosins must accumulate and traffic to different compartments inside the cell. However, not much information is available regarding cardosin A biogenesis, sorting or trafficking to the different compartments, mainly because the transformation protocols available are difficult to apply in cardoon plants. To solve this obstacle we obtain transgenic *Arabidopsis thaliana* lines' stably expressing cardosins constructs. In order to validate these mCherry-based constructs in *Arabidopsis* we succeed in their transient expression, adapting a method described by Marion and co-workers (2008). Moreover, this technique also allowed us to conclude that the cardosins trafficking events are conserved between the *Nicotiana tabacum* leaf and *Arabidopsis thaliana* cotyledon epidermal cells. Despite the great achievements using mCherry, the possibility of using photoinducible fluorescent proteins is a powerful addition to track cardosins fusions. Therefore, we obtained mEos-fusions both to cardosins and to the Plant-Specific Insert (PSI) even though these fusions will need further optimization. Despite the similarity between cardosins protein sequences the *N*-glycosylation pattern is different. The presence of a glycosylated PSI is a conserved characteristic of plant aspartic proteases that is absent from cardosin A, contrarily to cardosin-B PSI. The absence of a conserved glycosylation site in the PSI seems to be related with the already described PSI-dependent Golgi bypass. To understand the relevance of *N*-glycosylation, one of the main goals of this work was to obtain point mutations of the glycosylation sites. The results obtained during this work strongly suggest that glycosylation seems to be a key feature in determining the PSI-driven route and renew the debate about the importance of glycosylation for protein trafficking. Furthermore, the transgenic plants preliminary analysis are the starting point for a detailed study of cardosin A and cardosin B expression, localisation, sorting and trafficking routes, in the whole-plant context and to explore the role of cardosins during plant development.

Trânsito e direcionamento intracelular das cardosinas em *Arabidopsis* e tabaco

Resumo

A cardosina A e a cardosina B são proteinases aspárticas de *Cynara cardunculus* L. e foi sugerido um papel importante das cardosinas durante vários estados de desenvolvimento da planta, nomeadamente durante a reprodução da planta e a germinação da semente. Para participarem nestes eventos, as cardosinas devem acumular-se e deslocar-se para diferentes compartimentos dentro da célula. Contudo, não há muita informação disponível sobre a biogénese, direcionamento e trânsito para os diferentes compartimentos principalmente, porque os protocolos de transformação existentes são difíceis de aplicar no cardo. Para ultrapassar este obstáculo, obtivemos linhas de *Arabidopsis thaliana* a expressar estavelmente os constructos das cardosinas. Para validar estas fusões com a proteína fluorescente mCherry em *Arabidopsis*, obtivemos com sucesso, a sua expressão transiente utilizando um método adaptado de Marion e colaboradores (2008). Para além disso, esta técnica permitiu-nos concluir que os eventos no trânsito das cardosinas são conservados entre as células da epiderme da folha de *Nicotiana tabacum* e dos cotilédones de *Arabidopsis thaliana*. Apesar dos excelentes resultados obtidos usando a mCherry, a utilização de proteínas fluorescentes foto-indutíveis é uma ferramenta valiosa para seguir *in vivo* a síntese e trânsito das fusões das cardosinas. Por conseguinte, obtivemos fusões da mEos às cardosinas e ao Plant-Specific Insert (PSI) de cada uma, contudo, estas fusões precisam de mais optimização. Apesar das semelhanças entre as sequências proteicas das cardosinas o padrão de *N*-glicosilação é diferente. A existência de um PSI glicosilado é uma característica conservada entre proteases aspárticas mas que está ausente na cardosina A, contrariamente ao PSI da cardosina B. A ausência de um local de glicosilação conservado no PSI parece estar relacionado com a via já descrita que evita o Golgi dependente do direcionamento pelo PSI. Para perceber a relevância da *N*-glicosilação, um dos principais objetivos deste trabalho era obter mutações pontuais dos locais de glicosilação. Os resultados obtidos durante este trabalho sugerem fortemente que a glicosilação parece ser uma característica-chave na via dependente do Golgi e reacendem o debate sobre a importância da glicosilação para o trânsito das proteínas. Para além disto, a análise preliminar das plantas transgénicas é um ponto de partida para um estudo detalhado da expressão, localização, direcionamento e vias de trânsito das cardosinas em toda a planta e para explorar o papel das cardosinas durante o desenvolvimento da planta.

Table of Contents

Acknowledgements.....	i
Summary.....	ii
Resumo.....	iii
1 Introduction	1
1.1 The endomembrane system	2
1.1.1 The key-players of the endomembrane system	2
The endoplasmic reticulum and the Golgi apparatus.....	3
TGN and endosomes	3
Vacuoles.....	4
1.2 Secretory pathways.....	4
1.2.1 Protein secretion	4
1.2.2 ER-to-Golgi trafficking	5
1.2.3 Post-GA transport	6
Protein trafficking and sorting to the vacuole	6
1.3 Cardosins: model proteins to study different trafficking pathways.....	8
1.3.1 Processing, accumulation and biological function: an overview	8
1.3.2 Trafficking and sorting in heterologous systems.....	10
1.4 The protein <i>N</i> -glycosylation in plants.....	12
1.4.1 Plant <i>N</i> -linked glycans	12
1.4.2 Cardosin A and B glycosylation patterns	14
1.5 Fluorescent reporters to study cardosins trafficking	16
1.5.1 Fluorescent proteins: Green fluorescent protein and mCherry.....	16
1.5.2 Photoconvertible Proteins	17
The tetrameric Kaede	18
mEos: a powerful addition to study trafficking dynamic events	18
2 Materials and Methods.....	19
2.1 mEos-based constructs	19
2.1.1 Construction of Cardosins-mEos fusions	20
2.1.2 Fusion of Cardosin-A PSI and Cardosin-B PSI to mEos	22
SP-PSI A-mEos fusion.....	22
SP-PSI B-mEos	23
2.1.3 Cardosin-A and Cardosin-B PSI fused to mCherry in pMDC83.....	24

2.2	Constructs used for the study of cardosins expression in <i>Arabidopsis thaliana</i>	25
2.3	Obtaining of cardosins glycosylation mutants	25
2.3.1	SP-PSI A mut gly -mcherry	26
2.3.2	Cardosin A mut gly 1+2-mcherry	27
2.4	Molecular biology protocols and tools	27
	Polymerase Chain Reaction	27
	Site-Directed Mutagenesis	28
	RNA extraction	30
	RT-PCR analysis	30
	DNA Gel Electrophoresis	31
	DNA extraction and purification from agarose gel	32
	Ligation of DNA fragments.....	32
	Gateway® pENTR4™ Dual Selection Vector cloning	32
	Zero Blunt® PCR Cloning	32
	pFAST-GO2 Gateway® cloning.....	32
	pMDC83 and pVKH18-En6 cloning	32
	Bacterial Strains and growing conditions.....	33
	Preparation of “High efficiency” <i>Escherichia coli</i> Competent Cells.....	34
	Transformation of competent <i>Escherichia coli</i>	34
	Plasmid DNA extraction (miniprep).....	35
	Pure plasmid DNA extraction	35
	Plasmid DNA digestion.....	35
	Preparation of Electrocompetent <i>A. tumefaciens</i> Cells	35
	Transformation of <i>A. tumefaciens</i> by Electroporation	36
	Plasmid DNA extraction (miniprep) of <i>A. tumefaciens</i>	36
2.5	Biological material - maintenance and transformation	37
2.5.1	<i>Arabidopsis thaliana</i> system	37
	Germination and Maintenance of <i>A. thaliana</i>	37
	Transient transformation of <i>Arabidopsis thaliana</i>	38
	Stable expression in <i>Arabidopsis</i>	39
	Floral-dip method	39
2.5.2	<i>Nicotiana tabacum</i> system	40
	Germination and Maintenance of <i>N. tabacum</i>	40

	<i>Agrobacterium</i> -mediated infiltration of <i>N. tabacum</i> Leaves	40
	Dominant Negative Mutants Assay	41
2.6	Confocal laser scanning microscopy	41
	Preparation of sections	41
	Imaging and Photoconversion	42
3	Results	43
3.1	Validation of cardosins expression in <i>Arabidopsis</i> cotyledons	43
3.1.1	Cardosin A and B accumulate in the vacuole.....	43
3.1.2	Cardosin A truncated versions	45
	3.1.3 Cardosins vacuolar sorting determinants	47
	3.1.4. Cardosins vacuolar accumulation in <i>Arabidopsis thaliana</i> is a fast process	49
3.2	Stable expression in <i>Arabidopsis thaliana</i>	50
3.2.1	PSI A fused to mCherry	51
3.2.2	Cardosin A Δ PSI (deletion of the PSI region) fused to mCherry	51
3.2.3	Cardosin B-mCherry.....	52
	RT-PCR from Cardosin B-mCherry stable line	53
3.3	mEos chimeric proteins engineering and imaging.....	54
3.3.1	Cardosins PSIs cloning into pMDC and imaging	55
3.4	Glycosylation mutated versions expression analysis	62
3.4.1	Non-glycosylated cardosin A	62
3.4.2	Cardosin-A Glycosylated PSI version	63
3.4.3	Non-glycosylated cardosin-B PSI version	67
4	4. Discussion	68
4.1	Cardosins A and B and its mutated versions accumulate in the vacuole in <i>A. thaliana</i> seedlings	68
4.1.1	Transient expression: outcomes and limitations.....	69
4.1.2	Stable transformation: tracking cardosins accumulation along development.....	71
4.2	The glycosylation role in Cardosins trafficking and sorting	71
4.2.1	The sorting mediated by PSI domain and effect of <i>N</i> -Glycosylation	72
4.3	Fluorescent reporters.....	74
4.3.1	mcherry: photostability and brightness in highlighting cardosins trafficking	74
4.3.2	The undeniable profit in mEos addition to cardosins expression studies.....	74
	Approaches to optimize mEos constructs.....	75

5	Conclusions and perspectives.....	77
6	References.....	79

Abbreviations

µg - microgram

µL - microliter

APs – Aspartic Proteinases

Arg – Arginine (aminoacid)

Asn – Asparagine (aminoacid)

BFA – Brefeldin A

CaMV – Cauliflower Mosaic Virus

CCV – Clathrin Coated Vesicle

cDNA – Complementary DNA

CLSM – Confocal Laser Scanning Microscopy

C-ter – C-terminal peptide

ctVSD – C-terminal vacuolar sorting determinant

cv. - cultivar

d - day

DIC – Differential Interference Contrast

DNA – Deoxyribonucleic acid

dNTPs – Deoxyribonucleotides tri-phosphate

DV – Dense vesicle

EDTA - Ethylenediaminetetraacetic acid

EE – Early Endosome

En6 – 6 times enhancer

ER – Endoplasmic reticulum

FP – Fluorescent protein

GA – Golgi apparatus

GAP - GTPase-activating protein

GDP - guanine diphosphate

GEF - guanidine-nucleotide exchange factor

GFP – Green Fluorescent Protein

Glc – Glutamine (aminoacid)

GTP - Guanosine-5'-triphosphate

H - hour

HEPES - 4-(2-hydroxyethyl)-1-piperazineethanesulfonic acid

Kb - Kilobase

kDa - Kilodalton

KPa - kilopascal

LB – Luria Bertani medium

LE – late endosome

LV – Lytic vacuole

Min - minute

mL – milliliter

mM - millimolar

MOPS - 3-Morpholinopropanesulfonic acid

RFP – Red Fluorescent Protein

MS – Murashige and Skoog medium

MVB – Multivesicular Body

Nm - nanometer

OD – Optical Density

ON - Overnight

PAC – Precursor accumulating vesicles

PCR – Polymerase Chain Reaction

PM – Plasma membrane

Pre – Signal peptide present in aspartic proteinases precursor

Pro – Prosegment present in aspartic proteinases precursor

PSI – Plant Specific Insert

PSV – Protein Storage Vacuole

psVSD – physical structure vacuolar sorting determinant

PVC – Prevacuolar Compartment

RGD - Arginine-Glycine-Asparagine motif

RMR - Receptor Homology-transmembrane-RING H2 domain

Rpm – rotation per minute

RT – Room Temperature

SAPLIP – saposin-like protein

SDS – Sodium dodecyl sulphate

Ser – Serine (aminoacid)

SNARE - soluble N-ethylmaleimide sensitive factor adaptor protein receptor

SP – Signal Peptide

ssVSD – sequence specific vacuolar sorting domain

STET – sucrose-triton-EDTA-Tris buffer

TAE – Tris-acetate-EDTA buffer

TEM – Transmission Electron Microscopy

TGN – Trans-Golgi network

UDP – Uranyl diphosphate

UV - UltraViolet

V - volt

VSD – vacuolar sorting determinant

VSR – vacuolar sorting receptor

WT – Wild type

Table of figures

Figure 1.1.: Overview of the secretory pathway in plants.	6
Figure 1.2.: Schematic representation of cardosins processing steps.	8
Figure 1.3.: Putative models for the trafficking of cardosin A to the plant vacuole.	11
Figure 1.4.: Schematic representation of cardosin A and cardosin B glycosylation patterns.	15
Figure 1.5.: Diversity of the different fluorescent proteins available for cloning.	16
Figure 1.6.: Green-to-red photoconversion mechanism for Kaede and mEos 17	17
Figure 2.1.: Flowchart representation of the steps performed for obtaining, cloning and screening the mEos constructs analyzed during the work.	19
Figure 2.2.: Schematic representation of mEos-based constructs engineered during this work and detailed in this section.....	20
Figure 2.3.: Schematic representation of cardosin-A and cardosin-B PSI cloning into pMDC83.	24
Figure 2.4.: Schematic representation of the chimeric proteins already available in our lab that were used for <i>Arabidopsis</i> transformation.	25
Figure 2.5.: Schematic representation of cardosins glycosylation mutants..	26
Figure 2.6.: <i>Arabidopsis</i> germination in liquid MS medium for RNA extraction.....	38
Figure 2.7.: <i>Arabidopsis</i> seedlings infiltration protocol illustration.....	38
Figure 2.8.: Floral dip method proceedings.....	39
Figure 2.9.:Tobacco leaf infiltration with a needleless syringe.	41
Figure 3.1. Subcellular localisation of pFAST-Cardosin A-mCherry in <i>Arabidopsis</i> cotyledon epidermal cells..	44
Figure 3.2.: Subcellular localisation of pFAST-Cardosin B-mCherry in <i>Arabidopsis</i> cotyledon epidermal cells..	45
Figure 3.3.: Subcellular localisation of pFAST-Cardosin A Δ C-ter-mCherry (C-terminal domain deletion) in <i>Arabidopsis</i> cotyledon epidermal cells.	46
Figure 3.4.: Subcellular localisation of pFAST-Cardosin A Δ PSI-mCherry-C-terminal (Plant-specific insert deletion) in <i>Arabidopsis</i> cotyledon epidermal cells.	46
Figure 3.5.: Subcellular localisation of pFAST-SP-mCherry-C-terminal (cardosin-A C-terminal domain) in <i>Arabidopsis</i> cotyledon epidermal cells..	48
Figure 3.6.: Subcellular localisation of pFAST-SP-PSIA-mCherry (cardosin-A plant-specific insert) in <i>Arabidopsis</i> cotyledon epidermal cells..	48
Figure 3.7.: Subcellular localisation of mCherry fusions analysed during this work in <i>Arabidopsis</i> cotyledon epidermal cells 20 hours after vacuum-infiltration.....	50
Figure 3.8.: pFAST-Cardosin-A PSI-mCherry (SP-PSIA-mCherry) stable expression in <i>Arabidopsis thaliana</i> (T2).....	51
Figure 3.9.: pFAST-Cardosin A Δ PSI-mCherry stable expression in <i>Arabidopsis thaliana</i> (T2).	52
Figure 3.10.: pFAST-Cardosin B-mCherry stable expression in <i>Arabidopsis thaliana</i> (T2).	52
Figure 3.11.: RT-PCR product analysis of cardosin B-mCherry transgenic line (T2).in agarose gel electrophoresis.	53
Figure 3.12.: Electrophoretic separation of reaction products..	54
Figure 3.13.: Electrophoretic separation of reaction products.	55
Figure 3.14.: Electrophoretic separation of reaction products.	56
Figure 3.15.: Electrophoretic separation of reaction products.	56

Figure 3.16.: Positive clone of pMDC-SP-PSIB-mCherry determined by Xba I and Pst I restriction mapping.	57
Figure 3.17.: Observation and photoconversion of pMDC-SP-PSIA-mEos.....	58
Figure 3.18.: Observation and photoconversion of pMDC-SP-PSIB-mEos.	58
Figure 3.19.: Positive clone of pMDC-SP-PSIB-mCherry determined by Xba I and Pst I restriction mapping.	59
Figure 3.20.: Subcellular localisation of pMDC–SP-PSIA-mCherry (cardosin-A PSI) in <i>Arabidopsis</i> cotyledon epidermal cells.....	60
Figure 3.21.: Subcellular localisation of pMDC–SP-PSIB-mCherry (cardosin-B PSI) in <i>Arabidopsis</i> cotyledon epidermal cells.....	60
Figure 3.22.: Subcellular localisation of pMDC-SP-cardosin-B PSI-mCherry in <i>Arabidopsis</i> cotyledon epidermal cells 20 hours after vacuum-infiltration.....	61
Figure 3.23.: Electrophoretic separation of reaction products.	63
Figure 3.24.: Electrophoretic separation of reaction products.	64
Figure 3.25.: Subcellular localization of mCherry-tagged cardosin-A PSI (non-glycosylated version) and cardosin-A PSI glycosylated version (mutated version) and co-expression with the mutant Sar1 H74L.	65
Figure 3.26.: Electrophoretic separation of pure DNA extraction from a positive clone.	67

List of tables

Table 2-1: Primers used in the amplification of Cardosins-mEos-C-terminal fusions.	21
Table 2-10: Selectable markers for the plasmid vectors used to transform bacteria during this work.	34
Table 2-2: Primers sent to Eurofins MWG Operon for the sequencing of pENTR4-Cardosins-mEos-C-terminal constructs	22
Table 2-3: PCR reaction used for amplification of cardosins-mEos constructs	28
Table 2-4: Conditions of PCR reaction for Cardosin A/B-mEos-C-terminal amplification	28
Table 2-5: Primers designed for site-directed mutagenesis.	29
Table 2-6: PCR reaction performed for site-directed mutagenesis	29
Table 2-7: Conditions for site-directed mutagenesis reactions	29
Table 2-8: Primers used in the PCR reaction for cDNA product from RT-PCR amplification	31
Table 2-9: Cloning reaction into pMDC83 and pVKH18-En6 binary expression vectors.	33
Table 3-1: Quantitative analysis of the fluorescence patterns observed for cardosin-A glycosylated PSI fluorescent fusion and co-expression with Sar I H74L dominant-negative mutant known to block ER-Golgi trafficking (n, number of cells expressing fluorescent proteins in three independent experiments).	66

1 Introduction

Cardosins are members of the plant aspartic proteinases family (APs; EC 3.4.23) are a class of enzymes optimally active at acid pH, contain two aspartic residues at their active sites and are specifically inhibited by microbial oligopeptide pepstatin A. The tertiary structure of these enzymes has usually two domains separated by a deep and large cleft where the active site is located. APs are synthesized as inactive precursor proteins (zymogens) which are subsequently processed to produce the mature active polypeptides. In most cases, either these cleavages which can be intramolecular or intermolecular, are catalysed either by peptidases acting on themselves (autocatalytic) or by activating partners. The zymogen contains an N-terminal region with pre- and pro-sequences (cleaved during maturation) and one C-terminal region. Precursor protein processing yields either a monomeric or a dimeric protein which is generated by the removal of an internal peptide sequence of approximately 50–100 amino acids called the Plant Specific Insert (PSI). The PSI sequence is highly similar to saposins and saposin-like proteins (SAPLIPs) which are lysosomal sphingolipid-activator proteins (Simões and Faro 2004).

APs are widely distributed in nature, being found in viruses, fungi, yeasts, nematodes, protozoans, vertebrates and plants. To this class of enzymes have been attributed important roles, namely in the processing/activation of several precursor proteins in viruses, animals, yeasts and plants (Davies, 1990; D'Hondt *et al.*, 1993; Runeberg-Roos *et al.*, 1994). The Plant APs, characterised from a number of monocots, dicots and gymnosperms, perform a number of vital cellular processes such as protein maturation and protein degradation associated with tissue restructuring and cell maintenance, as well as in plant senescence, stress responses, programmed cell death and reproduction (Simões and Faro, 2004).

Proteinases play an important role in biotechnology because proteolysis modifies the chemical, physical, biological, and immunological properties of proteins. Some plant proteinases are used in the food industry, in the manufacturing of cheese and drinks, meat tenderizing, cookie baking, and the production of protein hydrolysates (Uhlig, 1998). In Portugal and Spain, APs of *Asteraceae* flowers are used in the production of cheese with organoleptic features different from those obtained with bovine chymosin or microbial rennins. Two cardoon groups of APs have been described: proteinases isolated under alkaline conditions are termed “cynarases” or “cyprosins” (Cordeiro *et al.*, 1994a; Cordeiro *et al.*, 1994b; Heimgartner *et al.*, 1990; White *et al.*, 1999) and those isolated at acidic pH from fresh stigmas of *Cynara cardunculus*, were

named “cardosins” (Faro *et al.*, 1999; Frazao *et al.*, 1999; Ramalho-Santos *et al.*, 1998; Verissimo *et al.*, 1996; Vieira *et al.*, 2001).

Recently, a great focus has been given to aspartic proteinases, and in particular cardosins, trafficking and sorting to plant vacuoles given some particular features as the presence of an unconventional vacuolar sorting determinant, the co-existence of two sorting signals or the hints that point out to a specialization of sorting and trafficking pathways according to cell needs (Pereira *et al.*, 2008; Oliveira *et al.*, 2010 Pereira *et al.*, 2013).

In the next section, a bibliographic survey on the endomembrane system and associated secretory pathways will be presented to introduce the concepts that will serve as basis for the section to follow where the current knowledge about cardosin A and cardosin B processing, localisation, sorting and trafficking routes will be focused.

1.1 The endomembrane system

The eukaryotic cell requires the exchange of proteins, lipids, and polysaccharides between membrane compartments, via transport intermediates. Plant growth and development are dependent on vesicular trafficking in the endomembrane system, facilitating the delivery of molecules and cargo to different destinations through the secretory pathway (including biosynthesis and sorting) and the through the endocytic pathway. Connection between the various endosomal compartments is achieved through tightly controlled, constant budding and fusion of vesicles (Rojo and Denecke, 2008). The secretory pathway is a complex structure of organelles where the synthesis, transport, modification and secretion of proteins and other macromolecules occurs. The route followed by a protein depends on the interactions between sorting motifs present in the protein and the motif-recognizing machinery (Xiang *et al.*, 2013).

1.1.1 The key-players of the endomembrane system

The endomembrane system functionally compartmentalizes the inside of the cell into distinct membrane compartments: the endoplasmic reticulum (ER), the Golgi apparatus (GA), the *trans*-Golgi network (TGN), endosomes, the vacuole and transport vesicles (Frigerio and Hawes, 2008).

The endoplasmic reticulum and the Golgi apparatus

In plants, the endoplasmic reticulum emerge from the nuclear envelope, may be subdivided into several functionally distinct domains (Staehelein, 1997) and is pushed to the cortex of the cell by the large central vacuole. The ER is the entrance into the endomembrane system for newly synthesized proteins carrying an N-terminal signal peptide and is an important checkpoint of correct protein folding and assembly, known for the stringent quality control. Misfolded proteins are recognized by molecular chaperones and retained in the lumen of the ER in an attempt to refold them to their correct structure. Persistent misfolded proteins are transferred to the cytosol and degraded by the proteasome system (Ellgaard and Helenius, 2003; Hebert and Molinari, 2007). Proteins that have erroneously reached the Golgi can also return when ER retention signals are present (Pimpl *et al.*, 2006). Both soluble and membrane proteins are *N*-glycosylated upon entry into the ER lumen (Vitale and Denecke, 1999).

The Golgi apparatus is a sorting station for distribution of cargo proteins to multiple destinations. Plant cells have between several and hundreds of Golgi stacks (Staehelein and Moore 1995, Dupree and Sherrier 1998). The Golgi apparatus consists of several stacked, flattened membrane sacs called cisternae. In each Golgi stack, the cisternae are polarized between the *-cis* side, receiving cargo from the endoplasmic reticulum (ER), and the *-trans* side, sending cargo forward to post-Golgi organelles. Based on resident enzyme activities each Golgi stack is subdivided into distinct cisternae from the *-cis* to *-medial* and the *-trans* side followed by a *trans*-Golgi network (TGN). Some of the more important Golgi functions are the glycosylation of passenger proteins and the synthesis of noncellulosic polysaccharides for the cell wall (Staehelein and Moore 1995, Dupree and Sherrier 1998).

TGN and endosomes

The *trans*-Golgi network sorts various cargo proteins destined for the plasma membrane and endosomes and also receives cargo from endosomal compartments. *Arabidopsis* mutants of TGN-localized proteins have demonstrated that the TGN plays essential roles in several physiological processes, including cell expansion and biotic and abiotic stress responses (reviewed in Uemura *et al.*, 2013)

Endosomes regulate the recycling and degradation of plasma membrane (PM) proteins. In plants, the TGN acts as an early/recycling endosome whereas prevacuolar compartments/multivesicular bodies (MVBs) take PM proteins to the vacuole for degradation.

The late endosomes/MVBs also carry newly synthesized vacuolar proteins from the Golgi to the vacuoles (Reyes *et al.*, 2011). Endosomal sorting of signalling receptors, transporters, and other PM proteins is a key regulatory process that controls the protein composition of the PM and therefore, regulates many cellular responses triggered at the cell surface. PM proteins are continuously internalized by endocytosis and delivered to endosomes for sorting, either back to the PM (recycling) or to degradation in vacuoles (Reyes *et al.*, 2011).

Vacuoles

The vacuoles are plant-specific compartments that typically store water, ions, secondary metabolites and nutrients but they also act as a depository for waste products, excess solutes and toxic substances (Revised by Xiang *et al.*, 2013) and are also implicated in cell death phenomena. There are two types of vacuoles: the protein storage vacuole (PSV) and the lytic vacuole (LV) (Bolte *et al.*, 2011). PSVs have higher pHs and lower hydrolytic activities than LVs, and predominate in storage tissues (e.g. cotyledons and endosperm in seeds, tubers), as well as in vegetative tissues of adult plants (e.g. bark, leaves, pods). Proteins stored in PSVs are mainly used as nutrient reserve during seed germination and plant development. However, PSVs can also contain large amounts of toxic proteins such as protease inhibitors. LVs are usually found in vegetative tissues. They have an acidic pH and contain an abundance of hydrolytic enzymes). LVs are used for storage and as a container of unwanted materials in plant cells. They receive extracellular components via endocytosis and phagocytosis, and intracellular material via autophagy, as well as via the biosynthetic trafficking pathway and membrane-bound transport systems (Revised by Xiang *et al.*, 2013).

1.2 Secretory pathways

1.2.1 Protein secretion

In plants, secreted proteins play an important role in cell wall assembly, modification and in the response to biotic and abiotic stresses (Surpin *et al.*, 2004). Recently, evidences for two types of secretion have been reported: conventional and unconventional protein secretion (reviewed by Drakakaki and Dandekar, 2013). Conventional protein secretion refers to ER-Golgi

mediated secretory routes. In post-Golgi trafficking, secretory vesicles fuse with the plasma membrane and release their contents into the extracellular space (Surpin *et al.*, 2004).

Unconventional protein secretion (UPS) is described for leaderless cytoplasmic proteins lacking the presence of a signal peptide. Many plant proteins have been identified in the extracellular space, even though they lack either a canonical signal peptide or proper recognition signals that direct them to the endomembrane system (Revised by Drakaki and Drakekar).

1.2.2 ER-to-Golgi trafficking

Vesicular transport can occur in the forward (anterograde) direction, export newly synthesized proteins from the endoplasmic reticulum (ER) towards the Golgi, or in the reverse direction (retrograde) for proteins that are ER resident but accidentally escape through incorporation into the lumen of export carriers and for recycling of proteins that are involved in the export machinery (revised by Hanton *et al.*, 2005).

The formation of vesicles is induced by the cytoplasmic coat protein complexes (COPs) that polymerize on the membrane surface, capturing in the process both cargo molecules and those that function in vesicle direction, such as soluble N-ethylmaleimide-sensitive factor attachment protein receptors (SNAREs). The membrane alters its morphology during the polymerization of the coat, resulting in the formation of a vesicle. Small proteins with GTPase activity regulate the assembly and disassembly of the vesicle coat by cycling between GTP/GDP forms corresponding to activated/inactivated forms, respectively. The activated form initiates the recruitment of coat proteins to the membrane, whereas hydrolysis of GTP to GDP alters the conformation of the GTPase and triggers uncoating of the vesicle. The GTPase activity is regulated by guanine-nucleotide exchange factors (GEFs) and GTPase-activating proteins (GAPs), which prevent unproductive cycles of membrane coating and uncoating. SAR1 GTPase and its GDP/GTP exchange factor SEC12 mediate COPII-dependent cargo export from the ER - the anterograde traffic. The retrograde transport from the Golgi to the ER is accomplished via COPI vesicles, which are morphologically and biochemically different from the COPII vesicles of the retrograde system. The distribution of proteins between ER and Golgi is maintained by the balanced modulation of COPI and COPII transport routes by the transport machinery (Revised in Jurgens *et al.*, 2004; Hanton *et al.*, 2005; Xiang *et al.*, 2013).

1.2.3 Post-GA transport

Protein trafficking and sorting to the vacuole

Vacuolar proteins reach the different types of vacuoles through a vesicle-mediated biosynthetic trafficking pathway that includes the ER, the Golgi apparatus, the TGN and the endosomes/prevacuoles (Fig. 1.1). For proper vacuolar sorting, positive information is needed from the protein – Vacuolar Sorting Determinant (VSD) – that must be recognized by a specific receptor – Vacuolar Sorting Receptor (VSR). In plant cells, two different types of membrane receptors are known: the vacuolar sorting receptor (VSR) family (De Marcos Lousa *et al.*, 2012) and the receptor membrane ring-H2 (RMR) family (Cao *et al.*, 2000). In regard to the plant VSDs, three major groups have been identified so far.

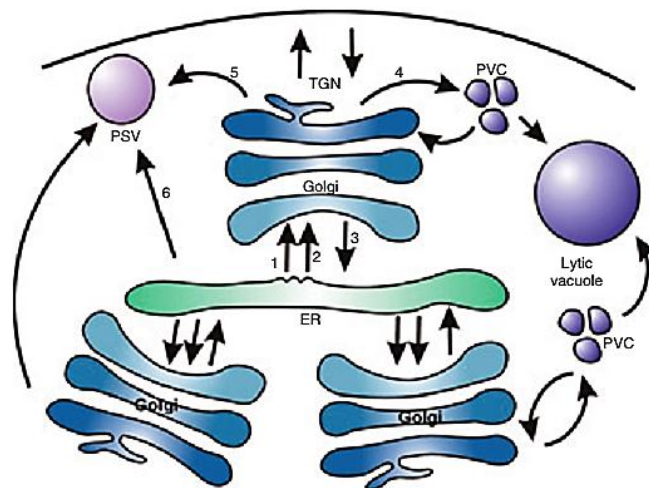


Figure 1.1.: Overview of the secretory pathway in plants. Schematic representation of organelles and their connecting protein transport routes in the plant-secretory pathway. Routes are numbered as follows: 1 –COPII-mediated endoplasmic reticulum (ER)–Golgi traffic; 2 –COPII-independent ER–Golgi traffic; 3 – COPI-mediated Golgi–ER traffic; 4 – traffic in clathrin-coated vesicles (CCVs) from the trans-Golgi network (TGN) to the prevacuolar compartment (PVC);5 – traffic via dense vesicles(DVs) to the protein storage vacuole (PSV); 6 – direct ER–PSV traffic. (Adapted from Hanton *et al.*, 2005)

The sequence-specific VSDs (ssVSDs) consist of conserved motifs usually located in the N-terminus of a protein. The second group of VSDs comprises the C-terminal VSDs (ctVSDs). These signals are not conserved, nor do they have a defined size; however, common to all C-terminal VSDs is that they are rich in hydrophobic amino acid residues, and they need to be surface-exposed. A third group of VSDs are those dependent on the physical structure of proteins (psVSDs), located in the centre of the protein and may involve one or more motifs, which become

exposed only when the protein acquires its folded conformation. Without these motifs, vacuolar proteins follow the default pathway and are secreted to the surface of the cell and though their introduction into a secreted protein redirects it to the vacuole. Inside the TGN, specific sorting signals are recognized by TGN membrane localized receptors, recruited into clathrin-coated vesicles (CCVs) and transported into the Lytic Vacuole. Remarkably, and uniquely in plants, LV resident proteins can be transported directly from the ER to the LV by means of ER bodies as intermediate compartments, through a Golgi-independent route (Revised by Xiang *et al.*, 2013)

Storage proteins are transported to the PSV in a Golgi-dependent or -independent manner depending on the cargo protein and the plant developmental stage. The trafficking of storage proteins from the Golgi apparatus into the PSV is mediated by dense vesicles (DVs). DVs are transferred to the TGN and eventually released. As mature DVs are not protein coated, they can directly fuse with the PSV or first with multivesicular bodies where they discharge their contents. Transport of storage proteins to the PSV can also take an alternative route from the ER bypassing the Golgi and reaching the PSV via precursor-accumulating compartments (PACs), which are much larger than DVs, and reach the PSV directly from the ER). Although directly generated from the ER, PACs can accept glycosylated proteins derived from the Golgi during their transport to the PSV). The incorporation into the lumen of the PSV follows one of two models: fusion between precursor-accumulating compartments and PSV through autophagy or by direct membrane fusion (Revised by Xiang *et al.*, 2013).

1.3 Cardosins: model proteins to study different trafficking pathways

Cardosins were originally isolated from the flowers of *Cynara cardunculus* L. (cardoon) and are representative of a complex protein trafficking routes and sorting mechanisms. These two aspartic proteases are superb models to study intracellular trafficking since their high similarity in terms of aminoacid and nucleotide sequences, translates into different subcellular localization in the native system (Ramalho-Santos *et al.*, 1997; Vieira *et al.*, 2001).

1.3.1 Processing, accumulation and biological function: an overview

Cardosin A and cardosin B have been isolated and extensively characterised and are the majority of the total soluble protein content found in floral organs (Ramalho-Santos *et al.*, 1996, 1997, 1998a, b; Verissimo *et al.*, 1996; Faro *et al.*, 1998; Vieira *et al.*, 2001).

Cardosin A is the more abundant and is mainly accumulated in protein storage vacuoles of the stigmatic papillae and vacuoles of the epidermic cells of the style. Considering this accumulation pattern and because it contains an Arg-Gly-Asp (RGD) motif, which is a well-known integrin-binding sequence, it was suggested a possible role in the pollen–pistil interaction (Faro *et al.*, 1999; Ramalho-Santos *et al.*, 1997, Duarte *et al.*, 2006).

The precursor form, procarnosin A, undergoes proteolytic processing as the flower matures and, during this process, the PSI is completely removed prior to the prosegment (fig. 1.2). The proenzyme is an active enzyme since its pro-segment is unable to block access to the catalytic cleft, as does for other APs (Simões and Faro 2004).

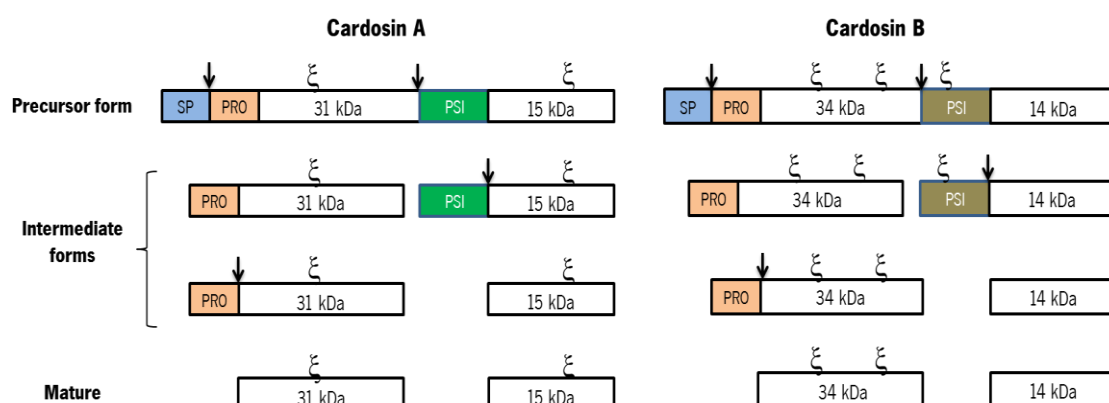


Figure 1.2.: Schematic representation of cardosins processing steps. Cardosins preproenzymes have a signal peptide (SP), followed by a prosegment (PRO) and a Plant-Specific Insert (PSI) between the heavy and light chains. There are two N-glycosylation sites (ξ) in cardosin A, one in the heavy chain and one in the light chain. Cardosin B has three putative glycosylation sites, two in the heavy chain and one in the PSI region. SP is removed upon

entrance in the ER and a first cleavage occurs between the heavy chain and the PSI; the PSI is removed by a cleavage between this region and the light chain; finally the pro-segment is removed and the two chains of the processed form are held together by hydrophobic interactions and hydrogen bonds. The arrows correspond to the cleavage sites.

The processed, mature, form of cardosin A was shown to be located in the vacuoles (Ramalho-Santos *et al.*, 1997). The conversion into the mature form is likely to occur inside the vacuoles (Ramalho-Santos *et al.*, 1998b, Simões and Faro 2004). Transmission electron microscopy (TEM) observations of developing cardoon pistils revealed swollen cisternae of ER with similar appearance to cardosin A-containing vacuoles (Duarte *et al.*, 2006). This observation led to the hypothesis that cardosin A could reach the vacuole through a Golgi independent route, although the presence of modified *N*-glycans indicates involvement of the Golgi complex (Costa *et al.*, 1997).

In cardoon seeds, procardosin A is accumulated in protein bodies and cell walls where it may also have a role in germination and post-germination developmental events, in addition to the possible involvement in storage protein conversion and/or degradation. The presence of procardosin A in seeds could be related to the proposed role of the plant-specific insert that could act as a membrane destabilising domain in membrane lipid conversion during water uptake and solute leakage in actively growing tissues (Egas *et al.*, 2000; Pereira *et al.*, 2008). The PSI was found to interact with phospholipid membranes, promoting the release of the aqueous contents of phospholipid vesicles in a pH-dependent manner, with higher leakage activity at acidic pH (Egas *et al.*, 2000). Procardosin A was also found to induce vesicle leakage of aqueous contents in a pH-dependent manner. Contrary to procardosin A, the mutated form lacking the PSI domain only presented a residual leakage activity.

The PSI sequence is highly similar to saposin-like proteins (SAPLIPs) (Guruprasad *et al.*, 1994), a protein family that includes saposins, which are lysosomal sphingolipid-activator proteins (O'Brien and Kishimoto, 1991). The main characteristics of this family of proteins are three conserved disulfide bridges, several hydrophobic residues, and a consensus glycosylation site. This last feature is not present in cardosin-A PSI (Verissimo *et al.*, 1997; Costa *et al.*, 1997). In fact, PSI is not a true saposin because of the swap between N- and C-terminal domains when compared to SAPLIPs, so it is denominated swaposin (Revised by Egas *et al.*, 2000). Some data point to a possible role for the PSI in the correct vacuolar sorting of some plant APs (Mutlu and Gal 1999; Tormakangas *et al.*, 2001; Simões and Faro 2004) like the barley phytepsin

(Tormakangas *et al.*, 2001) and for the soybean aspartic proteinase soyAP2, but not for soyAP1 in which deletion of the PSI has no effect on the vacuolar targeting (Terauchi *et al.*, 2006).

Cardosin B has been shown to be localised in the extracellular matrix of the stilar transmitting tissue (Vieira *et al.*, 2001, Duarte *et al.*, 2006) which led to a suggested role in the remodelling or degradation of the pistil extracellular matrix during pollen tube growth. The presence of cardosin B in specific regions of pollen tube may be associated with a role in softening and loosening of the cell wall, presumably facilitating pollen tube progression and/or the passage of nutritive substances through this region, nourishing the embryo sac (Figueiredo *et al.*, 2006). In seeds, cardosin B was only detectable in the first stages of germination and it was suggested that could have a role in loosening the constraining structures in the first hours after seed imbibition (Vieira *et al.*, 2001; Figueiredo *et al.*, 2006; Pereira *et al.*, 2008). Cardosin B has been found in tissues undergoing programmed cell death (Faro *et al.*, 1998). It is possible that the vesicle leakage of PSI may function as part of a defensive mechanism against pathogens and as an effector of cell death (Egas *et al.*, 2000).

Given the specific and preferable localisation of these two cardosins in cardoon flowers and seeds, it is probable that both may perform important roles during plant sexual reproduction and germination.

1.3.2 Trafficking and sorting in heterologous systems

Cynara cardunculus (cardoon) is a biannual plant and a lack of efficient transformation protocols restricts its use for the study of intracellular trafficking and sorting dynamic events. Cardosin A and cardosin B sorting and processing have then been characterized in heterologous systems (Duarte *et al.*, 2008; Soares da Costa *et al.*, 2010; Soares da Costa *et al.*, 2011; Pereira *et al.*, 2013).

Processing of cardosin A is conserved in the native and heterologous species (Duarte *et al.*, 2008). In *Nicotiana tabacum* and *Arabidopsis thaliana* seedlings cardosin A is correctly targeted to the vacuoles and highly stable when expressed in these two distinct heterologous systems (Duarte *et al.*, 2008). Cardosin A was shown to enter the secretory pathway and reach the vacuole in a Golgi-dependent manner (Duarte *et al.*, 2008; Pereira *et al.*, 2013). Recently the vacuolar sorting elements of cardosin A were dissected in *Nicotiana tabacum* (Pereira *et al.*, 2013). In this study, two vacuolar sorting determinants of cardosin A were identified and characterised and two different pathways through which the protein reaches the vacuole were

scrutinized. The C-terminal peptide VGFAEAA is a vacuolar sorting domain that mediates sorting through a probable COPII-dependent ER-to-Golgi pathway to the vacuole (Pereira *et al.*, 2013). The results obtained suggest a PVC–vacuolar route for cardosin A but the authors consider the existence of PVC independent routes in other tissues/organs, probably mediated by PAC vesicles (Pereira *et al.*, 2008; Pereira *et al.*, 2013). In this same study, a Golgi bypass mediated by the PSI was suggested in *Nicotiana tabacum* heterologous system (Pereira *et al.*, 2013). Pereira and co-workers (2013) demonstrated that the PSI is a VSD capable of directing cardosin A to the vacuole in the absence of the C-terminal domain. Furthermore, they showed that the PSI alone is able of targeting another protein besides cardosin, to the large vacuole of tobacco epidermal cells (Pereira *et al.*, 2013).

Cardosin B passes the Golgi complex by a RAB-D2a-dependent route and reaches the vacuole via the prevacuolar compartment in a RAB-F2b dependent pathway (Soares da Costa *et al.*, 2010). Contrary to cardosin-A plant specific insert, cardosin-B PSI needs to travel through the Golgi to reach the vacuole (Pereira *et al.*, 2013) (fig.1.3).

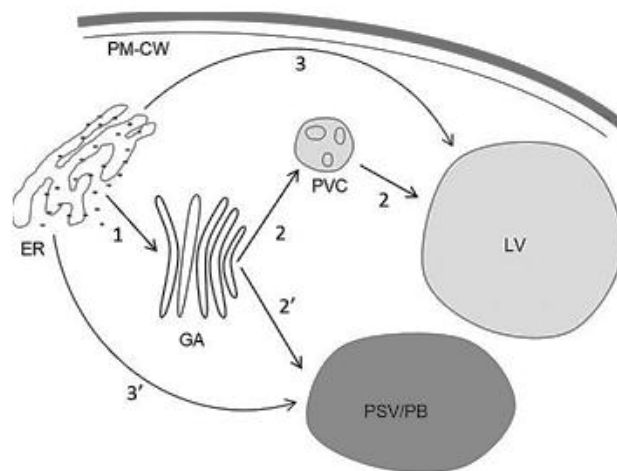


Figure 1.3.: Putative models for the trafficking of cardosin A to the plant vacuole. (1) COPII-dependent pathway, mainly mediated by C-terminal vacuolar sorting determinants (VSDs, black arrows), or a glycosylated plant-specific insert (PSI) determinant. (2) Pre-vacuolar compartment (PVC) route observed for cardosin A and C-terminal-mediated trafficking. (2') Putative route from the Golgi apparatus (GA) to the vacuole (mediated by PAC vesicles) that can be observed in storage organs (not confirmed). (3) COPII-independent pathway, sorted by PSI vacuolar sorting determinant without glycosylation site. (3') Cardosin A trafficking route to the protein body in cardoon seeds. Abbreviations: ER, endoplasmic reticulum; GA, Golgi apparatus; PAC, precursor accumulating vesicles; PM–CW, plasma membrane–cell wall complex; PSV/PB, protein storage vacuole/protein body; PVC, prevacuolar compartment; V, vacuole. Adapted from Pereira *et al.*, 2013.

1.4 The protein N-glycosylation in plants

Protein glycosylation is the attachment of a saccharide moiety to a protein, which occurs either co-translationally or post-translationally. The two major types of glycosylation, N-linked and O-linked, are both involved in the maintenance of protein conformation and activity, in protein protection from proteolytic degradation, and in protein intracellular trafficking and secretion (Varki, 1993). N-glycans also play a key role in the folding, processing, and secretion of proteins from the endoplasmic reticulum (ER) and the Golgi apparatus (Varki, 1993). In this section we will focus on N-glycosylation that is the most studied in plant cells and the one that occurs to the proteins that travel through the secretory pathway.

N-glycosylation starts in the endoplasmic reticulum (ER), with the co-translational transfer of an oligosaccharide precursor, Glc₃Man₉GlcNAc₂. These glycans are initially synthesized on a lipid-like molecule termed dolichol phosphate, followed by the transfer of the entire glycan of 14 sugars to protein. The N-glycosylation sites are the tripeptide Asn-X-Ser/Thr where X can be any amino acid except proline and aspartic acid (). The processing of the Glc₃Man₉GlcNAc₂ precursor occurs along the secretory pathway as the glycoprotein moves from the ER and through the Golgi apparatus to its final destination. Glycosidases and glycosyltransferases that catalyse the trimming and addition of sugar residues, respectively, are present in the ER and Golgi complex. A transient reglucosylation by an ER UDP-glucose: glycoprotein glucosyltransferase may occur subsequent to the elimination of these three glucose residues). This reglucosylation has been shown to act on unfolded proteins and is involved in the quality control of glycoproteins in the ER (revised by Rayon *et al.*, 1998).

1.4.1 Plant N-linked glycans

In plants, in the early steps of the protein biosynthesis when the nascent polypeptide enters the lumen of the ER and the oligosaccharide transferase attaches the oligosaccharide precursor to specific asparagine residues, the presence of N-glycans affects both the co- and post-translational folding of the protein. N-linked glycans strongly influence the glycoprotein conformation, stability and biological activity and they can protect the protein from proteolytic degradation, as well as the fact that they are responsible for the thermal stability, solubility and biological activity of glycoproteins (Rayon *et al.*, 1998).

Rayon and co-workers (1998) have proposed alterations in the classification due the different types of complex-type glycans found in plants. In this section we will adopt the nomenclature described by Lerouge and co-workers (1998) into the three following classes: high-mannose-type, complex-type, paucimannosidic-type and hybrid-type *N*-glycans.

The high-mannose-type *N*-glycans having the general structure $\text{Man}_{5-9}\text{GlcNAc}_2$ arise from the limited trimming of glucose and mannose residues from the precursor oligosaccharide $\text{Glc}_3\text{Man}_9\text{GlcNAc}_2$ ().

The complex-type *N*-glycans are characterized by the presence of α (1,3)-fucose and/or a β (1,2)-xylose residues respectively linked to the proximal N-acetyl glucosamine and to the β -mannose residues of the core and by the presence of β (1,2)-*N*-acetyl glucosamine residues linked to the α -mannose units (). More complex bi-antennary plant *N*-glycans have been described. They have one or two terminal antennae containing an oligosaccharide sequence, Gal β (1-3) [Fuc α (1-4)] GlcNAc, named Lewis a (Le_a) (Fitchette-Lainé *et al.*, 1997). Le_a containing *N*-glycans are present on glycoproteins from mosses, ferns, gymnosperms, monocots, and dicots (except for members of the *Cruciferae* family), but are absent on glycoproteins from lower organisms such as algae, lichens, and fungi (Fitchette *et al.*, 1999).

Paucimannosidictype *N*-glycans results from the elimination of terminal residues from complex-type *N*-glycans. Most vacuolar glycoproteins and seed storage glycoproteins described so far were found to be *N*-glycosylated with paucimannosidic-type *N*-glycans containing fucose and/or xylose residues but devoid of terminal glucosamine residues, whereas most extracellular glycoproteins bear complex-type *N*-glycans with terminal *N*-acetyl glucosamine residues or Le^a antennae (Lerouge *et al.*, 1998).

Hybrid-type *N*-glycans are a result from the processing of only the α (1,3)-mannose branch of the intermediate $\text{Man}_5\text{GlcNAc}_2$ leading to oligosaccharides having α (1,3)-fucose and/or a β (1,2)-xylose residues linked to $\text{GlcNAcMan}_5\text{GlcNAc}_2$

The polypeptide folding can influence the availability of potential glycosylation sites in the ER therefore glycans that are located on the protein surface will mature into complex-type *N*-glycans, whereas oligosaccharides that are masked in the protein structure remain unmodified high-mannose glycans.

Concanavalin A (ConA) is a lectin accumulated in the PSV of jack bean (*Canavalia ensiformis* L.). ConA is synthesized as a glycosylated precursor, proConA that has no lectin activity in contrast to mature ConA. Inhibition of the proCon A *N*-glycosylation reduces its

transport from ER to the protein storage vacuole. Deglycosylation of the prolectin appears as a key step in the lectin activation (Ramis *et al.*, 2001). These results indicate that the *N*-glycosylation of Con A is important for its transport to the vacuole and the regulation of its lectin activity.

On the other hand, the expression in transgenic tobacco plants of a vacuolar lectin, the bean phytohaemagglutinin (PHA) cDNA mutagenized on both *N*-glycosylation sites did not alter the accumulation of the unglycosylated lectin in the protein bodies of transgenic tobacco seeds. Another example is the barley lectin, a vacuolar protein that is initially synthesized as glycosylated precursor and subsequently processed to mature nonglycosylated protein by the post-translational cleavage of a C-terminal terminal glycopeptide. Localization of mature barley lectin derived from the glycoprotein in vacuoles of tobacco demonstrated that the high-mannose glycan attached to the C-terminal propeptide was not an absolute requirement for the targeting of barley lectin to vacuoles. This indicates that glycans of the barley lectin proprotein and PHA are not essential for processing and targeting of these proteins to vacuoles. However, the glycan of pro-ConA apparently plays a direct role in processing and transport of ConA to vacuoles (Revised in Rayon *et al.*, 1998).

In the presence of tunicamycin, an *N*-glycosylation inhibitor, most extracellular *N*-glycosylated glycoproteins are not secreted any more). However, the processing of high-mannose-type to complex-type *N*-glycans is not required for transport and secretion of extracellular glycoproteins in plants (Lerouge *et al.*, 1996). Therefore we can conclude that, Golgi-mediated maturation of *N*-glycans is dispensable for an efficient secretion of plant glycoproteins (Revised by Rayon *et al.*, 1998).

1.4.2 Cardosin A and B glycosylation patterns

The glycosylation of aspartic proteinases was suggested to have a role in the stabilization of the enzymes, as found for recombinant renin expressed in fibroblast-like cell line (COS cells), or in their secretion, as found for the recombinant aspartic proteinase from *Mucor* expressed in yeast (Revised by Costa *et al.*, 1997).

Cardosin A has two N-linked glycosylation sites (at Asn-67 and Asn-257), one in the 15-kDa subunit and another in the 31-kDa subunit (fig. 1.4). The oligosaccharides in cardosin-A light chain contain residues of both β (1, 2)-linked xylose and α (1, 3)-linked fucose (complex-type glycans), whereas the heavy chain contain only the proximal fucose residue (Verissimo *et al.*,

1996; Costa *et al.*, 1997). The N-glycan identified for the 31 kDa subunit is a plant-type specific glycan classified as paucimannosidic-type by Lerouge *et al.* (1998). The two glycans, of the plant complex type, attached to the polypeptide backbone are extensively visible in cardosin-A crystal structure (Frazão *et al.*, 1999). A hydrogen bond turns the monosaccharide inaccessible to accept a xylosyl residue (Costa *et al.*, 1997). Both sites are away from the aspartic proteinase catalytic site and from the specificity determining cleft. Therefore, it is unlikely that the oligosaccharides will play an important role in the activity and specificity of the enzyme although they may act to stabilize the protein conformation.

Cardosin B has three putative N-glycosylation sites: Asn138-Gly139-Thr140, Asn252-His253-Thr254 and Asn396-Glu397-Thr398 (fig. 1.4). The first two glycosylation sites are localised in the heavy chain and the last one on the PSI region (Soares da Costa *et al.*, 2010). The glycosylation pattern of cardosin B in *Arabidopsis* and *Nicotiana tabacum* heterologous systems was in accordance with that observed in cardoon high-mannose-type glycans, suggesting that either the glycans are inaccessible to the Golgi processing enzymes due to cardosin B conformation or the protein leaves the Golgi in an early step before Golgi-modifying enzymes are able to modify the glycans.

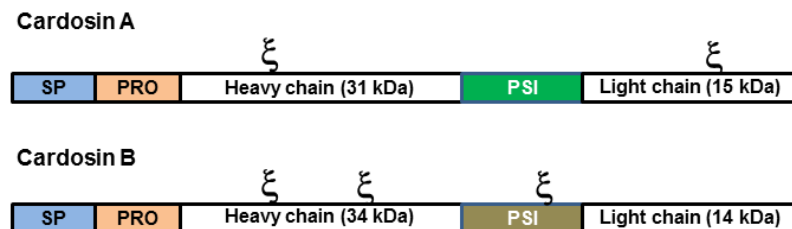


Figure 1.4.: Schematic representation of cardosin A and cardosin B glycosylation patterns. Cardosin A has two glycosylation sites, one in the heavy chain and another in the light chain. Cardosin B has three putative glycosylation sites, two in the heavy chain and one in the PSI domain. ξ- represents a glycosylation site.

1.5 Fluorescent reporters to study cardosins trafficking

Advances in fluorescence probes and microscopy technologies have provided valuable approaches that present advantages and complement traditional western and immunostaining assays. Since the discovery of green fluorescent protein (GFP) (Prasher *et al.*, 1992; Chalfie *et al.*, 1994; Tsien, 1998), a variety of fluorescent proteins (FPs) with different colours has been developed. Limitations of single-coloured FPs become apparent when the aim is to understand spatiotemporal aspects of interactions between similar organelles and local and often transient alterations in the organization of dynamic subcellular elements like the cytoskeleton and endomembranes. Nowadays fluorescent proteins covering the entire visible spectrum (Fig. 1.5) are considered essential tools for studying gene activity, protein localization, and subcellular interactions. In the recent years, a diversity of optical highlighters namely, photoactivatable, photoswitchable, and photoconvertible fluorescent proteins, have become available. These proteins react to specific wavelengths and undergo structural changes that result in changing from a dark to a bright fluorescent state (photoactivatable FPs) or cause a shift in their fluorescence emission wavelength (photoconvertible FPs) (revised in Shanner *et al.*, 2007).

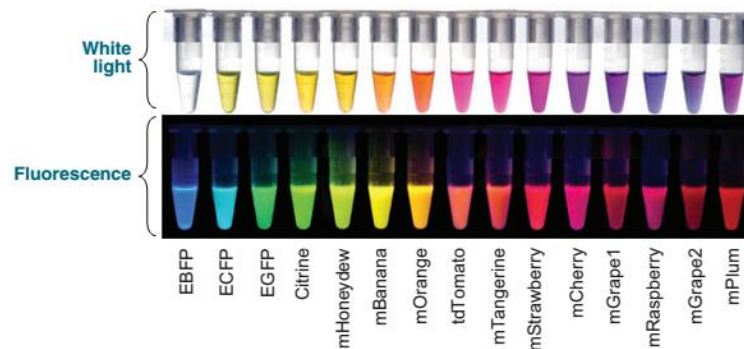


Figure 1.5.: Diversity of the different fluorescent proteins available for cloning. The top panel shows the FPs under white light and the bottom panel demonstrates the fluorescence of these FPs. (Adapted from Wang *et al.*, 2008).

1.5.1 Fluorescent proteins: Green fluorescent protein and mCherry

GFP complex was first isolated from the jellyfish *Aequorea Victoria*. The fusion of wild-type GFP sequence with genes encoding target molecules allows the tracking of subcellular localisations and dynamic motions by fluorescence microscopy. Recently it has been demonstrated new fluorescent protein-based technologies with this protein reinforcing that GFP is a valuable tool for *in vivo* studies (revised by Sparkes and Branzzini, 2012).

Several proteins have been purified from *Anthozoa* species. Among them, the red fluorescent protein (RFP) was of particular interest. A large amount of effort has been devoted to producing a monomeric RFP such as mCherry (Shanner *et al.*, 2004). mCherry has excellent photostability, fast maturation rate and high resistance to pH variations.

Despite highlighting their target clearly the green and red fluorescent probes are limited in their applications since their colours cannot be switched on or altered as and when required.

1.5.2 Photoconvertible Proteins

Improved classes of chromophores that are photoswitchable or photoconvertible, capable of pronounced light-induced spectral changes, have enabled users to study the subcellular dynamics *in vivo*. More recent optical highlighters have chromophores that can be activated either to initiate fluorescence emission from a quiescent state (photoactivation) or to be optically converted from one fluorescence emission bandwidth to another (photoconversion) through a cleavage in peptide backbone represented in the figure 1.5. These tags allow specific tracking of one subcellular structure (organelle or cell subdomain) within a differentially labelled population that used to be a methodological challenge for the cell biologist. Like green fluorescent protein (GFP), monomeric EosFP (mEos) and Kaede are bright green in colour but are efficiently photoconverted into a red fluorescent form using a violet-blue excitation. Moreover mEos and Kaede are fully compatible with cyan fluorescent protein, GFP, yellow fluorescent protein, and red fluorescent protein for use in simultaneous, multicolor labeling schemes. In this section we focus in these two photoconvertible proteins that were optimized in our laboratory for cardosins expression studies, Kaede and mEos, that have different applications due to their different properties.

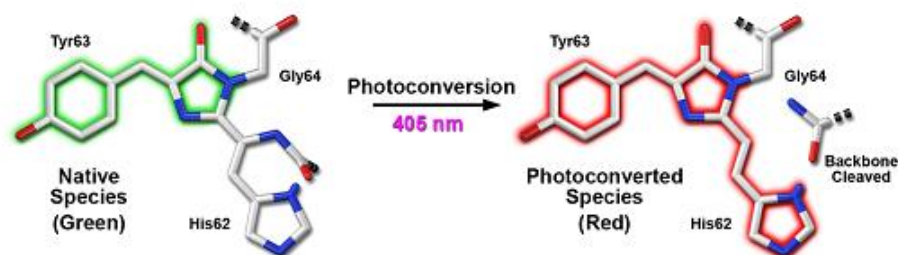


Figure 1.6.: Green-to-red photoconversion mechanism for Kaede and mEos that occurs when the FP is illuminated with ultraviolet or violet radiation to induce cleavage between the amide nitrogen and α carbon atoms in the His62 residue leading to subsequent formation of a conjugated dual imidazole ring system. (Adapted from Shanner *et al.*, 2007)

The tetrameric Kaede

The Kaede gene codes for a tetrameric protein found in the stony coral *Trachyphyllia geoffroyi*. Emits green fluorescence and irreversibly shifts to red fluorescence following irradiation with UV or violet light (Ando *et al.*, 2002). The emission spectra of Kaede before and after photoconversion are distinct from each other which enable simultaneous dual-colour labelling. Kaede has been reported as an excellent subcellular marker for endomembrane compartments such as Golgi bodies (Brown *et al.*, 2010). In this work Kaede proved to be a great reporter to track the dynamic behaviour of designated subpopulations of Golgi within living cells, while visualizing the *de novo* formation of proteins and structures (Brown *et al.*, 2010). Brown and co-workers demonstrated the applicability of Kaede to explore the secretory pathway in plant cells. The tetrameric structure of Kaede represents advantageous properties like its robustness, the stability of its green and red forms, its high contrast (high absorptivity and distinctness of its forms), and its sensitivity to violet light (Brown *et al.*, 2010). It was suggested that this three-dimensional nature possibly retains protein fusions which induced artefacts in Golgi compartments (Brown *et al.*, 2010).

mEos: a powerful addition to study trafficking dynamic events

EosFP, a homolog of Kaede derived from *Lobophyllia hemprichii*, has been engineered to a monomeric form without loss in fluorescence and photoconversion properties (Wiedenmann *et al.*, 2004). In its unconverted form, mEos displays bright green fluorescence that, upon illumination with an approximately 390- to 405-nm waveband, changes irreversibly to red fluorescence (emission maximum of 581 nm). Monomeric fluorescent proteins of different colours are widely used to study behaviour and targeting of proteins in living cells. mEos is especially useful for application in plants as it provides the ability to differentially colour and track a single organelle within a population, as well as follow endomembrane and cytoskeletal dynamics over time (Mathur *et al.*, 2010). An important property of monomeric EosFP (mEosFP) is the high stability and irreversibility of its red fluorescent photoconverted form. Thus, if green fluorescence of a target organelle or cell increases and reappears after photoconversion it can be attributed largely to newly synthesised green fluorescent form (recovery after photoconversion).

2 Materials and Methods

In order to study cardosins trafficking and their respective targeting signals, classical molecular biology tools were employed to obtain fusions with fluorescent proteins. These constructs were used to transform *Arabidopsis thaliana* using *Agrobacterium tumefaciens* mediated methods, either to achieve a transient expression or to obtain stably transformed plants expressing cardosins. Several truncated and mutated versions (already available in our lab) were used and tested for the first time in *A. thaliana* through transient expression. The same constructs and the ones produced during this work (represented in the figure 2.2) were used to obtain transgenic *A. thaliana* plants. Cardosins expression was evaluated by confocal microscopy and confirmed by RT-PCR analyses.

2.1 mEos-based constructs

The methodology to obtain mEos constructions and subsequent screening is showed schematically in figure 2.1 and will be detailed in this chapter.

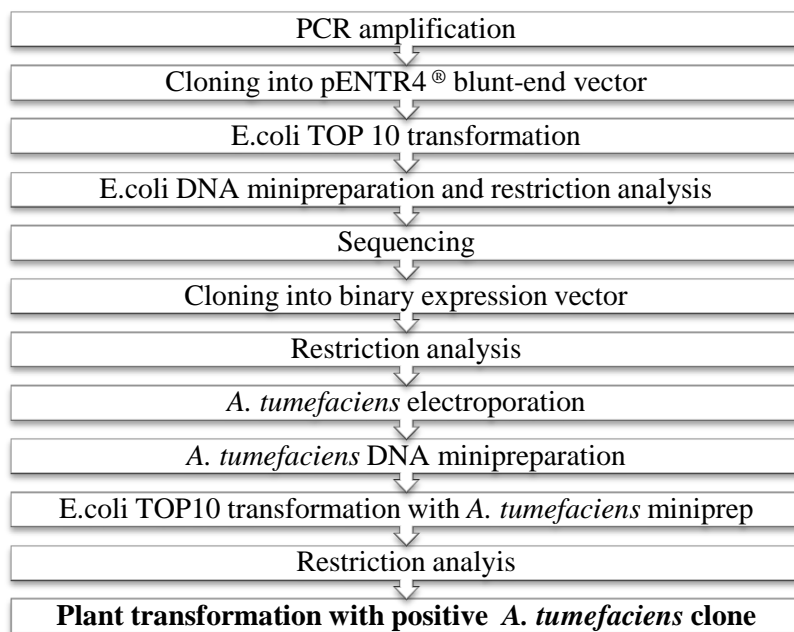


Figure 2.1.: Flowchart representation of the steps performed for obtaining, cloning and screening the mEos constructs analyzed during the work.

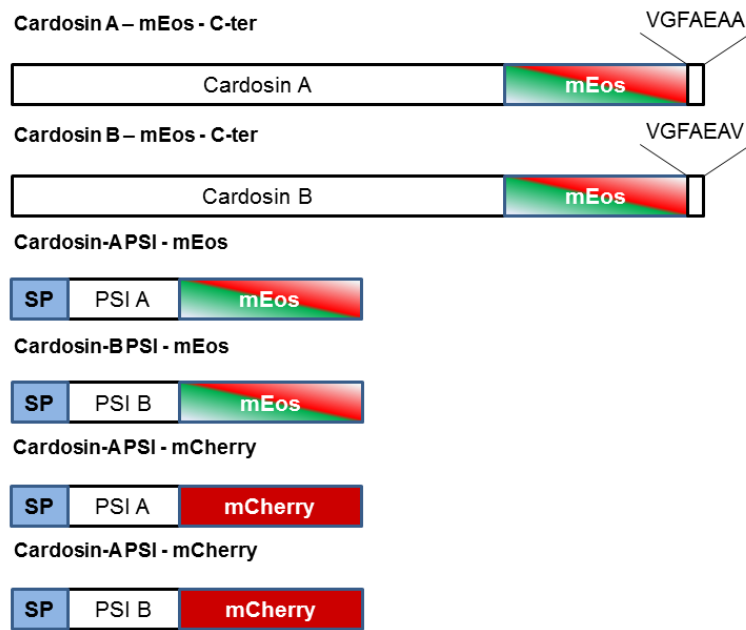


Figure 2.2.: Schematic representation of mEos-based constructs engineered during this work and detailed in this section. Cardosin A and B fused to mEos fluorescent protein with cardosins C-terminal sequence fused to the C-terminus of mEos and cardosin-A and cardosin-B PSI fused to the N-terminal of mEos and mCherry were obtained.

2.1.1 Construction of Cardosins-mEos fusions

The sequence of unmodified cardosin A (Duarte *et al.*, 2008) and B (Soares da Costa *et al.*, 2010) were fused to the monomeric photoconvertible fluorescent protein mEos (Wiedenmann *et al.*, 2004) and were already available in our laboratory from a previous work (Vieira, data). The expression of these versions in *N. tabacum* leaf epidermis cells showed a pattern suggesting that cardosins were retained in the early endomembrane compartments. Similarly to what happens with mCherry fusions we propose that the cardosins' C-terminal region may not be exposed to vacuolar receptors due to the conformation of the fusions with mEos that would not allow the proper folding of the protein. In order to obtain chimeric proteins, a C-terminal region was introduced in the 3' end of the chimeric fusions by amplification with a set of primers (Table 2-1).

Table 2-1: Primers used in the amplification of Cardosins-mEos-C-terminal fusions

Primer name	Sequence	Description
RevEOS-CterA_Sac	TTGAGCTCTTAAGC TGCTTCTGCAAATCCAACTCGTCT GGCATTGTCAGGCAATCCAGAA	Introduces a cardosin A C-terminal region at the 3' end of the mEos sequence (green), alters the STOP codon of cardosin sequence (red) and introduces a Sac I recognition site (yellow) at the 3' end of the fusion sequence
A 5' Xba	TCTAGAGCCGCCAC CATGGGTACCT	Introduces a Xba I restriction site (yellow) at the 5'end of Cardosin A sequence
RevEOS-CterB_Sac	TTGAGCTCTTAAGC TGCTTCTGCAAATCCAACTCGTCT GGCATTGTCAGGCAATCCAGAA	Introduces a cardosin B C-terminal region at the 3' end of the mEos sequence (green), alters the STOP codon of cardosin sequence (red) and introduces a Sac I recognition site (yellow) at the 3' end of the fusion sequence
B F KZ Xba	5'- CATCTAGACTCGAG CCACCATGGGAACCCC AATCAAAGCAAACG-3'	Introduces a Xba I restriction site (yellow) at the 5'end of Cardosin B sequence

PCR fragments were cloned into pENTR4® (Invitrogen) digested with Hinc II restriction enzyme that permits the blunt-ended cloning. Positive clones were selected using Xba I and Sall restriction enzymes and sent for sequencing using the universal primer pENTattL2rev (Eurofins MWG Operon, <http://www.eurofinsdna.com/home.html>) and the listed primers in table 2-2.

Table 2-2: Primers sent to Eurofins MWG Operon for the sequencing of pENTR4-Cardosins-mEos-C-terminal constructs

Primer name	Sequence	Description
Card A 5' Xba	TCTAGAGCCGCCACCATGGGTA CCTCAATCAAA	Primer designed for the 5' end of Cardosin A heavy chain.
A15F	GGTGCTGCAGGTGGTACTTCAT CTGAAGAATTAC	Primer designed for the 5' end of Cardosin A light chain.
Card B1	AAAAC TCGAGCCACCATGGGAA CCCCAATCAAAGCAAGCC	Primer designed for the 5' end of Cardosin B heavy chain.
B15F	GCTGCAGGTGGTTTCGATGGTAG ACTGCAAT	Primer designed for the 5' end of Cardosin B light chain

Positive sequenced clones were selected and used for cloning in the Gateway-compatible cloning vectors designed for expression in *Arabidopsis*. Cardosin B construct was subcloned into pFAST-G02 (Shimada *et al.*, 2010) and pMDC83 (Curtis *et al.*, 2003) adapted for classical cloning was used for Cardosin A construct. Positive cardosin B-mEos-C-terminal clones were selected using the Eco RI restriction enzyme. Cardosin A-mEos-C-terminal clones were screened with Sal I and Sac I enzymes.

2.1.2 Fusion of Cardosin-A PSI and Cardosin-B PSI to mEos

SP-PSI A-mEos fusion

The construction SP-PSIA fused to mCherry fluorescent protein (Shanner *et al.*, 2004) cloned into pVKH18-En6- was already available in our laboratory. The restriction enzymes Xba I and Sac I were used to excise SP-PSIA-mCherry insert. The reaction product was analysed by agarose gel electrophoresis and the fragment of interest was excised from the gel and purified. The purified DNA was used for cloning into pMDC83 for expression in *Arabidopsis*. The ligation product was used for TOP10 *E.coli* transformation and the clones were screened using Xba I and Sac I enzymes.

A positive clone was selected and the DNA extracted from this clone was partially digested for 15 minutes with Sal I and Sac I restriction enzymes to avoid excision of the PSI sequence but

the removal of mcherry. The enzymes were heat-inactivated at 65°C for 20 minutes. The plasmid digestion product was analysed in agarose gel electrophoresis and pMDC83-SP-PSIA fragment was extracted and purified.

mEos sequence was obtained from pVKH18-En6-cardosin A-mEos construct after prediction analyses of the open reading frame of the fusion sequence (SP-PSIA-mEos) in pDRAW (<http://www.aacalone.com>). Plasmid DNA was digested with the restriction enzymes Sal I and Sac I to extract the sequence corresponding to mEos (Fig. 2.3.). The plasmid digestion product was analysed by agarose gel electrophoresis and mEos corresponding fragment was extracted and purified. The obtained fragments pMDC83-SP-PSI A and mEos were used in a ligation reaction and Top10 *E. coli* cells were used for transformation. The colonies were screened using the enzymes Sal I and Sac I and a second digestion to confirm identity of mEos with Hind III that has no recognition site in mCherry sequence. Purified DNA (Sigma GenElute™ Miniprep Kit) of a positive PMDC83-SP-PSIA-mEos clone was used to transform *Agrobacterium* cells.

SP-PSI B-mEos

In order to obtain pMDC-SP-PSIB-mEos the SP-PSIA-mEos mentioned above was digested with Sal I restriction enzyme to excise PSIA. The digestion product was separated by agarose gel electrophoresis and the fragment corresponding to pMDC-SP_mEos was purified and used in the ligation reaction. The PSIB DNA sequence with Sall restriction site adapters obtained by PCR was already available in our lab into pCRblunt® vector. The clones were screened and the PSIB sequence was excised using Sal I restriction enzyme, purified and used in the pMDC-SP-PSIB-mEos ligation reaction. The ligation was used to transform Top10 *E.coli* cells. The clones were screened using Xba I and Pst I restriction of the plasmids to confirm correct orientation of the insert.

The classical cloning detailed above is illustrated in the figure 2.3 for better visualization.

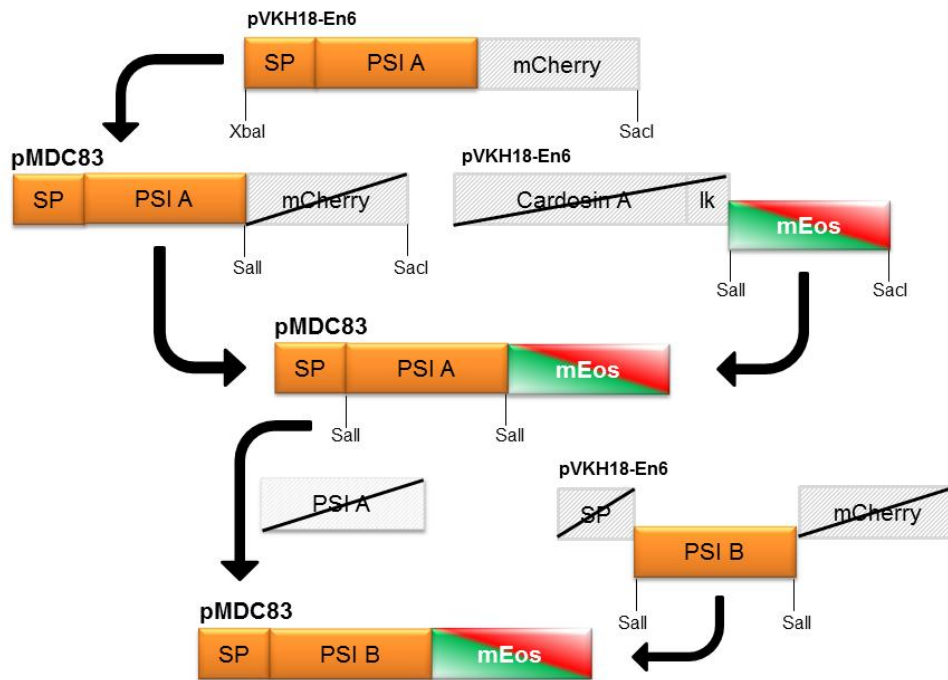


Figure 2.3.: Schematic representation of cardosin-A and cardosin-B PSI cloning into pMDC83. The restriction sites used for the cloning are pointed out and the vector containing the sequence to be excised is marked.

2.1.3 Cardosin-A and Cardosin-B PSI fused to mCherry in pMDC83

The mEos fluorescent protein coding sequence was replaced by mCherry sequence since the results obtained with the mEos-based constructs pointed to a misfolding of the fusion protein. pMDC83-SP-PSI A/B-mcherry constructs allowed us to validate the pMDC83 (adapted for classical cloning) as a suitable expression vector for *Arabidopsis* transformation.

pMDC83-SP-PSIA-mCherry was obtained in the intermediate steps of the SP-PSIA-mEos construct as mentioned above and it was used to obtain pMDC83-SP-PSIB-mCherry. The sequence was digested with Sal I enzyme restriction, the digestion product was analysed in agarose gel electrophoresis and the fragment corresponding to pMDC-SP_mcherry was extracted from the gel and purified. This purified vector containing the signal peptide and the fluorescent tag was used in a ligation reaction with PSIB already purified as mentioned above. Ligation product was used to transform TOP10 *E. coli* cells. Clones were screened using the same approach as for the PSIB-mEos constructs.

2.2 Constructs used for the study of cardosins expression in *Arabidopsis thaliana*

The mCherry fusions of cardosins, its truncated versions and isolated VSDs used in this work were already available in our laboratory (Fig. 2.4) and were obtained using Gateway cloning technology. The chimeric sequences have been subcloned into pFAST-G02 and were tested for expression in *Arabidopsis* during this work. Cardoso-B PSI fused to mCherry was obtained during this work as detailed above and was also used for stable *Arabidopsis* transformation.

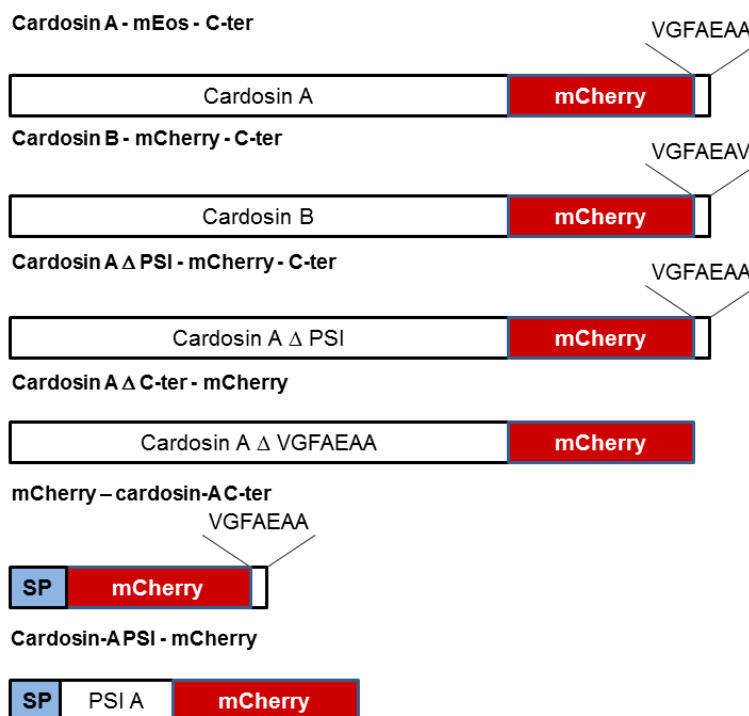


Figure 2.4.: Schematic representation of the chimeric proteins already available in our lab that were used for *Arabidopsis* transformation. Cardoso A and B fused to mCherry fluorescent protein with cardosins C-terminal sequence fused to the C-terminus of mCherry, cardosin A mutated versions without PSI or C-terminal and cardosin-A VSDs fused to the C-terminal or the N-terminal of mCherry were tested.

2.3 Obtaining of cardosins glycosylation mutants

N-glycosylation is an important post-translational modification that plays a role in protein trafficking and processing. Cardoso A has two glycosylation sites, one in the heavy chain and another in the light chain (Fig. 2.5). Three glycosylation mutants have been produced where the glycosylation sites were either removed (one by a point-mutation in the first site and another by a point-mutation in the second site) or added (by introducing a glycosylation site in the PSI region) (Fig. 2.5). These constructs were tested in a previous work and are already available in our

laboratory (Pereira, PhD thesis, 2012). In order to discuss the importance of glycosylation sorting two other constructs were obtained during this work: a non-glycosylated cardosin A version and a cardosin-A glycosylated PSI, since the presence of a glycosylated PSI is a conserved characteristic in most plant aspartic proteases. Also, cardosin B has a putative N-glycosylation site that was removed by site-directed mutagenesis in this work (fig. 2.5).

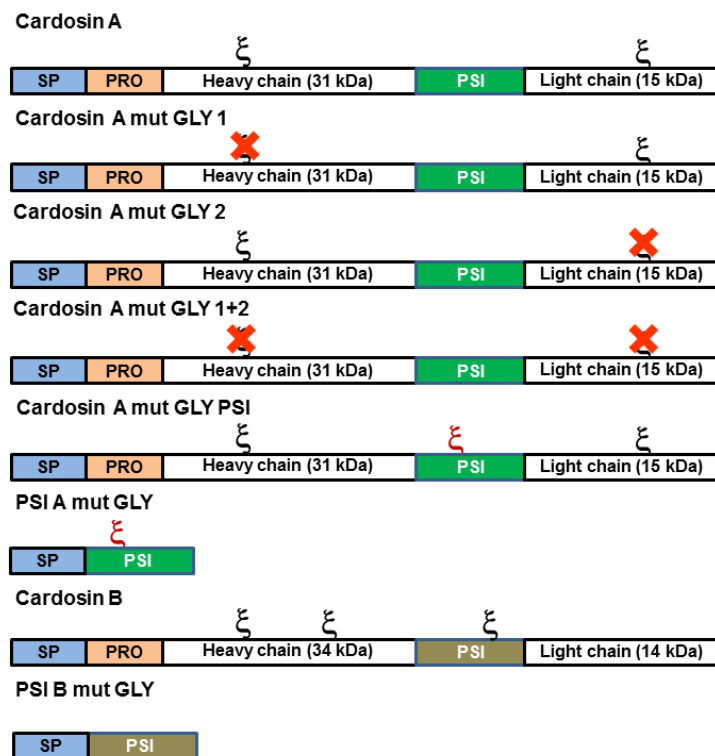


Figure 2.5: Schematic representation of cardosins glycosylation mutants. Cardosin A glycosylation sites 1 and 2 were removed by site-directed mutagenesis in previous works. Cardosin A mutated in both sites was constructed in pEntr4 vector and was subcloned into pVKH18-En6 and fused to mCherry during this work. Cardosin-A PSI glycosylated version was engineered using the same technique and was available in pCRBlunt® vector already fused to mCherry and was subcloned into pVKH18-En6. Cardosin-B PSI glycosylated version was produced during this work.

2.3.1 SP-PSI A mut gly -mcherry

Cardosin A-PSI mutated version fused to a signal peptide and to mCherry was already available in our lab. In this work SP-PSIA mut gly-mCherry was subcloned into pVKH18-En6 for expression in plant cells. This construct was digested with Xba I and Sac I restriction enzymes and the fragment of interest corresponding to SP-PSIA mut gly was isolated. The purified product was used as insert in the ligation reaction to pVKH18-En6_mcherry. The DNA extracted from *E. coli* transformed with the ligation mentioned above was digested with Sal I and Sac I enzymes for

screening. Plasmids from positive clones were used to transform *Agrobacterium* cells required for *N. tabacum* transient transformation.

2.3.2 Cardosin A mut gly 1+2-mcherry

Non-glycosylated Cardosin A version was already obtained in our lab. In this work cardosin A mut gly 1+2 sequence was excised from pCRblunt® and subcloned into pVKH18-En6 using the restriction enzymes Sal I and Sac I. The screening of clones was performed by plasmid restriction with the referred enzymes and plasmids were selected for *Agrobacterium* transformation. *A. tumefaciens* was used to transform *Nicotiana tabacum* epidermal cells.

Glycosylation pattern of cardosin A and B and other aspartic proteins was predicted using the “NetNGlyc” tool (version 1.0) (<http://www.cbs.dtu.dk/services/NetNGlyc/>).

2.4 Molecular biology protocols and tools

Polymerase Chain Reaction

For amplification of the cardosins-mEos fusions a polymerase with proofreading activity - "Pfu DNA polymerase (recombinant)" (Fermentas) – was used to minimize the inclusion of errors in the amplified sequence. The PCR reaction was performed as described in Table 2-3, and pVKH18-En6-cardosinA/B-mEos were used as template.

Table 2-3: PCR reaction used for amplification of cardosins-mEos constructs

Reagents	Concentration
DNA	20-50 ng
10X Pfu buffer plus MgSO4	1X
dNTPs	0.2 mM
5' Primer	0.3 μ M
3' Primer	0.3 μ M
Pfu DNA polymerase	1U
Sterile distilled water	Up to 25 μ L

The reactions were performed in a thermal cycler 'Mastercycler Gradient' (Eppendorf), according to the conditions in the table 2-4:

Table 2-4: Conditions of PCR reaction for Cardosin A/B-mEos-C-terminal amplification.

Step		Temperature / Duration
Initial denaturation		94 °C / 30 min
35 Cycles	Denaturation	94 °C / 30 sec
	Annealing	54 °C / 30 sec
	Extension	72 °C / 90 sec
Final elongation		72 °C / 7 min

Site-Directed Mutagenesis

The N-glycosylation site of cardosin B-PSI was mutated by site-directed-mutagenesis using the modified primers described in Table 2-5. pCRblunt-SP-PSIB was used as template in the reactions. Positive clones were confirmed by sequencing with M13 primer [M13 uni (-21) (Eurofins MWG Operon, <http://www.eurofinsdna.com/home.html>).

Table 2-5: Primers designed for site-directed mutagenesis

Primer name	Sequence	Description
PSI B mut gly fwd	GCAGAATGAAATCAAACGAAGCAGACTGAAG ATAACATAA	Introduction of a point mutation in the 245 th nucleotide [AAC (asparagine) changes to AGC (serine) -grey]
PSI B mut gly rev	TTATGTTATCTTCAGTCTCGCTTCGTTTGATTT CATTCTGC	

The mutated version of cardosin-B PSI was obtained by PCR using a polymerase with proofreading activity - "Pfu DNA polymerase (recombinant)" (Fermentas). The PCR reaction and conditions are summarized in Table 2-6 and Table 2-7 respectively.

Table 2-6: PCR reaction performed for site-directed mutagenesis

Reagents	Concentration
Template DNA	500 ng – 1 µg
10x Pfu buffer with MgSO4	1x
10 mM dNTPs mix	0,3 mM
5' Primer	0,4 mM
3' Primer	0,4 mM
Pfu DNA polymerase	2,5 U
Sterile distilled water	Up to 25 µL

Table 2-7: Conditions for site-directed mutagenesis reactions

Step	Temperature / Duration	
Initial denaturation	94 °C / 5 min	
12 Cycles	Denaturation	94 °C / 30 sec
	Annealing	54 °C / 30 sec
	Extension	72 °C / 2 min per Kb
Final elongation	72 °C / 15 min	

The PCR product obtained was digested with Dpn I restriction enzyme (Fermentas) for 1 hour at 37 °C, followed by inactivation of the enzyme at 65 °C for 15 minutes. This enzyme requires the presence of Dam methylation type (N6-methyladenine) in the recognition sequence, which is only present in the template DNA molecules obtained from the expression in DH5 α *E. coli*. Therefore by digesting the PCR product with this enzyme, the synthesized molecules during the PCR reaction (Cardosin-B PSI mutated version fused to pCRBlunt vector) are not damaged. The total volume resulting from of Dpn I restriction was used to transform competent DH5 α *E. coli* cells.

RNA extraction

The proceedings to extract RNA from *Arabidopsis* Cardosin B-mCherry transgenic line were according to the “RNeasy® Plant Mini Kit For purification of total RNA from plants and filamentous fungi” (Qiagen) instructions. RNA samples were stored at -80°C.

DNase I is commonly used to treat RNA preparations to degrade trace to moderate amounts of genomic DNA that could otherwise result in false positive signals in subsequent RT-PCR. The RNA samples were then treated with DNase I (Thermo Fisher Scientific Inc.) according to manufacturer instructions.

RT-PCR analysis

The *Arabidopsis* Cardosin B-mCherry transgenic line produced during this work was analysed using the RevertAid™ First Strand cDNA Synthesis Kit (Thermo Fisher Scientific Inc.) to confirm expression of the fusion proteins. The Reverse transcriptase PCR (RT-PCR) was performed according to the kit manufacturer instructions followed by a PCR reaction also according to the RevertAid™ First Strand cDNA Synthesis Kit manufacturer.

In order to confirm the presence of the fusion proteins the cardosin B plant specific insert was amplified by PCR with the primers listed in the table 2-9. In order to validate these primers as suitable for this PCR screening the Primer-Blast® alignment (<http://www.ncbi.nlm.nih.gov/tools/primer-blast/>) was used to compare primer sequences with *Arabidopsis thaliana* genome database.

Table 2-8: Primers used in the PCR reaction for cDNA product from RT-PCR amplification

Primer name	Sequence	Description
PSI B Fwd	TTAAACCAACAATGCAAAACATTGG	Primer designed for the 5' end of Cardosin-B PSI.
PSI B Rev II	TTCTGCACTTGAAGTGGGTA	Primer designed for the 3' end of Cardosin-B PSI.

DNA Gel Electrophoresis

DNA samples were analysed in 0.8-1.0 % (w/v) agarose gel in 1X TAE buffer [40 mM Trizma-base, 10 % (v/v) glacial acetic acid and 10 mM EDTA] and 0.5 µg/mL ethidium bromide added before polymerization. The samples were prepared with 10X loading dye [15 % (w/v) Ficol 400 and 0.25 % (w/v) Bromophenol Blue]. The electrophoretic separation was carried out at 200 V, non-limiting amperage and using 0.25X TAE running buffer. The molecular weight marker used was the “GeneRuler DNA Ladder Mix” (Fermentas). The DNA was visualized by ethidium bromide fluorescence in a UV light box (302-365 nm) and the images captured in an Alpha Innotech - “Alpha imager mini” (Biorad).

DNA extraction and purification from agarose gel

The bands of interest were rapidly cut from the agarose gel in order to reduce UV light exposure damages. The DNA was extracted with the GenElute™ Gel Extraction Kit (Sigma, Spain) according to the producer instructions.

Ligation of DNA fragments

Gateway® pENTR4™ Dual Selection Vector cloning

The ligation of DNA fragments obtained by PCR was performed using a pENTR4® vector digested previously with Hinc II (Fermentas) to produce blunt ends and dephosphorylated to allow the ligation of phosphorylated PCR products according to the pENTR4® manufacture instructions. The ligation reaction into pENTR4® was performed according to the manufacture instructions (Invitrogen™) for blunt cloning of PCR products.

Zero Blunt® PCR Cloning

The ligation of DNA fragments obtained by PCR was performed with a commercial kit for cloning of blunt-ended PCR products - “Zero Blunt® PCR Cloning Kit” (Invitrogen™) according to the producer instructions in 1.5 mL sterile microtubes tubes for an 1h, at room temperature.

pFAST-G02 Gateway® cloning

A positive pENTR clone with Cardosin B-mEos-C-terminal insert in the correct orientation was used in the recombination reaction with pFast-G02 (Shimada *et al.*, 2010) according to “Gateway®LR Clonase™II Enzyme Mix” manufacture (Invitrogen™). TOP10 *E.coli* cells were transformed with the ligation product.

pMDC83 and pVKH18-En6 cloning

The pMDC83 (Curtis *et al.*, 2003) vector was digested with Xba I and Sac I restriction enzymes in order to excise the recombination cassette and the GFP6his-tagged. The digestion product was separated in agarose gel electrophoresis and the band corresponding to the vector without the recombinant cassette was recovered and purified. The ligation of fragments excised from pENTR positive clones was performed according to the table 2-10, overnight at room temperature.

For pVKH18-En6 (Batoko *et al.*, 2000) constructions, the reaction was prepared according to table 2-10. The reaction occurred overnight, at room temperature.

Table 2-9: Cloning reaction into pMDC83 and pVKH18-En6 binary expression vectors

Reagents	Concentration
vector	1 μ L
Insertion fragment	2.5 μ L
10 X T4 DNA ligase buffer	1 μ L
T4 DNA ligase	1 μ L
Sterile water	To a total volume of 10 μ L

Bacterial Strains and growing conditions

In order to achieve multiple copies of a gene of interest or to obtain expression in plant cells several bacterial strains were used: *Escherichia coli*, strains DH5 α , TOP10 and DB 3.1 and *Agrobacterium tumefaciens*, strain GV3101::pMP90. The bacteria were grown in Luria Bertani medium (LB) [10 g tryptone, 5 g yeast extract, 10 g NaCl to 1 L of medium; to obtain a solid medium 1.5 % (w/v) microagar was added (LB-Agar)] at 37 °C for *E.coli* and 28 °C for *A. tumefaciens*, under orbital agitation for liquid cultures. The LB medium was supplemented with 50 μ g/mL of antibiotic for selection of plasmid containing the gene of interest and *Agrobacterium* was also selected for helper plasmid resistance with 20 μ g/mL gentamycin. The antibiotics used for selection of transformed cells are listed in the table 2-11 according to the plasmid vector.

Table 2-10: Selectable markers for the plasmid vectors used to transform bacteria during this work.

Plasmid Vector	Selectable marker 50 µg/mL
pENTR4*	Kanamycin
pCRBlunt*	Kanamycin
pVKH18-En6	Kanamycin
pFAST-G02	Spectinomycin
pMDC83	Kanamycin

Preparation of “High efficiency” *Escherichia coli* Competent Cells

In order to obtain chemically competent cells 50 µL of competent DH5α cells were inoculated in 25 mL of Luria Bertani (LB) medium [10 g of triptone, 5 g of yeast extract, 10 g of NaCl, to a final volume of 1 L] and the culture placed at 37 °C with orbital shaking (150 rpm). Bacteria were allowed to grow overnight and the pre-culture was added to 225 mL of LB medium supplemented with sterile 0.4 M MgCl₂ and 0.4 M MgSO₄, and was allowed to grow under the same conditions, until the optical density (OD) at 600 nm ranges 0.7. The culture was then placed on ice for 10 minutes, after that aliquots of 25 mL were centrifuged in 50mL tubes and centrifuged at 800 xg for 5 minutes at 6 °C. The supernatant was discarded and the pellet resuspended in 100 mL of RF1 [100 mM RbCl, 30 mM CaCl₂ and 15 % glycerol (v/v), pH 5.8, 50 mM KAc]; the cell suspension was incubated on ice for 15 min. The cell suspension was centrifuged at 800 xg for 5 minutes and the supernatant was removed. The pellet was resuspended in 16 mL of RF2 (1 mM RbCl, 223 mM CaCl₂, 10 mM MOPS and 1.5 % (v/v) glycerol, pH 8.0) and divided into aliquots of 100 µL. The cells were preserved in aliquots at -80°C.

Transformation of competent *Escherichia coli*

A 50 µL aliquot of competent cells was thawed on ice. The cells were added to the ligation product (or appropriate volume of plasmid DNA) and incubated for 30 minutes on ice. A heat shock was performed by incubation at 42 °C for 90 seconds followed by 1 minute on ice. 300 µL of LB medium was added and the cells were incubated at 37 °C in a GFL-shaking incubator (180

RPM), for 30 minutes to allow recovery. The cells were centrifuged at 775 xg for 2 minutes. 300 μ L of the supernatant was removed and the pellet resuspended in the remaining volume. The cells were plated in LB-agar medium with selective antibiotics.

Plasmid DNA extraction (miniprep)

A new culture from a stock aliquot or from a single colony was initiated the day before the extraction. 1.5 mL of that culture was transferred to a sterile eppendorf tube and centrifuged at maximum speed for 30 seconds. The supernatant was discarded and the pellet was resuspended in 200 μ L of Sucrose-Tris-EDTA-Triton (STET) buffer [8 % (w/v) sucrose; 0.1 % (v/v) Triton X-100; 50 mM EDTA; 50 mM Tris-HCl, pH 8.0] and 5 μ L of lysozyme (50 mg/ml). The samples were incubated for 5 minutes at room temperature. The samples were boiled for 45 seconds for inactivation of DNases and lysozyme and centrifuged was performed for 5 minutes at maximum speed. The pellet was removed with a sterile toothpick and 200 μ L of 2-propanol was added to the tube for DNA precipitation. The samples were homogenized by vortexing, followed by a 10 minutes spin. The supernatant was removed and the pellet was washed with 70 % (v/v) ethanol. The pellet was air-dried, at room temperature. The DNA was resuspended in 20 μ L of sterile water with RNase (10 μ g/ml) and stored at -20 °C.

Pure plasmid DNA extraction

Extraction of plasmid DNA to be used in DNA sequencing and *A. tumefaciens* transformation was performed after an overnight growth of the *E. coli* containing the plasmid DNA of interest and using the GenElute™ Miniprep Kit (Sigma, Spain) according to the manufacturer's instructions except for the final elution that was made in 30 μ L sterile water.

Plasmid DNA digestion

The Plasmid DNA digestion whether for cloning in an expression vector or screening after cloning, was realized according to the manufacturer of the restriction enzymes (Fermentas).

Preparation of Electrocompetent *A. tumefaciens* Cells

An aliquot of *A. tumefaciens* GV3101 electrocompetent cells was inoculated in 10 mL of LB medium and the culture placed at 28 °C with orbital shaking. After saturation, the pre-culture was added to 200 mL of LB medium and returned to the same growing conditions until the optical density at 600 nm corresponds to an absorbance between 0.5 and 0.6. The culture was incubated on ice for 30 minutes and the volume was separated in 50 mL tubes. The tubes were

centrifuged for 10 minutes at 1800 xg and the supernatant discarded. The pellet was resuspended in 25 mL of 1 mM HEPES buffer, cooled in ice and the cultures were centrifuged once more and the pellet resuspended in 25 mL of 1 mM HEPES buffer. The cells were recovered by centrifugation and the pellet was resuspended in 20 mL of 1 mM HEPES buffer supplemented with 10 % (v/v) glycerol. The final centrifugation was performed similar to the previous ones and the pellet was resuspended in 0.5 mL of 1 mM HEPES buffer with 10 % (v/v) glycerol and aliquoted in 50 µL per tube. The cells were stored at -80 °C.

Transformation of *A. tumefaciens* by Electroporation

Electrocompetent *Agrobacterium* GV3101 were thawed on ice and the electroporation cuvette [0,2 cm aperture, Sigma-Spain, washed with 1% (w/v) SDS, water and 70 % (w/v) ethanol] was pre-cooled on ice. 10 µL of pure plasmid DNA were added to the cells and the mixture was carefully transferred to the bottom of the cuvette. The Biorad Micropulser was set to “Agr” mode. The cuvette was placed in the chamber slide. After the pulse, 1 mL of LB medium was immediately added to the cuvette. This mixture was incubated for 4h without shaking at 28 °C (Shel Lab-shaking incubator) for recovery of the cells. The cells were centrifuged for 4 minutes at 1300 xg. 900 µL supernatant were discarded and the pellet was resuspended and plated in LB-agar supplemented with antibiotics. The plates were incubated for 48h at 28 °C.

Plasmid DNA extraction (miniprep) of *A. tumefaciens*

A spin was made using 1.5 mL of overnight culture at maximum speed for 30 seconds. The supernatant was discarded and the pellet was resuspended in 200 µL of sterile Solution I [50 mM glucose, 25 mM Tris, 10 mM EDTA] and 2 µL of lysozyme (50 mg/mL). The reaction occurred on ice for 10 minutes. 400 µL of lysis solution [0.2 M NaOH, 1 % SDS] was added and mixed gently. This mixture was left on ice for 10 minutes. 300 µL of sterile neutralization solution [3 M Kac pH 4.8] was added and the tube was inverted carefully to mix. This mixture was left on ice for 10 minutes. A spin was done at 10°C for 20 minutes and the supernatant transferred to a new tube. 0.7 vol isopropanol was added. A spin was performed at 10 °C for 30 minutes. The pellet was washed with 70 % (v/v) ethanol. The pellet was left to dry and resuspended in 20 µL sterile water. The DNA obtained was used to transform *E. coli* cells to obtain plasmid DNA, with the method described above, that can be used for restriction enzymes screening.

2.5 Biological material - maintenance and transformation

2.5.1 *Arabidopsis thaliana* system

In order to test the efficiency of the cloning and the functionality of the fusions in *Arabidopsis* system, a transient expression protocol was optimized for cardosins constructs based on an *Agrobacterium* vacuum infiltration method, described by Marion and co-workers (2008). After expression in *Arabidopsis* transient system the chimeric proteins were used to produce stable transgenic lines for each construct in order to obtain a constitutive expression system.

Germination and Maintenance of *A. thaliana*

A. thaliana seeds ecotype Col-0 were sterilized in 70 % (v/v) ethanol for 5 minutes under agitation and left to dry onto a filter paper in the flow hood. Seeds were transferred to Murashige and Skoog® (MS) medium (Duchefa Biochemie™) supplemented with 1.5 % (w/v) sucrose and 0.7 % (w/v) Bacto-agar and stratified for 2 days at 4 °C (Fig. 2.6).

For the transient transformation, Young Columbia (Col 0) sterile *Arabidopsis* seeds were placed on Murashige and Skoog® (MS) agar medium in six-well culture plates (Orange Scientific) and stratified for 2 days at 4° C. Seedlings were allowed to grow for 4 days (21 °C temperature, 60 % humidity, 24 h daylight) prior to infiltration.

To obtain transgenic *Arabidopsis* stable lines expressing mEos/mCherry fusions after stratification, seeds were incubated in the same growth conditions as above for 12-15 days and then transferred to individual pots with fertilized substrate (SiroPlant) and maintained in a growth chamber with the same conditions till flowering stage. The main floral stem was cut relieving apical dominance and encouraging synchronized emergence of multiple secondary bolts.

Transgenic lines were screened by RT-PCR technique (as described previously in this chapter) using RNA extracted from seedlings. The seedlings were germinated in liquid MS medium (fig. 2.6) supplemented with 1.5 % (w/v) sucrose during 5 days at room temperature, with gentle agitation and continuous light.



Figure 2.6.: Arabidopsis germination in liquid MS medium for RNA extraction.

Transient transformation of *Arabidopsis thaliana*

Agrobacterium tumefaciens cells transformed with the various constructs were grown overnight in 5 ml pre-culture and used to inoculate a 30 ml culture (LB liquid medium). After overnight growth at 28 °C, *A. tumefaciens* cells were centrifuged at 1537 xg and resuspended at the appropriate OD₆₀₀ in 2 ml of MS liquid medium. A 1/20 dilution of the cell suspension was made and the absorbance read at 600 nm. The infiltration solution was diluted in 4 mL of MS liquid medium supplemented with 200 μM acetosyringone to the final concentration OD₆₀₀= 2. Infiltration was performed by submerge the seedlings in the *Agrobacterium* solution and by applying vacuum (-70 KPa) twice for 1 min (figure 2.7). The remaining infiltration medium was subsequently removed and the plates were transferred to a culture room for 3 days (same growth conditions prior to infiltration).

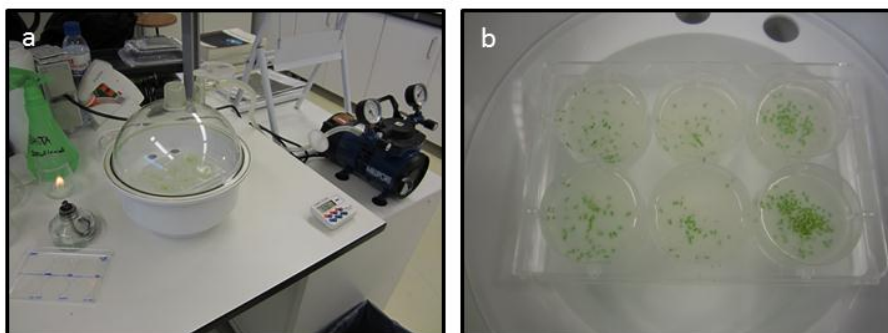


Figure 2.7.: Arabidopsis seedlings infiltration protocol illustration. a. Vacuum infiltration apparatus, b. detail of *Arabidopsis* 6-well plate during infiltration process.

Stable expression in *Arabidopsis*

Floral-dip method

Two days prior to *Arabidopsis* dipping an *Agrobacterium* pre-culture was started in 5 mL of LB (Luria Bertani medium) and allowed to grow for 18 hours. All the cultures were initiated with a 1:100 dilution of a pre-culture in the day before infiltration and grown for 18 hours. The cultures were centrifuged for 15 minutes at 1537 xg at room temperature. The supernatant was removed and the cells were resuspended in floral dip inoculation medium [5.0 % (w/v) sucrose, 0.05 % (v/v) Tween-20 to a final 250 mL volume of water]. The floral dip medium was added to a beaker and the plants were inverted into this suspension (Figure 2.8 c). A minimum of three robust plants without siliques (Figure 2.8 a and b) were used per transformation. The plants were submerged two times for 2 minutes each with gentle agitation (Figure 2.8 c). Plants were removed from the beaker and placed in a plastic tray and covered with a clear-plastic to maintain humidity (Figure 2.8 d). Plants return to greenhouse and plastic cover was removed 12-24 hours after dipping. Plants were grown until siliques were brown and dry. The pots from each construct were separated from the neighbouring pots. The seeds were recovered carefully placing the siliques into paper bags that were collected when plants were completely dry. The seeds were separated using a sieve and were stored at room temperature.



Figure 2.8.: Floral dip method proceedings. a. Flowering *Arabidopsis* plants used for floral dip transformation, b. *Arabidopsis* flower detail, c. *Arabidopsis* dipping with gentle agitation and d. covered plants for humidity maintenance after floral dip.

Selection of transgenic plants

Transgenic seeds were germinated and grown in soil. Seeds were spread in trays containing Siroplant® substrate, covered with transparent plastic lids and placed in a greenhouse under the same conditions of the wild-type seeds germination. Breather holes in the container were opened as the seeds started germinating to prevent excessive of humidity. When first true leaves start to emerge, BASTA® diluted in water (60 mg/L) was sprayed once every 3 days until most of the germinated seedlings are dying (yellowing of cotyledons, drying). A few plants stayed green and were transferred to large pots with SiroPlant® substrate.

2.5.2 *Nicotiana tabacum* system

Nicotiana tabacum leaves were used for glycosylation mutants expression analysis. Leaf epidermis of one month old plants was *Agrobacterium* infiltrated using a syringe-pressure mediated transient transformation.

Germination and Maintenance of *N. tabacum*

Seeds of *N. tabacum* cv. SRI Petit Havana were germinated in petri dishes on filter paper, moistened with water in a Sanyo Growth Cabinet – Model “MLR-350H”. After germination, seedlings were transferred to individual pots with fertilized substrate (SiroPlant®) and maintained in a growth chamber with continuous light, 60% humidity and 21° C and capped with cling film for acclimation. At the end of the first week, cling film was eliminated.

***Agrobacterium*-mediated infiltration of *N. tabacum* Leaves**

One mL of a fresh culture of *A. tumefaciens* transformed with the construct of interest was transferred to a 1.5 mL tube and centrifuged at 16000 xg for 1 minute. The pellet obtained was resuspended in 1 mL of infiltration buffer (10 mM MgCl₂ and 10 mM MES) and again centrifuged at 16000 xg for 1 minute. The pellet was resuspended in 1 mL of infiltration buffer, supplemented with 100 mM of acetosyringone (3', 5'-dimethoxy-4'-hidroxiacetofona to 97%, Sigma-Aldrich), which contributes to increase the virulence *A. tumefaciens*. The samples were centrifuged at 16000 xg for 1 minute and the supernatant resuspended in 1 mL of infiltration buffer with 100 mM acetosyringone. A 1/5 dilution of the cell suspension was made and the absorbance read at 600 nm. Then the infiltration mixture was prepared according to the following equation: (desired OD600 / dilution OD600) x 1000 = required volume (µL) of the dilution to prepare 1 mL of infiltration mixture. Using a 1 mL capacity syringe, without needle, a tobacco

leaf was infiltrated, controlling the pressure applied with the syringe on the lower epidermis (Fig. 2.9) until the liquid enters through the stomata and infiltrates in the intercellular spaces. The plants were placed in the same growth conditions during the time of the assay.



Figure 2.9. Tobacco leaf infiltration with a needleless syringe. a. *Nicotiana tabacum* plants used for infiltration and b. Infiltration proceedings.

Dominant Negative Mutants Assay

Sar I H74L (Andreeva *et al.*, 2000) dominant-negative mutant was used to affect ER-to-Golgi pathway in glycosylation mutants expression analyses in *Nicotiana tabacum*. The *Agrobacterium* containing the Sar I H74L dominant-negative mutant was co-infiltrated with the construct to be tested. The final optical density used for Sar I H74L dominant-negative mutant infiltration was 0.015. Three days after infiltration a sample was taken from the infiltrated leaf and cells were imaged using CLSM.

2.6 Confocal laser scanning microscopy

Preparation of sections

Three days after infiltration the *Arabidopsis* cotyledons were excised from the seedlings and placed on the top of a drop of water in a slide with the abaxial face upwards. The fresh material was covered with a cover slide.

Transgenic *Arabidopsis* plants were collected at different stages of development and mounted for observation in water under glass coverslips.

Small portions (about 1 cm²) of the tobacco leaf infiltrated area were cut and placed in a glass slide with abaxial face upwards. A drop of water and a coverslip were placed on top of the leaf. All

the samples were imaged in a Leica confocal microscope TCS SP2 (Leica Microsystems, Germany). The acquisition and imaging processing were obtained with the *Leica Confocal software* (Leica Microsystems, Germany).

Imaging and Photoconversion

Imaging of green mEos was performed using 488 nm laser excitation, and fluorescence emission was detected between 499 nm and 544 nm for non-converted FP. Red mEos and mCherry emission was detected at between 595 nm and 647 nm using a 561 nm laser for excitation. Transmission images were taken simultaneously in Nomarski mode Differential interference contrast (DIC). Routinely, dual-colour imaging was run with fast simultaneous scanning. The objective selected in all the experiments was the HCX PL APO CS 40.0x1.25 OIL UV.

Photoconversion of mEos occurred upon exposure to UV-violet light with a 405 nm laser pulse. To prevent the conversion of mEos by environment light, the preparations were kept in the dark.

3 Results

3.1 Validation of cardosins expression in *Arabidopsis* cotyledons

Cardosin A and B have different accumulation patterns in the native system according to the organ and stage of development (Pereira *et al.*, 2008; Oliveira *et al.* 2010). Recently, several studies focusing cardosins biogenesis and sorting pathways have been conducted in *Nicotiana tabacum* epidermal cells (Duarte *et al.*, 2008; Soares da Costa *et al.*, 2010; Pereira *et al.*, 2013). However, regardless of the great achievements accomplished in this system, it is necessary to study cardosins expression in other types of tissues and also during development, and *Arabidopsis thaliana* is a great choice for this task, due to the impossibility of using *Agrobacterium*-mediated transformation in the native system. The first goal of this work was, therefore, to validate the system for expression of cardosins constructs already available in the lab and already tested in *Nicotiana tabacum*. A transient system in *Arabidopsis* would also allow testing the constructs obtained in this work.

A method for transient transformation of *Arabidopsis* had already been described (Marion *et al.*, 2008) and was adjusted to our experimental purposes regarding the setup of the transformation protocol and the confocal microscopy analysis. In this part of the work, constructs already available in the laboratory were used to transform *Arabidopsis* plantlets through *Agrobacterium*-vacuum infiltration. The transgene cloned into pFAST-G02 (Shimada *et al.*, 2009) was under the control of different regulatory sequences, including the 35S promoter of cauliflower mosaic virus (CaMV). The cotyledons of *Arabidopsis* were analysed under a confocal microscope three days after vacuum infiltration. The blue-coloured channel was used to isolate chlorophyll autofluorescence and to confirm that the fluorescence observed in red channel was due to the mCherry fluorescence and not from vacuolar autofluorescence that can also be originated from stressed cells.

3.1.1 Cardosin A and B accumulate in the vacuole

Cardosin A and B fused to mCherry fluorescent protein were available in our laboratory cloned into pVKH18-En6 (Batoko *et al.*, 2000). Since this plasmid is optimized for maximum expression in tobacco cells, prior to this work the chimeric protein sequence was subcloned into pFAST-G02, a vector suitable for expression in *A. thaliana*. The pVKH18-En6 fusion has been

already used and tested in *Nicotiana tabacum* and the results showed a vacuolar accumulation of both proteins (Soares da Costa *et al.*, 2010; Pereira *et al.*, 2013). *Agrobacterium tumefaciens* transformed with pFAST-cardosin A/B-mCherry constructs was used for transient expression in *Arabidopsis thaliana* seedlings mediated by vacuum infiltration. Three days post-infiltration, the cotyledons were imaged for mCherry fluorescence detection.

In the observations of cardosins A/B-mCherry fusions mCherry fluorescence was detected in the large vacuole that occupies almost the entire epidermal cell (fig. 3.1 and 3.2) that has a typical “puzzle”-shape. It was not observed fluorescence in the early compartments of the secretory pathway that are pushed to the cell periphery due to the space occupied by the large vacuole. In the images obtained we were able to distinguish the limits of the cell without mCherry fluorescence which means that the protein fusion was not target to the cell wall or the extracellular space (fig. 3.1 and 3.2). It is worth to note that autofluorescence (fig. 3.1 and 3.2 b, f) does not correspond with the fluorescence observed in the vacuole and only with the chloroplasts (fig. 3.1 and 3.2 d, h).

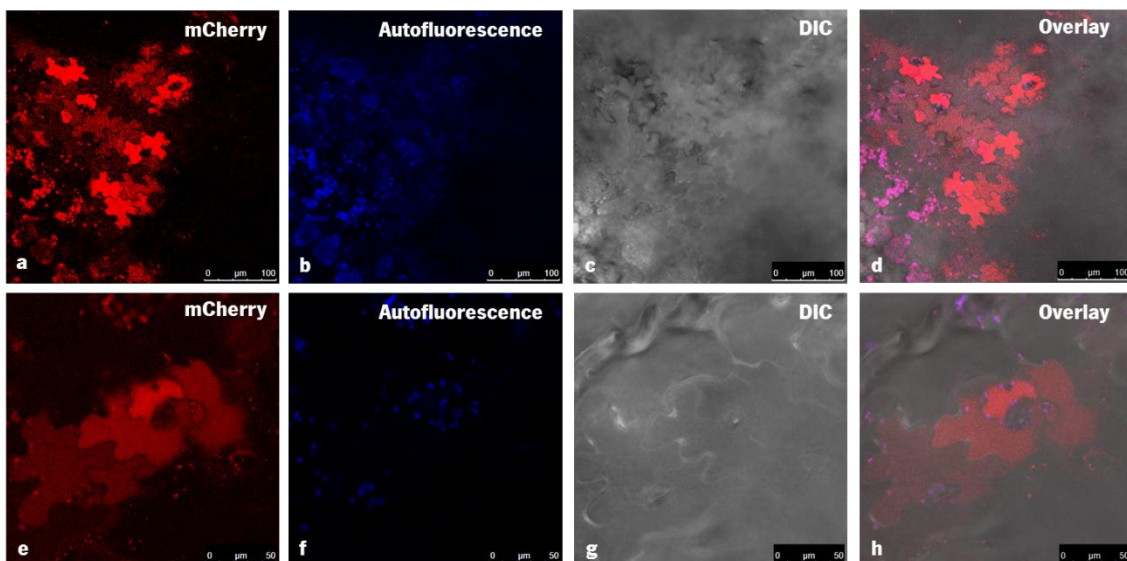


Figure 3.1. Subcellular localisation of pFAST-Cardosin A-mCherry in *Arabidopsis* cotyledon epidermal cells. mCherry fluorescence was observed in the vacuole 3 days post-vacuum infiltration using 561 nm laser-line for excitation. (a, e) red channel for mCherry fluorescence detection; (b, f) autofluorescence (in blue); (c, g) Differential interference contrast (DIC); (d, h) Overlay of red channel, autofluorescence (in blue) and DIC. Scale bars: a, b, c, d: 100 μm ; e, f, g, h: 50 μm .

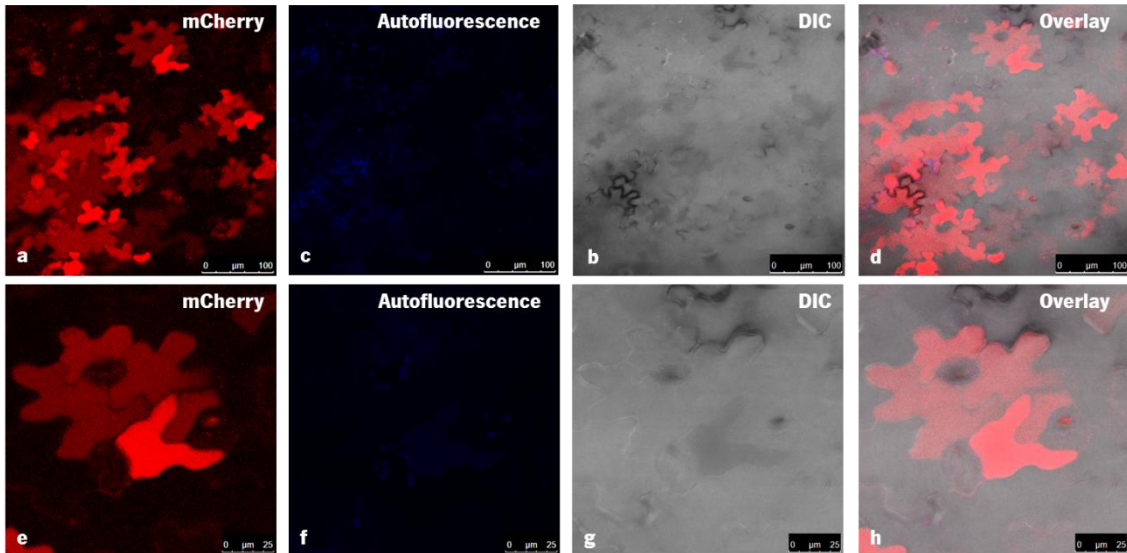


Figure 3.2.: Subcellular localisation of pFAST-Cardosin B-mCherry in *Arabidopsis* cotyledon epidermal cells. mCherry fluorescence was observed in the vacuole 3 days post-vacuum infiltration using 561 nm laser-line for excitation. (a, e) red channel for mCherry fluorescence detection; (b, f) autofluorescence (in blue); (c, g) Differential interference contrast (DIC); (d, h) Overlay of red channel, autofluorescence (in blue) and DIC. Scale bars: a, b, c, d: 100 μm ; e, f, g, h: 25 μm .

In *Arabidopsis* transient system 3 days after infiltration fluorescence of mCherry tagging cardosins was totally observed in the vacuole. **mCherry was detected in the vacuole of cotyledon epidermal cells in a pattern very similar to that observed in *N. tabacum*.**

3.1.2 Cardosin A truncated versions

In order to understand the function and the importance in cardosins trafficking of its vacuolar sorting domains, the C-terminal and the plant-specific insert, two mutated versions were engineered and fused to mCherry in our lab (Pereira *et al.*, 2013). The mutated sequences fused to mCherry - Cardosin A without C-terminal (Cardosin A Δ C-terminal-mCh) and cardosin A without PSI domain (Cardosin A Δ PSI-mCh-C-terminal) - were also subcloned into pFAST-G02, for the reasons explained above and infiltrated in *Arabidopsis* seedlings.

In the *Arabidopsis* cotyledon cells the protein fusions could reach the vacuole only with one of the two vacuolar sorting domains, as already observed in *N. tabacum* (Pereira *et al.*, 2013), in other words, in the absence of the C-terminal domain or the PSI the protein fusion still reaches the vacuole. Similar to what was observed for non-mutated version of cardosins, mCherry fluorescence was observed in the lytic vacuole (fig. 3.3 and 3.4) occupying a substantial part of the epidermal cells. The deletion of one VSD did not interfere with the proper sorting of the protein to the vacuole. Furthermore, we did not observe any delay or retention of the protein

fusion in the protein quality control compartments such as the endoplasmic reticulum or any dot shaped early compartments. The protein fusions were not detected in the apoplast or the cell wall that corresponds to a non-fluorescent black colour in the red channel for mCherry detection (fig. 3.3 and 3.4 a, e).

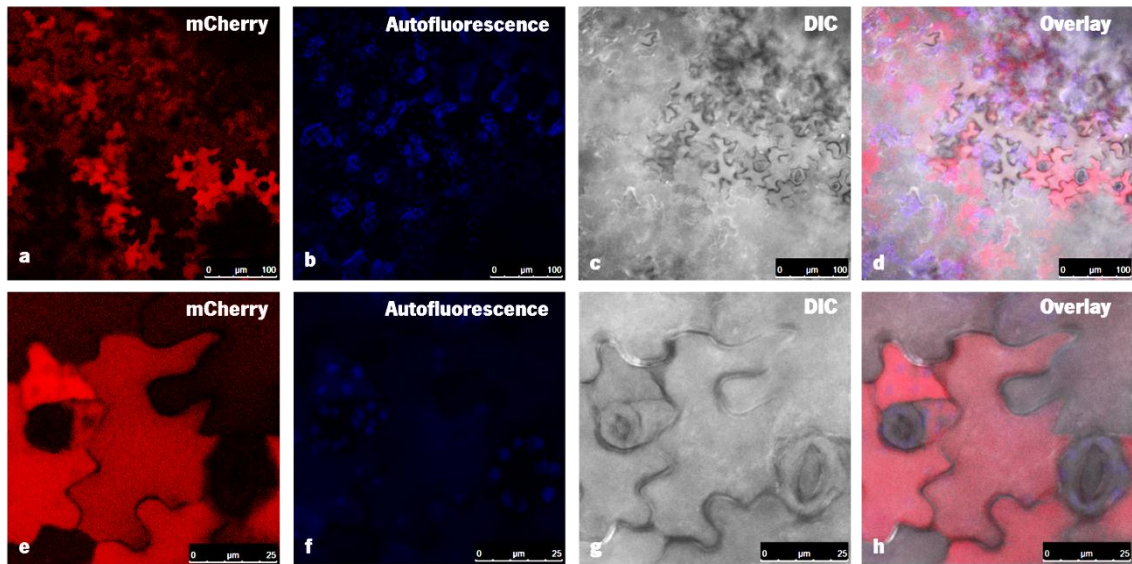


Figure 3.3.: Subcellular localisation of pFAST-Cardosin A Δ C-ter-mCherry (C-terminal domain deletion) in *Arabidopsis* cotyledon epidermal cells. mCherry fluorescence was observed in the vacuole 3 days post-vacuum infiltration using 561 nm laser-line for excitation. (a, e) red channel for mCherry fluorescence detection; (b, f) autofluorescence (in blue); (c, g) Differential interference contrast (DIC); (d, h) Overlay of red channel, autofluorescence (in blue) and DIC. Scale bars: a, b, c, d: 100 μ m; e, f, g, h: 25 μ m.

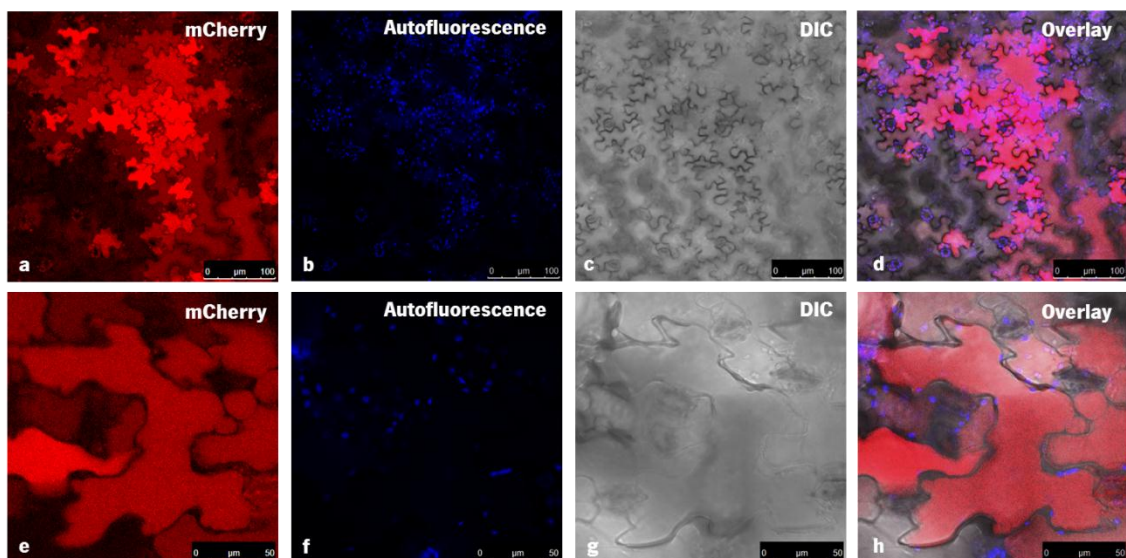


Figure 3.4.: Subcellular localisation of pFAST-Cardosin A Δ PSI-mCherry-C-terminal (Plant-specific insert deletion) in *Arabidopsis* cotyledon epidermal cells. mCherry fluorescence was observed in the vacuole 3 days post-vacuum infiltration using 561 nm laser-line for excitation. (a, e) red channel for mCherry fluorescence detection; (b, f) autofluorescence (in blue); (c, g) Differential interference contrast (DIC); (d, h) Overlay of red channel, autofluorescence (in blue) and DIC. Scale bars: a, b, c, d: 100 μ m; e, f, g, h: 50 μ m.

The results obtained showed that the **two VSDs have the same ability of driving the protein to the vacuole in *Arabidopsis thaliana* cotyledon epidermal cells**, since most of the cells imaged presented mCherry fluorescence in the vacuole (fig. 3.3 e 3.4).

3.1.3 Cardosins vacuolar sorting determinants

To validate in *Arabidopsis* that the PSI domain and the C-terminal peptide VGFAEAA from cardosin A were able to target other protein to the vacuole, the functionality of these VSDs was tested independently. Fusions between the PSI or the C-terminal peptide with mCherry were generated using a signal peptide (SP) in the N-terminal of the VSDs, to guarantee they are translocated to the ER and enter the secretory pathway. These fusion proteins were previously prepared and tested in *N. tabacum* cells (Pereira *et al.*, 2013). In this chimeric protein the C-terminal was fused to the C-terminal of mCherry to ensure recognition of the C-terminal by vacuolar receptors. In the case of PSI domain the mCherry protein was fused to the C-terminal of PSI that may be the proper folding of the fusion protein since PSI is an internal signal. In *Arabidopsis* seedlings expressing these chimeric proteins, the fluorescence of mCherry was limited to the vacuole after three days of infiltration (fig. 3.6). The expression protocol was followed as already described.

Both fusions were localised in the central vacuole of the epidermal cells (fig. 3.5 and 3.6). The cardosin-A C-terminal domain and the PSI were capable of sorting the fluorescent protein to the vacuole. mCherry fluorescence was not visualised in any other compartments of the cell namely the typical ER reticular network, cytoplasmic strands or dot-shaped vesicular compartments.

The cardosin-A VSDs independently are sufficient to target a protein like mCherry to the vacuole in the *Arabidopsis* transient expression system.

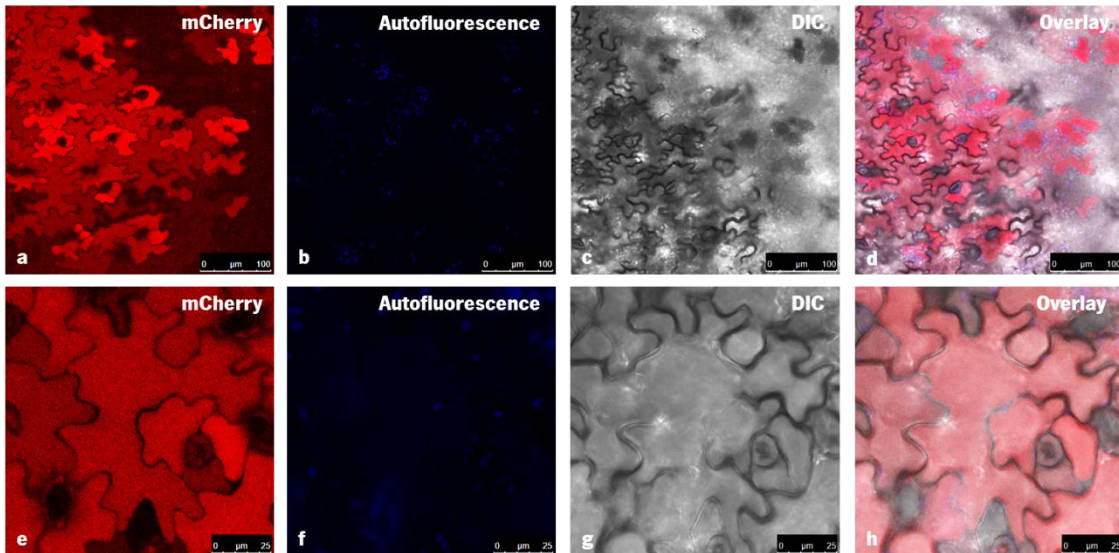


Figure 3.5.: Subcellular localisation of pFAST-SP-mCherry-C-terminal (cardosin-A C-terminal domain) in *Arabidopsis* cotyledon epidermal cells. mCherry fluorescence was observed in the vacuole 3 days post-vacuum infiltration using 561 nm laser-line for excitation. (a, e) red channel for mCherry fluorescence detection; (b, f) autofluorescence (in blue); (c, g) Differential interference contrast (DIC); (d, h) Overlay of red channel, autofluorescence (in blue) and DIC. Scale bars: a, b, c, d: 100 µm; e, f, g, h: 25 µm.

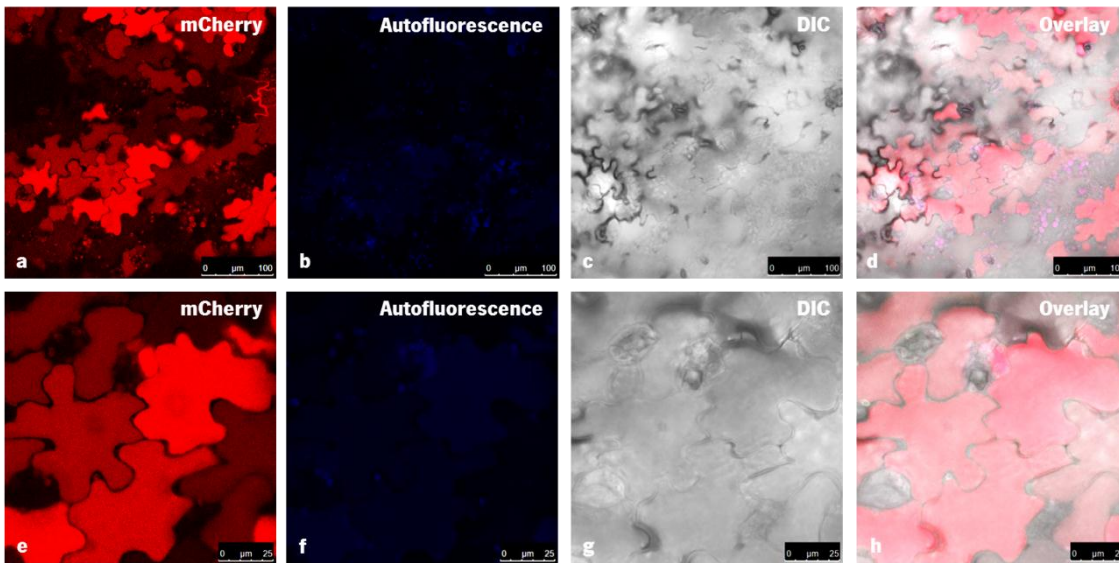


Figure 3.6.: Subcellular localisation of pFAST-SP-PSIA-mCherry (cardosin-A plant-specific insert) in *Arabidopsis* cotyledon epidermal cells. mCherry fluorescence was observed in the vacuole 3 days post-vacuum infiltration using 561 nm laser-line for excitation. (a, e) red channel for mCherry fluorescence detection; (b, f) autofluorescence (in blue); (c, g) Differential interference contrast (DIC); (d, h) Overlay of red channel, autofluorescence (in blue) and DIC. Scale bars: a, b, c, d: 100 µm; e, f, g, h: 25 µm.

Summarizing, this protocol revealed to be an excellent tool to study cardosins expression in heterologous systems as an alternative to *N. tabacum* epidermal cells. The efficiency of transformation with all the constructions was remarkable. It was possible to distinguish several transformed cells with different levels of expression. The tissue autofluorescence isolated in the blue channel was confined to the chloroplasts confirming the unstressed condition of the plants

during the transformation process. We were able to observe mCherry fluorescent protein in the huge vacuoles that exclude the cytoplasmic contents to the periphery in the epidermal cells, a pattern that was already observed in *Nicotiana tabacum*.

The results obtained with this system confirm the advantages and validate the efficiency of the *Arabidopsis* leaf epidermis transformation for studying cardosins sorting and trafficking.

3.1.4. Cardosins vacuolar accumulation in *Arabidopsis thaliana* is a fast process

The analysis of *Arabidopsis* vacuum-infiltrated cotyledons was performed 3 days after infiltration having as reference the observations of cardosins trafficking in *Nicotiana tabacum* (Pereira *et al.*, 2013; Soares da Costa *et al.*, 2010). In the *N. tabacum* leaf epidermal cells mCherry was observed in the vacuole 3 days after infiltration and before that the fusion proteins were still in trafficking to the vacuole. In order to evaluate the trafficking of these fusions in *Arabidopsis* transient system and establish a time-point to perform blocking assays we observe the cells few hours after infiltration.

Twenty-hours after Agroinfiltration all the protein fusions were restricted to the large vacuole and it was not observed fluorescence in the early compartments of the secretory pathway or in transit to the vacuole (fig. 3.7). Therefore, we assume that future blocking assays with drugs like Brefeldin A (BFA) or dominant-negative mutants will have to be applied soon after the infiltration procedure or even at the same time.

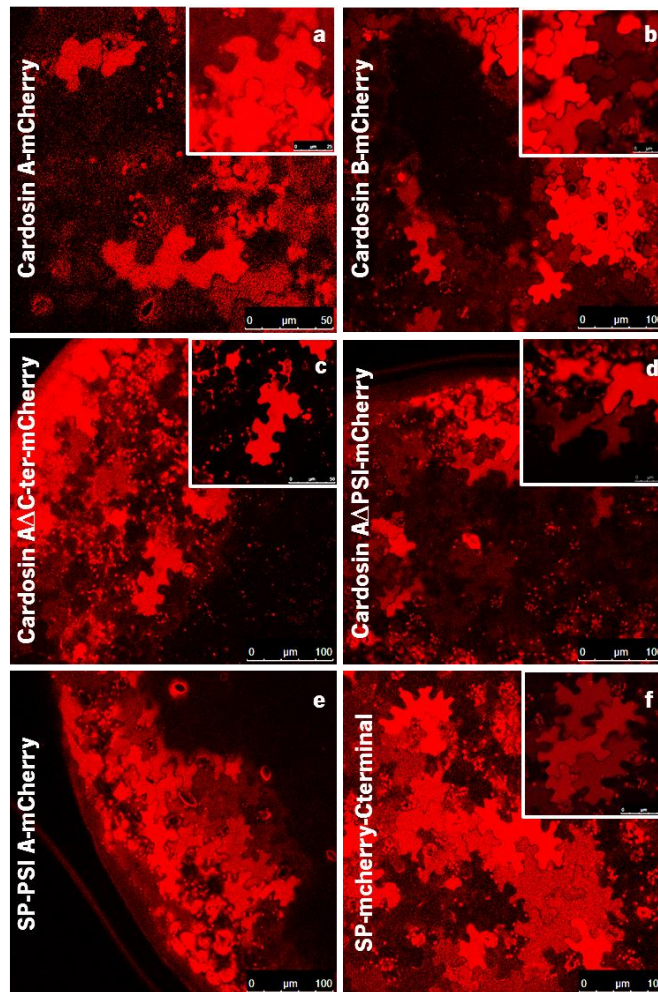


Figure 3.7.: Subcellular localisation of mCherry fusions analysed during this work in *Arabidopsis* cotyledon epidermal cells 20 hours after vacuum-infiltration. mCherry fluorescence was observed in the vacuole 20h post-vacuum infiltration using 561 nm laser-line for excitation. (a) pFAST-cardosin A-mCherry; (b) pFAST-cardosin B-mCherry; (c) pFAST-cardosin AΔC-terminal; (d) pFAST-cardosin AΔPSI-mCherry; (e) pFAST-SP-cardosin-A PSI-mCherry; (f) pFAST-SP-mCherry-Cterminal. Scale bars: (a): 50 μm; (b, c, d, e, f) 100 μm; detail of mCherry fluorescence in the large vacuole of a cell: (c, f) 50; (a, b, d, e) 25 μm.

3.2 Stable expression in *Arabidopsis thaliana*

After the validation of cardosins expression in *Arabidopsis thaliana* transient system we move on to the next goal of this work: obtain stable lines expressing cardosins and its VSDs fused to mCherry, that will allow to analyse them in different tissues and organs and also during development.

The *Agrobacterium* clones tested in *Arabidopsis* transient expression system were used for Floral-dip method (Clough and Bent, 1998). Transformed seeds were collected, germinated and screened until T2 generation when the first signals of mCherry fluorescent were obtained.

3.2.1 PSI A fused to mCherry

Seedlings from the T2 generation were observed under the confocal microscope and mCherry fluorescence was detected in the large vacuole of the cotyledon epidermal cells (fig. 3.8). The pattern observed was very similar to the one observed in the transient expression except for the higher number of cells expressing mCherry (fig. 3.8 a). The mCherry fluorescence was observed in the vacuole of epidermal cells (fig. 3.8 a) and, surprisingly, we did not observe mCherry fluorescence in intermediate compartments such as the ER or Golgi.

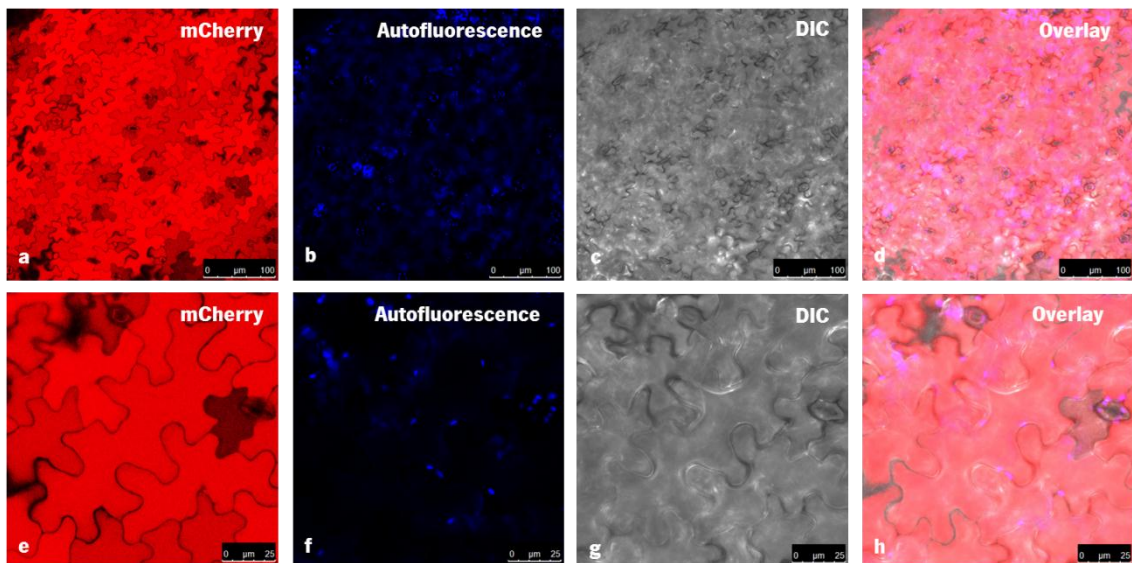


Figure 3.8.: pFAST-Cardosin-A PSI-mCherry (SP-PSIA-mCherry) stable expression in *Arabidopsis thaliana* (T2). mCherry fluorescence was detected in the vacuole of the imaged cotyledon epidermal cells. (a, e) red channel for mCherry fluorescence detection; (b, f) autofluorescence (in blue); (c, g) Differential interference contrast (DIC); (d, h) Overlay of red channel, autofluorescence (in blue) and DIC. Scale bars: a, b, c, d: 100 µm; e, f, g, h: 25 µm.

3.2.2 Cardosin A Δ PSI (deletion of the PSI region) fused to mCherry

Cardosin A with only one vacuolar sorting determinant, the C-terminal domain, was tested in the transient expression and consequently was used for stable transformation protocol. The fluorescence intensity was lower than the one observed for the SP-PSIA-mCherry but it was also observed in the large vacuole of the cotyledon epidermal cells similar to the localisation observed in the transient system (fig.3.9). As observed for the cardosin-A PSI fusion, the mCherry fluorescence was restricted to the vacuole and we did not observe fluorescence in any other compartment besides the vacuole.

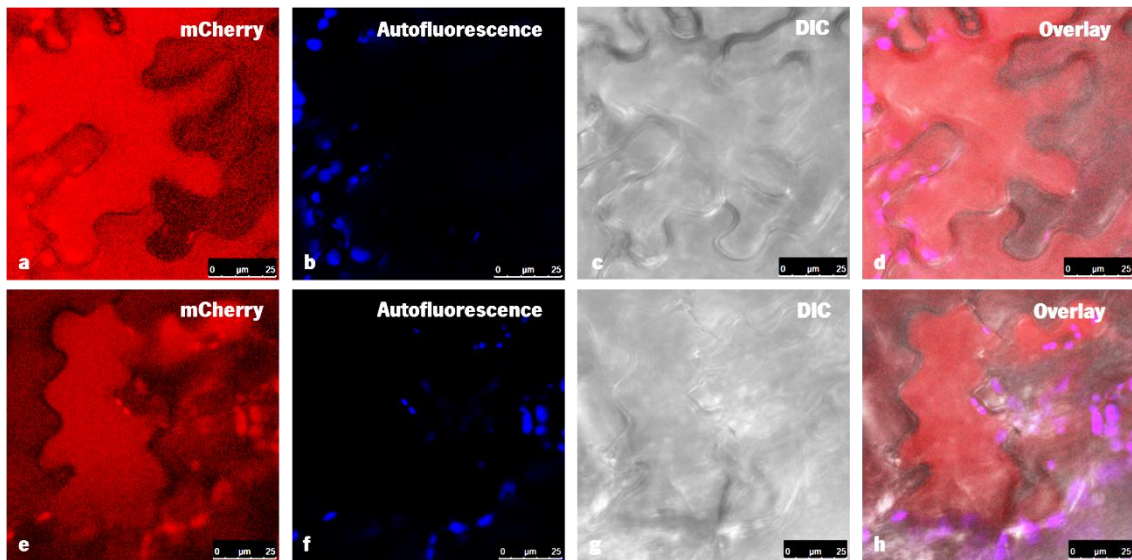


Figure 3.9.: pFAST-Cardosin A Δ PSI-mCherry stable expression in *Arabidopsis thaliana* (T2). mCherry fluorescence was detected in the vacuole of the imaged cotyledon epidermal cells. (a, e) red channel for mCherry fluorescence detection; (b, f) autofluorescence (in blue); (c, g) Differential interference contrast (DIC); (d, h) Overlay of red channel, autofluorescence (in blue) and DIC. Scale bars: a - h: 25 μ m.

3.2.3 Cardosin B-mCherry

Young *Arabidopsis* plants of T2 generation of 3 weeks-old were imaged under a confocal microscope. mCherry fluorescence was detected in the vacuoles of leaf epidermal cells (Fig. 3.10). This vacuolar accumulation of the chimeric protein confirms the success of the stable transformation in *Arabidopsis*. In this preliminary screening we did not observe accumulation of the protein in the other compartments of the secretory pathway.

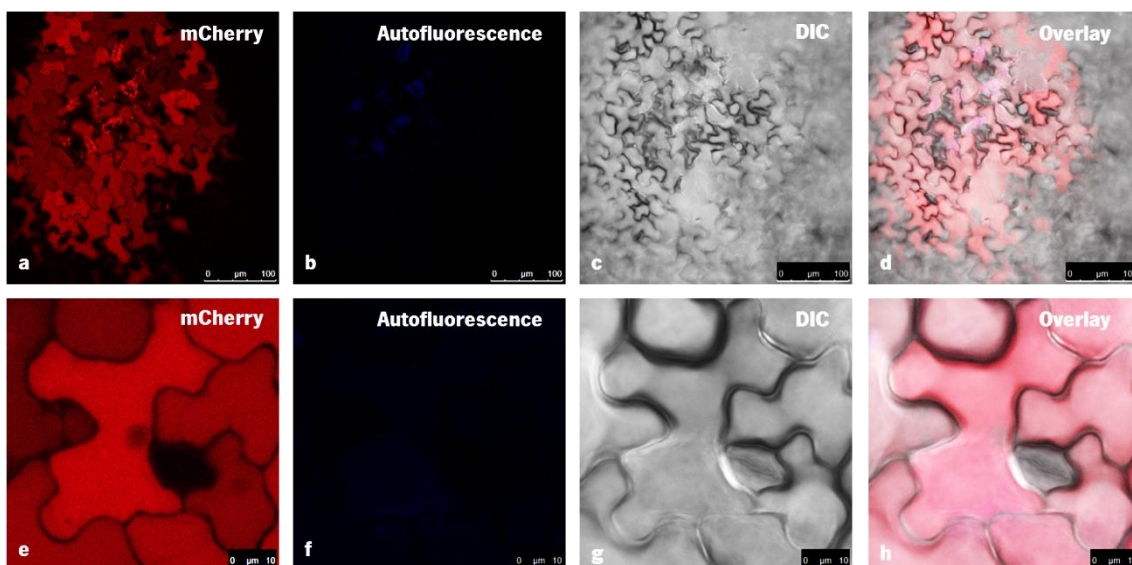


Figure 3.10.: pFAST-Cardosin B-mCherry stable expression in *Arabidopsis thaliana* (T2). mCherry fluorescence was detected in the vacuole of the imaged leaf epidermal cells, using 561 nm laser-line for excitation. (a, e) red channel

for mCherry fluorescence detection; (b, f) autofluorescence (in blue); (c, g) Differential interference contrast (DIC); (d, h) Overlay of red channel, autofluorescence (in blue) and DIC. Scale bars: a - d: 100 μm ; e - h: 25 μm .

RT-PCR from Cardosin B-mCherry stable line

The T2 generation of cardosin B-mCherry *Arabidopsis* stable line was screened for gene expression using reverse transcriptase polymerase chain reaction (RT-PCR). The primers used for reaction would amplify the PSI region of cardosin B. The PCR product was loaded in agarose gel and after electrophoretic separation it was possible to observe a band with approximately 300 bp, corresponding to the plant-specific insert amplification (fig.3.11).

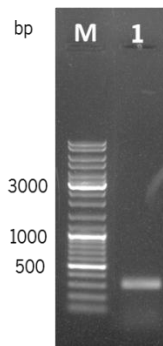


Figure 3.11.: RT-PCR product analysis of cardosin B-mCherry transgenic line (T2).in agarose gel electrophoresis. M- molecular weight marker GeneRuler™ DNA Ladder Mix (Fermentas).

Due to the limited time, only the cardosin B-mCherry line was screened by RT-PCR since it was the first line from which we obtained a positive result in the confocal screening for mCherry detection. Nevertheless, this is preliminary result for cardosin B-mCh line but already give us the indication of the transformation success.

For SP-mCherry-C-terminal the transformation rate was lower so we are currently obtaining the first generations and we soon be able to screen the T2 generation. For the Cardosin A-mCherry and the Cardosin A Δ C-ter-mCherry lines, the mCherry fluorescence was not detected in the T2 generation, probably because the plants are not homozygous yet.

The stable transformation was accomplished for the first lines screened and the mCherry protein was detected in the vacuole of cotyledon and leaf epidermal cells, a localization that was already observed in the transient transformation methods.

3.3 mEos chimeric proteins engineering and imaging

The photoconversion is a great improvement for cardosins studies and will allow to reveal details of protein trafficking so it was another goal for this study to obtain mEos fluorescent fusions of cardosins and the PSIs.

Cardosin A and cardosin B were fused to mEos in previous studies in our laboratory (Vieira, Data). Due to the previous inconclusive results cardosins C-terminal domain was amplified by PCR at the C-terminal of mEos to assure exposure of this domain to vacuolar receptors. The PCR product was loaded in agarose gel, purified after electrophoresis and quantified (Figure 3.12 a). The purified product was used in a ligation reaction with pENTR4[®] followed by *E.coli* transformation. Clones were screened with double digestion reactions and the product of reaction was separated in three bands of 2257, 1547 and 760 bp (Figure 3.12 b and c) by electrophoresis agarose gel.

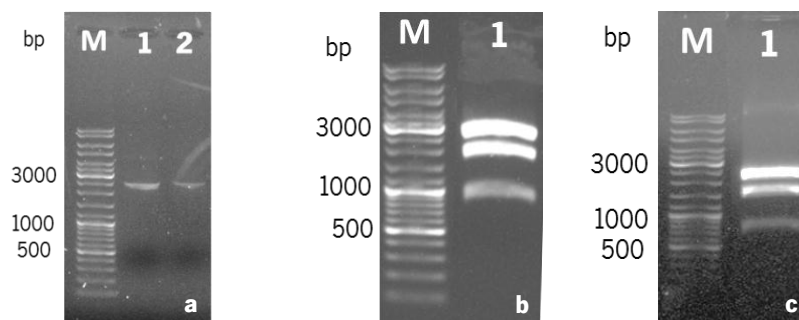


Figure 3.12.: Electrophoretic separation of reaction products. a- Analysis of amplified fragments of Cardosin A-mEos-C-terminal (1) and cardosin B-mEos-C-terminal (2); b and c- positive clones from cardosin A and cardosin B constructs respectively determined by Xba I and Sal I restriction mapping. M- molecular weight marker GeneRuler™ DNA Ladder Mix (Fermentas).

Positive clones were sequenced and after confirmation of correct cloning the insert was excised and used for subcloning into expression vectors. Cardosin A construct was cloned into pMDC83 (Curtis *et al.*, 2003) and cardosin B construct was subcloned into pFAST-G02 (Shimada *et al.*, 2009). Both constructions were screened using restriction enzymes. After electrophoretic separation the positive clones exhibited two bands with approximately 11512 bp and 730 bp (Figure 3.13 a) for cardosin A and for cardosin B a band with molecular weight above 14 Kb and a 730 bp band (Figure 3.13 b).

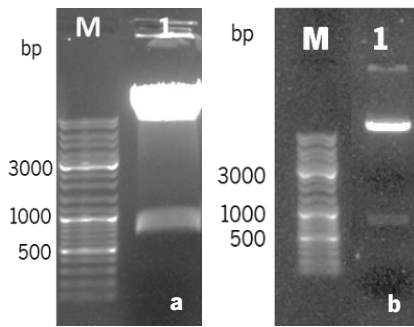


Figure 3.13.: Electrophoretic separation of reaction products. 1- positive clones from - pMDC-Cardosin A-mEos-C-terminal (a) and pFAST-cardosin B-mEos-C-terminal (b); determined by Sal I and Sac I for cardosin A and EcoRI for cardosin B restriction mapping. M- molecular weight marker GeneRuler™ DNA Ladder Mix (Fermentas).

Positive clones of each construction were used for *Agrobacterium* electroporation and after screening the positive *Agrobacteria* were selected for confocal imaging experiments. *Arabidopsis* seedlings were vacuum-infiltrated and three days after infiltration the cotyledons were imaged.

The confocal imaging results of cardosins-mEos fusions were inconclusive. We were unable to detect the mEos fluorescence localization. mEos never reached the vacuole so we assume that the fusions are not functional in cotyledon epidermal cells without further optimization and the results are not showed.

3.3.1 Cardosins PSIs cloning into pMDC and imaging

In order to obtain *Arabidopsis* transgenic plants expressing cardosin-A and -B PSIs, pVKH18-En6 fusions already available in the laboratory were used for subcloning into pMDC83, an optimized vector for expression in *Arabidopsis*.

SP-PSIA-mCherry and mEos were isolated from pVKH18-En6 by restriction digestion. The product of these reactions was loaded onto an agarose gel and the band corresponding to SP-PSIA-mCherry with approximately 1000 bp and the band corresponding to mEos with approximately 700 bp were excised and purified after electrophoretic separation. The purified SP-PSIA-mCh DNA was used for a reaction with pMDC vector already linearized and purified. The ligation was used for *E.coli* transformation and several clones were screened. A positive clone that showed a fragment of 1000 bp (Figure 3.14) after electrophoretic separation was selected for *Agrobacterium* electroporation.

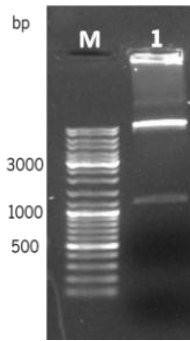


Figure 3.14.: Electrophoretic separation of reaction products. 1- positive clone of pMDC-Cardosin A-PSI-mCherry determined by Xba I and Sac I restriction mapping. M- molecular weight marker GeneRuler™ DNA Ladder Mix (Fermentas).

The DNA extracted from *E. coli* positive clone carrying SP-PSIA-mCh was digested in order to excise mCherry fragment. After agarose gel electrophoresis the band corresponding to pMDC-SP-PSIA was excised from gel and purified. This purified DNA was used in a ligation reaction with the purified mEos DNA already obtained. The ligation product was used for *E. coli* transformation. The colonies were screened and a positive clone with a 9575 bp band and a 1478 bp band after restriction mapping was selected for *Agrobacterium* electroporation. After screening, a positive *Agrobacterium* clone (Figure 3.15.) was vacuum-infiltrated in *Arabidopsis* seedlings.

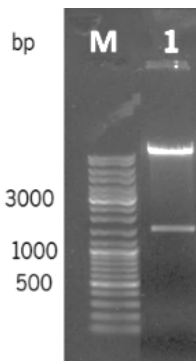


Figure 3.15.: Electrophoretic separation of reaction products. 1- positive clone of pMDC-Cardosin A-PSI-mEos determined by Hind III restriction mapping. M- molecular weight marker GeneRuler™ DNA Ladder Mix (Fermentas).

The pMDC-SP-PSIA-mEos construction was used for engineering a similar construct but encoding for cardosin B PSI. PSIA was excised from pMDC-SP-PSIA-mEos. The fragment of interest with approximately 10000 bp was excised from gel, purified and used in the ligation to obtain pMDC-SP-PSIB-mCherry. PSIB was excised from pCRBlunt-PSIB construct, which was also obtained during this work as described in Chapter 2. The fragment with 700 bp was extracted from gel, purified and used for ligation of fragments. The *E. coli* clones transformed with the ligation product were screened XbaI and PstI to verify the orientation of the insert. The correct

orientation of PSI appeared in the gel as two distinct bands of approximately 400 bp and 757 bp (Fig. 3.16.). A positive clone was selected for *Agrobacterium* electroporation.

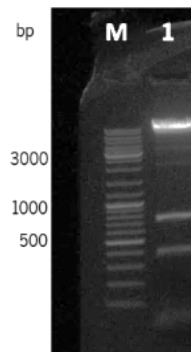


Figure 3.16.: Positive clone of pMDC-SP-PSIB-mCherry determined by Xba I and Pst I restriction mapping. (1). M-molecular weight standard Gene Ruler™ DNA Ladder Mix (Fermentas).

The PSI-mEos fusions were tested in *Arabidopsis* transient transformation and imaged in a confocal microscope. Similar to what happened for cardosins-mEos fusions we couldn't determine the localization of mEos green form (fig.3.17 and fig.3.18). The pattern observed suggests a cytoplasmic accumulation and ER retention suggesting by the perinuclear labelling (fig. 3.18 b, c and d). The mEos protein never reached the vacuole or the fluorescence was not detected in that compartment (fig.3.17 and fig.3.18 b, c, d). Contrary to what happened in previous mEos experiments in our lab, the red form was residually present in the same place as the green form (fig. 3.17 and fig. 3.18 f, g, h). In order to confirm that the fluorescence was due to the mEos expression we activated the 405 laser-line to photoconvert the protein and we examine the fluorescence alterations. In both fusions we observe a slight decrease in the green fluorescence but the photoconverted form was not detected even when we repeated the UV-pulse (fig.3.17 and fig.3.18 g, h).

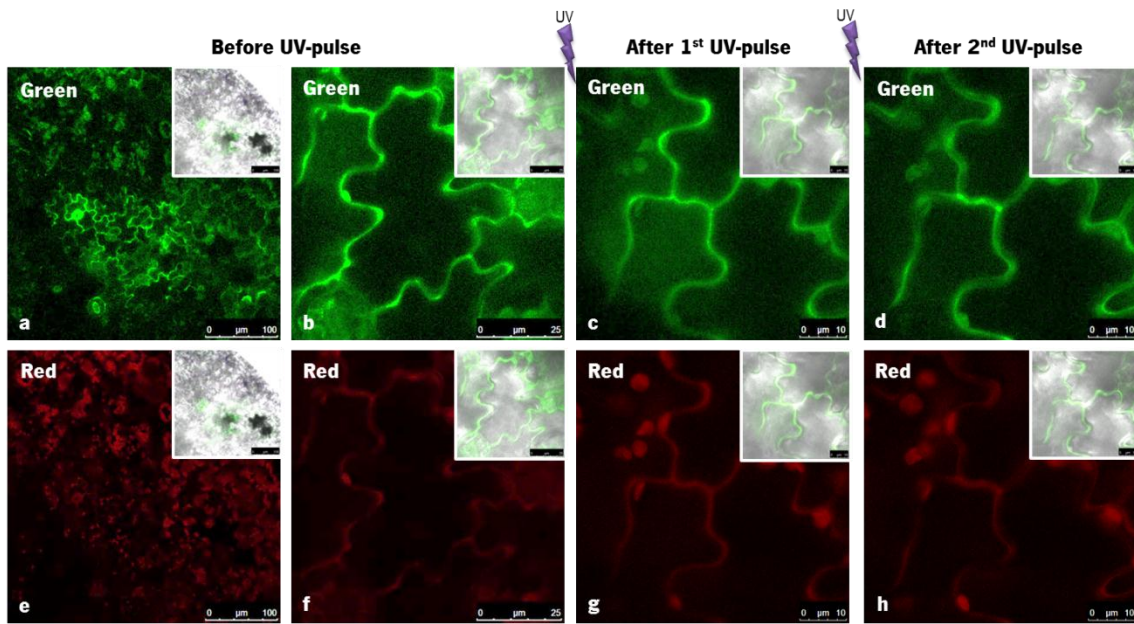


Figure 3.17.: Observation and photoconversion of pMDC-SP-PSIA-mEos. (a - d) green channel; (e - h) red channel. (a, b, e, f) mEos fluorescence before UV pulse; (c, d, g, h) mEos fluorescence after UV pulse. The overlap between green channel, red channel, autofluorescence (in blue) and Differential Interference Contrast (DIC) is shown in all the images. The mEos fluorescence was observed outside the vacuole. After excitation with 405 laser-line the green fluorescence decreased but the mEos red form was not visualized. Scale bars: a, e: 100 μm ; b, f: 25 μm ; c, d, g, h: 10 μm .

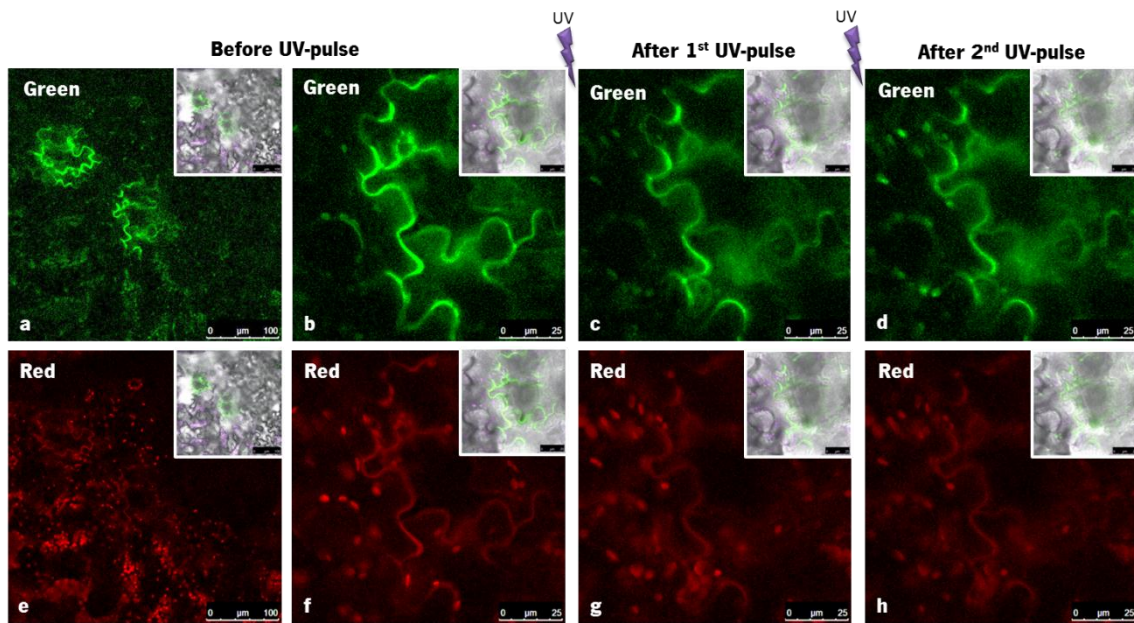


Figure 3.18.: Observation and photoconversion of pMDC-SP-PSIB-mEos. (a - d) green channel; (e - h) red channel. (a, b, e, f) mEos fluorescence before UV pulse; (c, d, g, h) mEos fluorescence after UV pulse. The overlap between green channel, red channel, autofluorescence (in blue) and Differential Interference Contrast (DIC) is shown in all the images. The mEos fluorescence was observed outside the vacuole. After excitation with 405 laser-line the green fluorescence decreased but the mEos red form was not visualized. Scale bars: a, e: 100 μm ; b - h: 25 μm .

The cloning in the vector pMDC83 modified for classical cloning was obtained for the first time with the mEos fusions. Therefore we needed to exclude the hypothesis that the retention observed for mEos fusions was due to the cloning vector. We decided to substitute mEos for mCherry in the constructs described above.

To engineer pMDC-SP-PSIB-mCherry the construction pCRBlunt-PSIB and pMDC-SP-PSIA-mCherry were digested in order to excise PSIB and PSIA respectively. The purified fragments of PSIB and pMDC-SP_mCherry were used for ligation reaction and *E.coli* was transformed with this reaction product. A positive clone was selected with Xba I and Pst I (Figure 3.19.) for *Agrobacterium* electroporation.

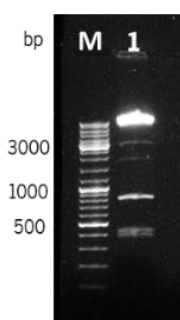


Figure 3.19.: Positive clone of pMDC-SP-PSIB-mCherry determined by Xba I and Pst I restriction mapping. (1). M-molecular weight standard Gene Ruler™ DNA Ladder Mix (Fermentas).

Agrobacterium carrying pMDC-SP-PSIA-mCherry and pMDC-SP-PSIB-mCherry were used to infiltrate *Arabidopsis* seedlings to obtain transient expression of the constructs. The cotyledons were analysed under confocal microscope after 3 days of infiltration.

The results obtained for the PSI-mCherry fusions cloned in the vector pMDC were very similar to the observations of pFAST constructs already described. The mCherry fluorescence was detected in the large vacuole 3 days after infiltration (fig. 3.20 and fig. 3.21). We did not observe fluorescence in any other compartment of the cell so we conclude the fusion protein was not retained or delayed in their trafficking to the vacuole. The most part of the observed cells were transformed and mCherry was correctly targeted to the vacuole (fig. 3.20 and fig. 3.21 a, e), which definitely excludes the cloning into pMDC vector as the cause of mEos-fusions retention.

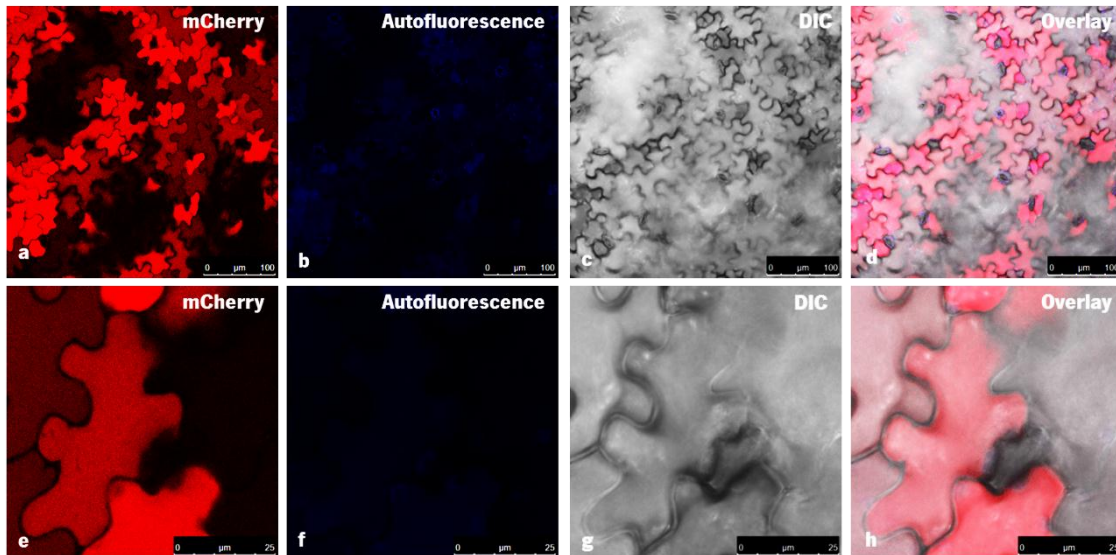


Figure 3.20.: Subcellular localisation of pMDC-SP-PSIA-mCherry (cardosin-A PSI) in *Arabidopsis* cotyledon epidermal cells. mCherry fluorescence was observed in the vacuole 3 days post-vacuum infiltration using 561 nm laser-line for excitation. (a, e) red channel for mCherry fluorescence detection; (b, f) autofluorescence (in blue); (c, g) Differential interference contrast (DIC); (d, h) Overlay of red channel, autofluorescence (in blue) and DIC. Scale bars: a - d: 100 µm; e - h: 25 µm.

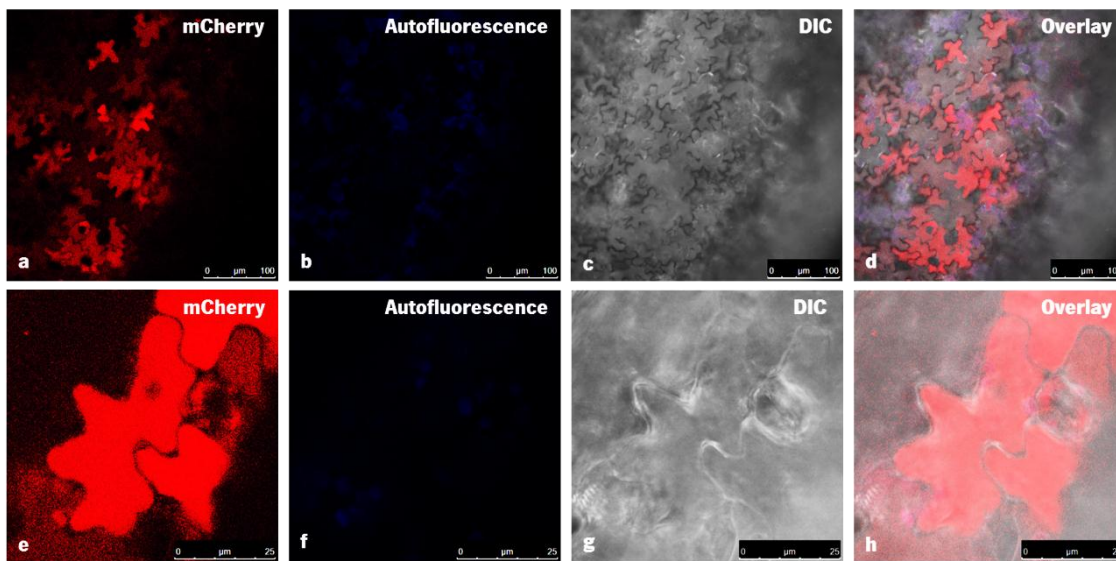


Figure 3.21.: Subcellular localisation of pMDC-SP-PSIB-mCherry (cardosin-B PSI) in *Arabidopsis* cotyledon epidermal cells. mCherry fluorescence was observed in the vacuole 3 days post-vacuum infiltration using 561 nm laser-line for excitation. (a, e) red channel for mCherry fluorescence detection; (b, f) autofluorescence (in blue); (c, g) Differential interference contrast (DIC); (d, h) Overlay of red channel, autofluorescence (in blue) and DIC. Scale bars: a - d: 100 µm; e - h: 25 µm.

As referred previously in this section we needed to establish a time-point for further studies using the *Arabidopsis* transient transformation so we observed cardosin-B PSI-mCherry fusion 20 hours after vacuum infiltration. The results were similar to the ones obtained for the pFAST constructs since the mCherry fluorescence was observed in the vacuole and we did not detect

mCherry fluorescence in any other compartment of the cells (fig.3.22). This result corroborates the fact that pMDC is a suitable vector for cardosins expression in *A. thaliana*.

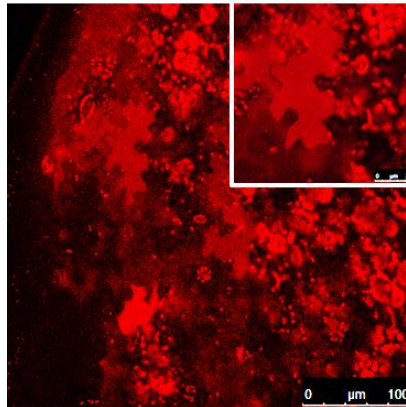


Figure 3.22.: Subcellular localisation of pMDC-SP-cardosin-B PSI-mCherry in *Arabidopsis* cotyledon epidermal cells 20 hours after vacuum-infiltration. mCherry fluorescence was observed in the vacuole 20h post-vacuum infiltration using 561 nm laser-line for excitation. Scale bars: 100 μm ; detail of mCherry fluorescence in the large vacuole of a cell: 25 μm .

The pMDC83 is a valuable vector for expression in *Arabidopsis* system since the PSI-mCherry fusions were correctly targeted to the vacuole and with high transformation efficiency. mEos is not working properly for cardosins tagging since the fusions never reached the vacuole and were observed in a pattern that could correspond the early compartments of the secretory pathway or near to the cell wall. Further studies are needed to fully interpret these data.

3.4 Glycosylation mutated versions expression analysis

The events that lead to cardosins different accumulation patterns and the routes along the endomembrane system are not fully understood. However, subtle differences in their protein sequence may be responsible for such different behaviour, namely the glycosylation pattern of each. The presence of a glycosylated PSI is a conserved characteristic of plant aspartic proteases (Vieira *et al.*, 2001) that is absent from cardosin A. Given the previous results obtained when exploring the role of the PSI in protein trafficking (Pereira *et al.*, 2013) we undertook a systematic analysis of cardosin A glycosylation pattern and its influence in the routes that cardosin takes to the vacuole. Previous to this work, three glycosylation mutants have been produced (Pereira, PhD thesis, 2012) where the glycosylation sites were either removed (one by a mutation in the first site and another by a mutation in the second site) or added (by introducing a glycosylation site in the PSI region). The results obtained showed that the protein is able to travel to the vacuole in the three studied cases but at a lower transport rate especially when the first site is removed (Pereira, PhD thesis, 2012). In order to discuss the importance of glycosylation in the sorting, two other constructs were tested during this work: a non-glycosylated cardosin A version and a cardosin-A glycosylated PSI. Along this work we also successfully remove the glycosylation site present in cardosin-B PSI through site-directed mutagenesis technique. To allow direct comparison with the already published results by Pereira and co-workers (2013) regarding cardosins glycosylation we used the *N.tabacum* transient expression system in this part of the work.

3.4.1 Non-glycosylated cardosin A

Cardosin A has two N-glycosylation sites that were modified by site-directed mutagenesis to better understand the importance of this pattern on cardosin A trafficking to the vacuole. This mutated version was already cloned in pCRBlunt® vector. During this work Cardosin A mutated in the two glycosylation sites (cardosin A mut GLY 1+2) was subcloned into pVKH18-En6-mCherry plasmid. *E. coli* was transformed with the obtained ligation product and the colonies were screened by double restriction. A positive clone was selected by the presence of a band of approximately 700 bp after agarose gel electrophoresis (Fig. 3.23).

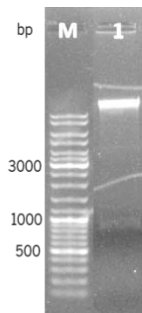


Figure 3.23.: Electrophoretic separation of reaction products. 1- positive clone of pVK-Cardosin A mut GLY 1+2-mCherry determined by Sal I and Sac I restriction mapping. M- molecular weight marker GeneRuler™ DNA Ladder Mix (Fermentas).

The cardosin A mut gly 1+2 (cardosin A mutated in both glycosylation sites) construct was used for *Agrobacterium* electroporation and subsequently for *Nicotiana tabacum* transformation. The leaf epidermal cells were imaged 3 days after infiltration under a confocal microscope. The results were inconclusive since in the most of the experiments we did not detect mCherry fluorescence. A few times, the mCherry fluorescence was observed in the vacuole but, morphologically, the tissues exhibited a stress condition reason why we decided that further optimization is needed to analyse this construct.

3.4.2 Cardosin-A Glycosylated PSI version

Cardosin-A PSI contrary to other aspartic proteases' PSIs has no identifiable glycosylation site (Frazão *et al.*, 1999). Using site-directed-mutagenesis a glycosylation site was introduced in cardosin-A PSI to understand the effect of the glycosylation in the trafficking to the vacuole and the influence in the recently proposed Golgi-bypass route (Pereira *et al.*, 2013). Cardosin-A PSI glycosylated version was already available in the laboratory cloned into pENTR4® vector and fused to mCherry. During this work SP-PSI A mut GLY-mCherry (PSI mutated version fused to signal peptide to enter the secretory pathway and a fluorescent tag) was excised from pENTR4® and subcloned into pVKH18-En6. The clones obtained from *E. coli* transformation with the fusion were screened with restriction enzymes and a positive one with a band of approximately 700 bp (fig. 3.24) after electrophoretic separation was selected for *Agrobacterium* electroporation to be used in tobacco infiltration.

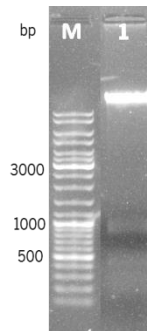


Figure 3.24.: Electrophoretic separation of reaction products. 1- positive clone of pVK-Cardosin-A PSI mut GLY-mCherry determined by Sal I and Sac I restriction mapping. M- molecular weight marker GeneRuler™ DNA Ladder Mix (Fermentas).

Three days after tobacco cells transformation glycosylated PSI-mCherry fusion to mCherry was mostly observed in the vacuole (figure 3.25 e and f) similar to fluorescence observed for the cardosin A non-glycosylated PSI (figure 3.25 a and b) and for the cardosin-B PSI, already described by Pereira and co-workers (2013). The SP-PSIA-mCherry images were kindly provided by Pereira and co-workers (2013) for comparison purposes.

Sar I H74L dominant-negative mutant was used to block the ER-to-Golgi trafficking. When co-expressed with SarI dominant-negative mutant, cardosin-A PSI continued to reach the vacuole (Pereira *et al.*, 2013) (fig. 3.25 c and d). When a glycosylation site is artificially placed in the PSI domain the fluorescent chimera never reached the vacuole and was retained in the early secretory compartments (figure 3.25 g and h) similar to what was observed for cardosin-B PSI (a glycosylated PSI) when the trafficking from ER to Golgi was blocked (Pereira *et al.*, 2013).

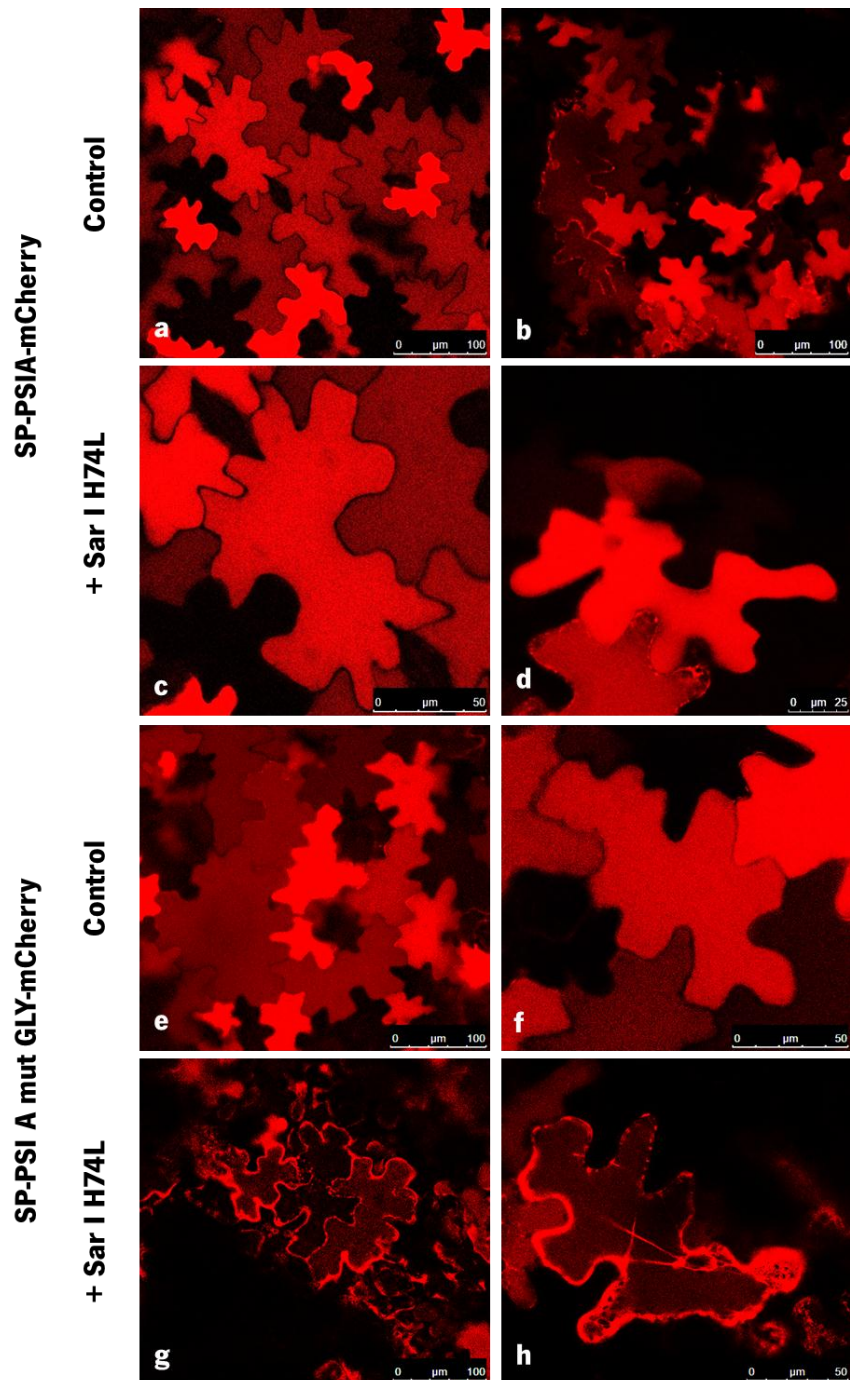


Figure 3.25.: Subcellular localization of mCherry-tagged cardosin-A PSI (non-glycosylated version) and cardosin-A PSI glycosylated version (mutated version) and co-expression with the mutant SarI H74L. (a-d) Cardosin-A PSI fused to mCherry. (e-h) Cardosin-A mutated PSI fused to mCherry. The cardosin-A PSI and PSI mutated version were infiltrated alone (a, b, e, f) or was co-infiltrated with SarI H74L (c, d, g, h). The SP-PSI A-mCherry and SP-PSI A mut GLY-mCherry accumulates in the vacuole but when it is co-infiltrated with blocking agent the PSIA continues to reach the vacuole and for the mutated version there is an accumulation of fluorescence in cytoplasmic strands and perinuclear labelling, indicative of retention in the endoplasmic reticulum (ER) induced by the Sar I dominant-negative mutant and absence of vacuolar accumulation. Scale bars: a, b, e, g: 100 μm ; c, f, h: 50 μm ; d: 25 μm .

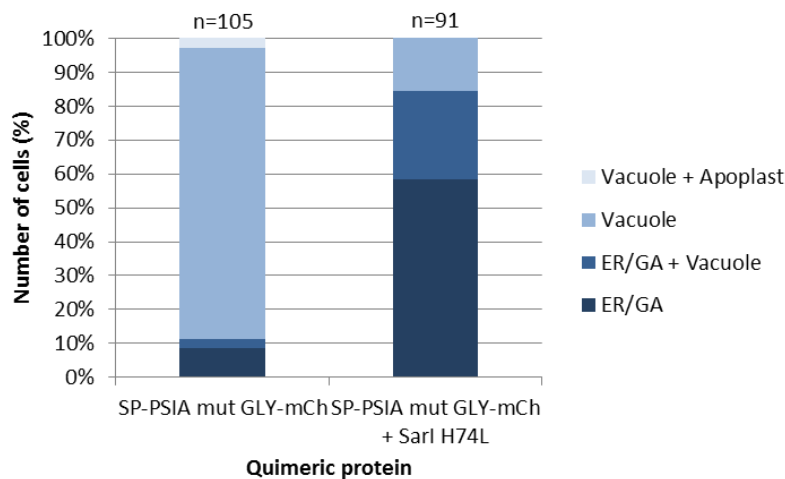
Given the novelty of the results obtained and to get a better view of the microscopic observations, quantitative analysis was performed on the results from the observation of more

than 90 cells from three independent experiments. For the quantification (table3-1) it was considered that the total number of cells with fluorescent signal will define a 100% value and among this population the different localization patterns were then scored.

Table 3-1: Quantitative analysis of the fluorescence patterns observed for cardosin-A glycosylated PSI fluorescent fusion and co-expression with Sar I H74L dominant-negative mutant known to block ER-Golgi trafficking (n, number of cells expressing fluorescent proteins in three independent experiments)

Chimeric proteins \ Localization	SP-PSIA mut GLY-mCh	SP-PSIA mut GLY-mCh + <i>Sar1</i> H74L
ER/GA	9	53
ER/GA + Vacuole	3	24
Vacuole	90	14
Vacuole + Apoplast	3	0
number of cells	105	91

Quantitative analysis of the fluorescence patterns



Data obtained from the quantification of fluorescence patterns reflects the subcellular localization observed in confocal analysis. The control cardosin-A C-terminal is mostly accumulated in the vacuole but when co-expressed with Sar I dominant-negative mutant becomes retained in the ER-Golgi compartments validating the efficiency of the blocking. The cardosin-A mutated PSI is correctly targeted to the vacuole but when co-infiltrated with the mutant gets retained in the early secretory compartments.

3.4.3 Non-glycosylated cardosin-B PSI version

In this work site-direct mutagenesis approach was used for removal of putative N-glycosylation site of cardosin-B PSI. The plant-specific insert of cardosin B is glycosylated as occurs in the majority of plant aspartic proteases. This VSD, contrary to what occurs for cardosin-A PSI, needs to travel through the Golgi to reach the vacuole in tobacco epidermal cells (Pereira *et al.* 2013). In order to evaluate the influence of N-glycosylation site in the trafficking to the vacuole cardosin-B PSI, its putative glycosylation site was disrupted. The mutation was already confirmed by sequencing and the plasmid DNA of a positive clone (fig. 3.26) will be used for *Agrobacterium* transformation in order to proceed with tobacco infiltration.

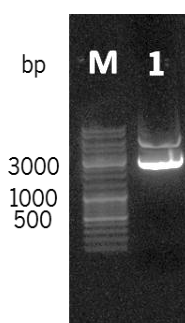


Figure 3.26.: Electrophoretic separation of pure DNA extraction from a positive clone. 1- positive clone of pCRBlunt-Cardosin-B PSI mut GLY-mCherry evaluation for DNA sequencing . M- molecular weight marker GeneRuler™ DNA Ladder Mix (Fermentas).

The glycosylation seems to be a key-feature in the PSI driven targeting to the vacuole since the cardosin-A PSI could not target mCherry efficiently to the vacuole and the fusion was retained in the early compartments of the secretory pathway upon Sar I H74L dominant-negative mutant co-infiltration. With further analysis of non-glycosylated cardosin A we will be able to understand the importance of these two glycosylation sites for the protein trafficking. The non-glycosylated cardosin-B PSI will be very important to confirm the relevance that we are suggesting after SP-PSI A mut gly-mCherry analysis.

4 Discussion

In the beginning of this work we had 4 main goals:

- The validation of *Arabidopsis thaliana* transient system for fluorescent-tagged cardosins expression
- To obtain *Arabidopsis* stable lines expressing cardosins-mCherry fluorescent fusions
- To obtain mEos fusions of cardosins and the Plant-Specific Insert
- To get further insights on the role of glycosylation in cardosins trafficking

In the end, we accomplished the majority of the proposed objectives and since we have validated *Arabidopsis thaliana* as a suitable system for cardosins expression; we obtained several transgenic lines expressing cardosins, its truncated versions or their VSDs tagged with mCherry; and we also added new insights to the role of glycosylation in cardosins trafficking between endomembrane compartments. These topics will be discussed in more detail in the following sections.

4.1 Cardosins A and B and its mutated versions accumulate in the vacuole in *A. thaliana* seedlings

In our group we have been using cardosins A and B as models to study intracellular trafficking but, despite many achievements so far, many aspects are yet to be deciphered. The localisation studies of cardosins in the native plant revealed intriguing results: very similar in sequence they have different accumulation patterns in distinct organs (Ramalho Dantos *et al.*, 1997; Vieira *et al.*, 2001; Duarte *et al.*, 2006, Figueiredo *et al.*, 2006, Pereira *et al.*, 2008; Oliveira *et al.*, 2010). Some theories have been raised in respect to the function of the two proteins in the tissues where they are predominantly accumulated, being hypothesised a role during plant reproduction and seed germination (Faro *et al.*, 1999; Ramalho-Santos *et al.*, 1997, Duarte *et al.*, 2006; Pereira *et al.*, 2008). In the past years, in an attempt to unveil important aspects of intracellular trafficking and sorting, *Nicotiana tabacum* was chosen as heterologous system to express cardosins, since there is a lack of transformation protocols for *Cynara cardunculus*. This system allowed the expression of fluorescent-tagged versions of cardosins, several mutated versions of cardosins and the isolation of its VSDs. The expression of cardosin A and cardosin B in tobacco leaf epidermis showed a final accumulation of both proteins in the

vacuole (Soares da Costa *et al.*, 2010; Pereira *et al.*, 2013). Then, cardosin A C-terminal domain and the Plant-Specific Insert were deleted from the protein sequence allowing to conclude that each of these domains are capable of target the proteins to the vacuole in the absence of the other (Pereira *et al.*, 2013). These vacuolar sorting determinants were also isolated, tested independently, and it was shown that they were able to drive mCherry to the vacuole as well. Finally, it was suggested, after several assays blocking the protein transit between specific endomembrane compartments, that cardosin-A PSI domain is capable of Golgi bypass to reach the vacuole, a characteristic that cardosin-B PSI does not have (Pereira *et al.*, 2013).

Given the limited approaches allowed by the *N. tabacum* leaf epidermis expression, it became essential to analyse the trafficking events in the different plant organs and tissues along development and during this work the tools necessary for this task were obtained.

First we wanted to test the fluorescent fusions in the *Arabidopsis* system, to show that cardosins sorting was as efficient in *Arabidopsis* as in tobacco and that we were in face of a conserved sorting mechanism. We applied a transient method and validated the chimeric proteins that accumulated in the vacuole of the *Arabidopsis* cotyledon epidermal cells. Cardosins, its truncated versions and cardosin-A VSDs fusions accumulated in the vacuole of the *Arabidopsis* cotyledons epidermal cells in a similar manner to that observed for *N. tabacum* (Pereira *et al.*, 2013).

Ultimately, the *Arabidopsis thaliana* and *Nicotiana tabacum* systems have different characteristics allowing different approaches that will enable great progress in cardosins localisation studies. *Arabidopsis* has a well-established protocol for stable expression, a short life cycle and tobacco requires minimum handling for high efficiency transient expression.

4.1.1 Transient expression: outcomes and limitations

The transient expression in *Arabidopsis* demonstrated to be a valuable tool in cardosins expression studies. This is a fast and simple method that requires minimum handling and allows high-throughput analyses since we can test six different experimental conditions in one single plate, generating a high number of transformed cells in a limited space. Co-expression of different fluorescent tags in a single well allows direct co-localization studies, using for example two fluorescent proteins with divergent excitation and emission spectra. It also allows blocking assays using expression in wild-type plants but also using the transgenic lines obtained during this work. This method as was optimized in this work, allowed rapid and robust monitoring of

protein localization in *Arabidopsis* seedlings since we detected our protein fusions in the final subcellular destination as early as twenty hours after infiltration. We also imaged the cells three days after infiltration and mCherry was still stable in the vacuole. Performing blocking assays is a challenging task because both fusion protein and blocking agent must be infiltrated simultaneously, which can have implications in the normal trafficking of the cell endogenous proteins. On the other hand, this is an advantage when comparing to tobacco where it takes three days after infiltration to have the entire protein pool accumulated in the vacuole. Furthermore, for transient expression in tobacco a month is necessary to have an optimum leaf size for infiltration while in the *Arabidopsis* system we obtain plants ready to infiltrate in 3-4 days. Moreover, tobacco requires a large greenhouse space to grow the plants. Most importantly, we can compare and integrate results from transient expression in *Arabidopsis* and tobacco systems and test new constructs before stable expression in *Arabidopsis* that takes much longer (several months) to get results.

We showed before (Results, section 3.1.4) that cardosins reach the vacuole in less than 24 h when transiently expressed in *Arabidopsis*. This was firstly surprising for us, but it may be due to the type of organ being infiltrated. *Arabidopsis thaliana* has a shorter life cycle than tobacco so the trafficking events along the secretory pathway may be faster in order to fulfil the growth needs.

The more relevant weaknesses of this technique is the stress caused by vacuum pressure in fragile young seedlings during infiltration process and the analysis of the cells in confocal microscopy can be very demanding due to the cells size and inherent tissue autofluorescence. However, this can be overcome if we excise the cotyledon and place them independently in the slide to avoid curling of the tissue and assure correct page (abaxial) observation. What concerns to autofluorescence we always perform the experiments using the blue-coloured channel for autofluorescence since the chlorophyll emission can be isolated and be also used the green channel to detect cell walls.

4.1.2 Stable transformation: tracking cardosins accumulation along development

The results obtained in the transient expression evidenced the correct target of cardosins-mCherry fusions in the leaf epidermis. We then generated stable *Arabidopsis* lines for each construction. The success of transformation was confirmed by confocal microscopy for some transgenic lines. These observations showed an accumulation pattern similar to the observed in the transient expression. The major goal will be to analyse other organs and tissues of the plant expressing cardosins and the mutated versions. The constitutive expression give us the opportunity to observe the cardosins accumulation through development and analyse the accumulation pattern of cardosin A VSDs that will allow us to determine the preferable accumulation when it is determined by the PSI or by the C-terminal. We are expecting that PSI would be located in the PSVs, in accordance with results previously obtained, an evaluation that we could not perform in the leaf epidermal cells that only contains a large LV. The PSIs stable expression may give us more information about the saposin-like function of membrane interaction that was proposed for this domain (Egas *et al.*, 2000). It will be possible to analyse development-dependent and organ-specific trafficking in the organs were the cardosins are thought to have an important function, namely more active tissues like flowers were the differential accumulation is more relevant, and seeds .

4.2 The glycosylation role in Cardosins trafficking and sorting

The glycosylation patterns of cardosin A and cardosin B are different and have been suggested as the main difference between cardosins protein sequence (Frazão *et al.*, 1999; Costa *et al.*, 2001; Pereira *et al.*, 2013). Cardosin A has two glycosylation sites, one in the heavy chain and another in the light chain, while cardosins B, and most plant Aps, has a conserved glycosylation site in the PSI domain. It has been suggested in the past that glycosylation may somehow influence the trafficking of proteins by slowing down the transport rates or by altering their intracellular routes (Wilkins *et al.*, 1990). Given cardosins A glycosylation pattern and the differences observed in relation to other plant Aps, it was questioned if it was indeed relevant for cardosin A trafficking, particularly in its Golgi-bypass. In order to understand the importance of the N-glycosylation in cardosins trafficking, cardosin A glycosylation sites were mutated in a

previous work (Pereira, PhD thesis, 2012). The preliminary conclusion from tunicamycin assay (known to affect *N*-glycosylation) was that glycosylation does not prevent the vacuolar accumulation of cardosin A. However, it does seem to interfere with the route taken by the protein to the vacuole as the mutant with an extra glycosylation site in the PSI was retained upon tunicamycin treatment and the removal of only one glycosylation site was sufficient for the protein accumulation not be affected by the drug.

In this work we obtained a cardosin A mutant without both glycosylation sites and expressed it in Tobacco epidermal cells (to allow direct comparison with the results obtained by Pereira, 2012). The results obtained were not conclusive because, despite repeating several times, the fluorescent pattern obtained was not clear. The cells did not look healthy and we concluded that this construction needed further optimization of the technique that will be focus on the titration of *Agrobacterium* carrying the construct. On the other hand, the *N*-glycosylation protects the protein from proteolytic degradation, and influences protein conformation, stability and biological activity. Mal-conformation of this mutated protein can possibly trigger the ER quality control and cause the protein to be retained in tis compartment and eventually be degraded by the cell proteasome. We did not observe expression of the non-glycosylated protein and this may be due either to proteolytic degradation of the fusion, or the protein becoming unstable during the trafficking to the vacuole or during accumulation inside the vacuole.

4.2.1 The sorting mediated by PSI domain and effect of *N*-Glycosylation

The role of the glycosylation in the vacuolar routes taken by proteins in the secretory pathway has been discussed, in particular in relation to a possible Golgi bypass (Rayon *et al.*, 1998; Paris *et al.*, 2010).

It has been described that cardosin-A PSI can drive cardosin and mCherry alone to the vacuole through a Golgi independent pathway (Pereira *et al.*, 2013). However it was also shown that cardosin-B PSI has to pass through the Golgi to reach the vacuole (Pereira *et al.*, 2013). Cardosin-A PSI is not glycosylated and cardosin-B PSI has a putative glycosylation site similar to most APs such as phytepsin where it was shown that this domain was essential to enter a COPII pathway (Törmäkangas *et al.*, 2001). The cardosin-B PSI has a glycosylation site similar to the

one of phytepsin's PSI so it was proposed that it may be also depending on COPII mediated trafficking (Pereira *et al.*, 2013).

In order to understand how the glycosylation of PSI affects the trafficking route we introduced an artificial glycosylation site on cardosin-A PSI to obtain a similar pattern with cardosin-B PSI and to evaluate if the glycosylation would influence the route taken by the cardosin-A PSI.

In contrast with the non-glycosylated PSI that accumulates in the vacuole despite the ER-to-Golgi blocking, the mutated version was retained when co-infiltrated with Sar I H74L a dominant-negative mutant, known to block the ER to Golgi trafficking preventing the formation of COPII vesicles (Andreeva *et al.*, 2000). Cardosin-A glycosylated PSI co-infiltrated with Sar I H74L dominant negative mutant was detected in a low percentage of cells but it must be emphasised that the titration of *Agrobacterium* carrying the mutant form of Sar I is much lower than the glycosylated PSI-mCherry fusion, to prevent irreversible damage to the cells since this assay blocks not only the protein-fusion but also the cell vital proteins that need COPII transport from ER to Golgi to get to the final destination (Andreeva *et al.*, 2000) Comparing these results with the non-mutated version, we observed that 2 days after infiltration part of the protein synthesised was still in transit to the vacuole, but after 3 days, all the protein pool had reached the final destination, the vacuole. In the case of mutated PSI (glycosylated), after 3 days we observe a retention and accumulation of the protein fusion in the early compartments of the secretory pathway in most of the cells. The morphological aspect of the tissue lead us to conclude that the mCherry fluorescence located in the vacuole in the glycosylated PSI observations was because these cells were not transformed by Sar I H74L dominant-negative mutant.

These results unleash a debate about the relevance of *N*-glycosylation in protein trafficking. It has been proposed that *N*-glycosylation is not determinant for the correct trafficking of the vacuolar protein but lead to a delay in the trafficking (Wilkins *et al.*, 1990; Ramis *et al.*, 2001). Here we show that the glycosylation may indeed be important for the route taken by protein, in particular in what concerns by their passage through the Golgi, but further studies are needed to prove this theory. Another tool we are preparing and we hope it will add more information and help to clarify this subject is the cardosins B PSI without its glycosylation site. Soon we will be able to evaluate if the route driven by the non-glycosylated cardosin-B PSI is the same when compared to the glycosylated (non-mutated) version. This will add more information to our hypothesis that glycosylation plays an important role in the cardosins trafficking mediated by the PSI domain.

4.3 Fluorescent reporters

4.3.1 mcherry: photostability and brightness in highlighting cardosins trafficking

The use of mCherry fusions was a great advance in cardosins studies. Before the use of mCherry the knowledge about cardosins was obtained from fixed tissues either by immunofluorescence studies (confocal microscopy) or ultrastructure analyses (transmission electron microscopy-TEM). These are exquisite approaches when the aim is the localization of cardosins in the native tissue. The use of mCherry does not substitute the previous approaches since every approach has a different purpose but in this work we wanted to study the dynamic process through which cardosins get to the final accumulation compartment, a task that needs in vivo analyses. In this work, we confirmed the stability of mCherry in the acidic central vacuole of epidermal cells during prolonged live cell imaging. It is a true monomeric protein since we never detected aggregation problems with our fusions. In this work we use mCherry in a stable expression and we confirm once more the photostability and efficiency of red fluorescence emission. Also in this constitutive expression we didn't observe any aggregation problems.

4.3.2 The undeniable profit in mEos addition to cardosins expression studies

The fusions with mCherry fluorescent protein were very stable in the vacuole and mCherry has the characteristic of being a monomeric structure that is the more suitable for tagging protein fusions. Unfortunately, mCherry is limited to a single emission wavelength which means we cannot alter its colour which would be very useful in for studying cardosins dynamic events. We expect to be able to track the protein movement, through the different cellular compartments, and observe in real-time the *de novo* synthesised molecules, if we couple cardosins with a photoconvertible protein. Therefore we have selected mEos, a monomeric photoconvertible fluorescent protein for tracking cardosins fusions.

The possibility of photoconversion will allow us to change the colour of the entire pool of the chimeric proteins in observation and then observe the newly synthesized molecules and track their behaviour separately from the entire red protein. This is possible only because photoconversion of mEos is irreversible, in other words, a residue is cleaved from the peptide backbone when irradiated with UV light and this is a permanent modification. In a stable

transformation this would be a powerful tool to follow cardosins and the VSDs, namely the Plant-Specific Insert. In a constitutive expression we will be able to observe the *de novo* protein synthesis since the protein is constantly being produced while observing the trafficking of the remaining protein that can be already in the final accumulation compartment. Moreover, we will observe cardosins trafficking in real-time in the several tissues of each organ of the plant. Photoconversion would be very useful to observe the vacuole remodelling proposed during seed germination which is one of the stages that cardosins could have a preponderant role (Pereira *et al.*, 2008). mEos allows simultaneous use of other fluorescent protein, for example fused to intracellular markers which allows track of two or more different fusions and co-localization studies.

Approaches to optimize mEos constructs

The fluorescence observed for the mEos fusions was located in the early compartments of the secretory pathway, namely the ER since we could observe perinuclear labelling and cytoplasmic strands for the PSI constructs indicating that the protein is retained in the first check point for the proteins that enter the ER. This retention can be due to the misfolding of the protein. For cardosins fusions our first hint was the recognition of the C-terminal domain for the vacuolar receptors and we obtain new constructs with the cardosin C-terminal fused to the mEos C-terminal. In the case of mCherry this worked very well but for the mEos fusions the results were very similar to the ones obtained with the C-terminal not exposed. mEos fusions may need a different linker between cardosins and mEos to be able to adopt the correct conformation. Curiously, this retained protein is not able to form its photoconverted structure since we applied UV laser and the red form was not detected even though the green form decreased, what can also be due to photobleaching of the protein.

In the case of PSIs fusions we were expecting to detect the fluorescence in the vacuole similar to the results obtained with mCherry but the results were similar to the cardosins fusions. The cardosins-mEos constructs were used to obtain the mEos DNA using classical molecular methods. In this process we linked additional nucleotides from the cardosins-mEos linker that may be influencing the protein conformation, even though we previously predict the open reading frame of the fusion. The first approach would be amplifying the fusion with specific primers that would allow the fusion without linker similar to the mCherry constructions.

On the other hand, we are expecting an accumulation of mEos in the lytic vacuole of *Arabidopsis thaliana* or previously in *Nicotiana tabacum* leaf epidermis and we cannot exclude the hypothesis that the protein is not stable in acidic pH of the lytic vacuole. Furthermore, in recent works new mEos versions have been created to overcome the aggregation tendency of the first versions. If mEos forms clusters it loses the advantage of a monomeric protein and could detain our fusions similar to what happens with a tetrameric protein like Kaede (Brown *et al.*, 2010). To examine if the protein reaches the vacuole but we are not able to detect fluorescence due to the instability of the fluorescent protein we could obtain protoplasts from the cotyledon epidermal cells, isolate vacuoles and perform a western blotting with the protein extracted from the vacuoles for immunodetection of cardosins or PSIs. Another approach is to obtain mEos fused to cardosin-A C-terminal domain by PCR since this construct with mCherry accumulates in the vacuole and with this approach we eliminate the presence of a linker.

5 Conclusions and perspectives

We managed to establish in our laboratory a protocol for the transient transformation in *Arabidopsis thaliana* using the *Agrobacterium* vacuum-mediated infiltration adapted from Marion *et al.* (2008). This approach was undertaken to test a set of constructs intended to be used in *A. thaliana* stable transformation. In *A. thaliana* mCherry tagged cardosins versions were detected in the vacuole of cotyledon epidermal cells in a pattern very similar to that observed in *N. tabacum*. Furthermore, the results obtained showed that the two cardosin-A VSDs and cardosin-B PSI have the same ability of driving the protein to the vacuole in *Arabidopsis thaliana* cotyledon epidermal cells, since most of the cells imaged presented mCherry fluorescence in the vacuole. These results confirm that cardosin-A VSDs independently are sufficient to target a protein like mCherry to the vacuole as it has been previously shown in *Nicotiana tabacum* leaf epidermis transient expression system (Pereira *et al.*, 2013), and that this mechanisms are conserved. This system revealed to be an excellent tool to study cardosins expression in heterologous systems as an alternative to *N. tabacum* epidermal cells and a method to test constructs previous to stable transformation. After the remarkable efficiency of transformation with all the mCherry constructions we also decided to test mEos-based constructs in this system. Results with mEos were inconclusive for cardosins tagging since the fusions never reached the vacuole and were observed in a pattern that could correspond the early compartments of the secretory pathway or near to the cell wall. This allowed us to conclude that these constructs will need further optimization to be used for cardosins stable expression studies. Further tests will allow to determine if the mEos fusions did reach the vacuole at some point but lost its fluorescence. For that a new construct will be obtained: mEos fused to the cardosin-A C-terminal, known to mark the vacuole (Pereira *et al.*, 2013). Also Western blotting analysis will allow to examine the vacuoles content.

During this work, the stable transformation was accomplished for the first lines screened and the mCherry protein was detected in the vacuole of cotyledon and leaf epidermal cells, a localization that was already observed in the transient transformation methods. These transgenic stable lines will be screened in order to observe the cardosins accumulation during development, namely in the flowers and during seed germination.

One of the main goals of this work was to explore the hypothesis that *N*-glycosylation plays an important role in cardosins trafficking, especially in what concerns the PSI-dependent routes. The glycosylation seems to be a key-feature in the PSI driven targeting to the vacuole since the

glycosylated cardosin-A PSI could not target mCherry efficiently to the vacuole and the fusion was retained in the early compartments of the secretory pathway upon Sar I H74L dominant-negative mutant co-infiltration contrarily to the non-glycosylated cardosin-A PSI which has been previously shown to reach the vacuole under the same conditions, probably bypassing the Golgi. Our results outline the potential effect of glycosylation on vacuolar transport: when a glycosylation site is added to cardosin-A PSI, the protein behaves differently upon blockage of the ER-to-GA transport, as it shifted from a vacuolar accumulation (possibly COPII-independent) to retention in the early endomembrane compartments, consistent with a COPII-dependent pathway. These observations strongly support previous results regarding the specificity of Cardosin-A PSI in directing the protein to the vacuole via an alternative route, bypassing Golgi, and add new and important insights indicating that the route taken by the PSI may be dependent on its N-glycosylation status.

Further analysis of non-glycosylated cardosin A will allow to understand the importance of these two glycosylation sites for the protein trafficking. Removal of the glycosylation site present in cardosin-B PSI will be a great addition to finally validate the importance of glycosylation in the route proteins take to reach the vacuole. The cardosin-B PSI mutated version will be cloned and will be transiently expressed in *Nicotiana tabacum* system. *Arabidopsis thaliana* stably expressing the glycosylation mutants will be essential to ascertain whether the PSI and the glycosylation role on protein trafficking is tissue/organ-specific.

6 References

- Ando, R., Hama, H., Yamamoto-Hino, M., Mizuno, H. and Miyawaki, A. (2002) An optical marker based on the UV-induced green-to-red photoconversion of a fluorescent protein. *Proc. Natl Acad. Sci. USA*, 99, 12651–12656.
- Andreeva, A.V., Zhengm, H., Kutuzov, M.A., Evans, D.E. and Hawes, C.R. (2000). Organization of transport from endoplasmic reticulum to Golgi in higher plants. *Biochem. Soc. Trans.*28: 505–512
- Batoko, H, Zheng, H.Q., Hawes, C & Moore, I, 2000a. A rab1 GTPase is required for transport between the endoplasmic reticulum and golgi apparatus and for normal golgi movement in plants. *The Plant cell*, 12(11), pp.2201-18.
- Bolte, S., Lanquar, V., Soler, M. N., Beebo, A., Satiat-Jeunemaitre, B., Bouhidel, K. and Thomine, S., (2011). Distinct lytic vacuolar compartments are embedded inside the protein storage vacuole of dry and germinating *Arabidopsis thaliana* seeds. *Plant & cell physiology*, 52(7), pp.1142-52.
- Brown, S.C., Bolte, Susanne, Gaudin, M., Pereira, C., Marion, J., Soler, M.-N. & Satiat-Jeunemaitre, Béatrice, (2010). Exploring plant endomembrane dynamics using the photoconvertible protein Kaede. *The Plant journal* 63(4), pp.696-711
- Cao X, Rogers SW, Butler J, Beevers L & Rogers JC (2000) Structural requirements for ligand binding by a probable plant vacuolar sorting receptor. *Plant Cell*12, 493–506.
- Chalfie M, Tu Y, Euskirchen G, Ward WW, Prasher DC. (1994) Green fluorescent protein as a marker for gene expression. *Science*. Feb 11; 263 (5148):802-5.
- Cordeiro, M.; Pais, M.; Brodelius, P. (1994) Tissue-specific expression of multiple forms of cyprosin (aspartic proteinase) in flowers of *Cynara cardunculus*. *Physiol. Plant.*, 92, 645-653.
- Cordeiro, M.; Xue, Z.; Pietrzak, M.; Pais, M.; Brodelius, P. (1994) Isolation and characterization of a cDNA from flowers of *Cynara cardunculus* encoding cyprosin (an aspartic proteinase) and its use to study the organ-specific expression of cyprosin. *Plant Mol.Biol.*, 24, 733-741.
- Costa, J., Ashford, A. D., Nimtz, M., Bento, I., Frazao C., Esteves L. C., Faro C., Kervinen J., Pires E., Verissimo P., Wlodawer A., and Carrondo A., M. (1997) The glycosylation of the aspartic proteinases from barley (*Hordeum vulgare* L.) and cardoon (*Cynara cardunculus* L.) *Eur. J. Biochem.* 243, 695-700
- Clough SJ, Bent AF (1998) Floral dip: a simplified method for *Agrobacterium*-mediated transformation of *Arabidopsis thaliana*. *Plant J*16:735–743
- Curtis, M. and Grossniklaus U. (2003) A Gateway Cloning Vector Set for High-Throughput Functional Analysis of Genes in Plants *Plant Physiology* Vol. 133, pp. 462–469

- Davies, D.R. (1990). The structure and function of the aspartic proteinases. *Annu. Rev. Biophys. Biophys. Chem.* 19, pp.189-215.
- De Marcos Lousa C, Gerschlick DC and Denecke J (2012) Mechanisms and concepts paving the way towards a complete transport cycle of plant vacuolar sorting receptors. *Plant Cell* 24,1714–1732
- D'Hondt, K., Bosch, D., Van Damme, J., Goethals, M., Vandekerckhove, J. and Krebbers, E. (1993) An aspartic proteinase present in seeds cleaves *Arabidopsis* 2 S albumin precursor *in vitro*. *J. Biol. Chem.* 268, 20884–20891.
- Duarte, P., Figueiredo, R., Pereira, Susana and Pissarra, José, (2006). Structural characterization of the stigma-style complex of *Cynara cardunculus* (*Asteraceae*) and immunolocalization of cardosins A and B during floral development. *Canadian Journal of Botany*, 84(5), pp.737-749.
- Duarte, P., Pissarra, J. and Moore, I.(2008) Processing and trafficking of a single isoform of the aspartic proteinase cardosin A on the vacuolar pathway. *Planta*, 227, 1255–1268.
- Dupree P, Sherrier DJ. (1998). The plant Golgi apparatus. *Biochim. Biophys. Acta* 1404:259–70
- Egas, C., Lavoura, N., Resende, R., Brito, R. M., Pires, E., de Lima, M. C. and Faro, C (2000). The saposin-like domain of the plant aspartic proteinase precursor is a potent inducer of vesicle leakage. *The Journal of biological chemistry*, 275(49), pp.38190-6.
- Ellgaard L & Helenius A (2003) Quality control in the endoplasmic reticulum. *Nat Rev Mol Cell Biol* 4,181–191.
- Faro C, Ramalho-Santos M, Veríssimo P, Pissarra J, Frazão C, Costa J, Lin X, Tang J, Pires E (1998) Structural and functional aspects of cardosins. *Adv Exp Med Biol* 436: 423–433
- Faro, C., Ramalho-Santos, M., Vieira, M., Mendes, A., Simões, I., Andrade, R., Veríssimo, P., Lin, X., Tang, J. and Pires, E. (1999) Cloning and characterization of cDNA encoding cardosin A, an RGD-containing plant aspartic proteinase. *J. Biol. Chem.* 274, 28724–28729
- Figueiredo, R., Duarte, P., Pereira, Susana & Pissarra, José (2006). The embryo sac of *Cynara cardunculus*: ultrastructure of the development and localisation of the aspartic proteinase cardosin B. *Sexual Plant Reproduction*, 19(2), pp.93-101.
- Frazão, C., Bento, I., Costa, J., Soares, C.M., Veríssimo, P., Faro, C., Pires, E., Cooper, J. and Carrondo, M.A.(1999) Crystal structure of cardosin A, a glycosylated and Arg-Gly-Asp-containing aspartic proteinase from the flowers of *Cynara cardunculus* L. *J. Biol. Chem.* 274, 27694–27701.
- Fitchette-Lainé A-C, Gomord V, Cabanes M, Michalski J-C, Saint Macary M, Foucher B, Cavelier B, Hawes C, Lerouge P, Faye L (1997) N-glycans harboring the Lewis x epitope are expressed at the surface of plant cells. *Plant J* 12:1411–1417

Fitchette C., Cabanes-Macheteau M., Marvin L., Martin B., Satiat-Jeunemaitre B, Gomord V., Crooks K, Lerouge P., Faye L., and Hawes C. (1999) Biosynthesis and Immunolocalization of Lewis a-Containing *N*Glycans. *Plant Physiology*, Vol. 121, pp. 333–343

Frigerio L and Hawes C (2008) The endomembrane system: a green perspective. *Traffic* 9, 1563.

Guruprasad, K., Tormakangas, K., Kervinen, J. & Blundell, T.L.(1994) Comparative modelling of barley-grain aspartic proteinase: a structural rationale for observed hydrolytic specificity. *FEBS Lett.* 352, 131–136.

Jurgens, G., 2004. Membrane trafficking in plants. *Annual review of cell and developmental biology*, 20, pp.481-504.

O'Brien, J.S. & Kishimoto, Y. (1991) Saposin proteins: structure, function, and role in human lysosomal storage disorders. *FASEBJ.* 5, 301–308

Oliveira, A., Pereira, C., da Costa, D.S., Teixeira, J., Fidalgo, F., Pereira, S. and Pissarra, J.(2010) Characterization of aspartic proteinases in *C. cardunculus* L. callus tissue for its prospective transformation. *Plant Sci.*178, 140–146.

Pereira, C.S., da Costa, D.S., Pereira, S., de Moura-Nogueira, F., Albuquerque, P.M., Teixeira, J., Faro, C. and Pissarra, J.(2008) Cardosins in postembryonic development of cardoon: towards an elucidation of the biological function of plant aspartic proteinases. *Protoplasma*, 232, 203–213

Pereira C. (2012) Cardosin A Molecular Determinants and Biosynthetic Pathways. *PhD Thesis*, Faculty of Sciences, University of Porto, Portugal.

Pereira C., Pereira S., Satiat-Jeunemaitre B. and Pissarra J.. Cardosin A contains two vacuolar sorting signals using different vacuolar routes in tobacco epidermal cells. (2013) *The Plant Journal*;76(1):87-100

Pimpl, P., Taylor, J. P., Snowden, C., Hillmer, S., Robinson, D. G. and Denecke, J., (2006). Golgi-mediated vacuolar sorting of the endoplasmic reticulum chaperone BiP may play an active role in quality control within the secretory pathway. *The Plant cell*, 18(1), pp.198-211.

Drakakaki G. and Dandekar A. (2013) Protein secretion: How many secretory routes does a plant cell have? *Plant Science* 203 204 74–78

Hanton, S.L., Bortolotti, L. E., Renna, L., Stefano, G. & Brandizzi, F., (2005). Crossing the divide-transport between the endoplasmic reticulum and Golgi apparatus in plants. *Traffic* (Copenhagen, Denmark), 6(4), pp.267-77.

Hebert DN & Molinari M (2007) In and out of the ER: protein folding, quality control, degradation, and related human diseases. *Physiol Rev* 87, 1377–1408

- Heimgartner, U.; Pietrzak, M.; Geertsen, R.; Brodelius, P.; Da Silva Figueiredo, A.; Pais, M. (1990) Purification and partial characterization of milk-clotting proteases from flowers of *Cynara cardunculus*. *Phytochemistry*, 29, 1405-1410
- Lerouge P, Fichette-Lainé AC, Chekkafi A, Avidgor V, Faye L: (1996) N-linked oligosaccharide processing is not necessary for glycoprotein secretion in plants. *Plant J* 10: 101–107
- Lerouge, P., Cabanes-Macheteau, M., Rayon, C., Fichette-Lainé, A. C., Gomord, V. & Faye, L, 1998. N-glycoprotein biosynthesis in plants: recent developments and future trends. *Plant molecular biology*, 38(1-2), pp.31-48.
- Mathur J, Radhamony R, Sinclair AM, Donoso A, Dunn N, Roach E, Radford D, Mohaghegh PSM, Logan DC, Kokolic K, et al(2010) mEosFP-based green-to-red photoconvertible subcellular probes for plants. *Plant Physiol* 154:1573–1587
- Mutlu, A. & Gal, S., (1999). Plant aspartic proteinases: enzymes on the way to a function. *Physiologia Plantarum*, 105(3), pp.569-576.
- Wiedenmann J.*, Ivanchenko S, Oswald F, Schmitt F Röcker C, Salih A. , Spindler K, and G. Nienhaus U (2004) EosFP, a fluorescent marker protein with UV-inducible green-to-red fluorescence conversion. *PNAS* 9, vol. 101 no. 45 15905–15910
- C. Prasher. Virginia K. Eckenrode, William W. Ward², Frank G. Prendergast¹, Milton J. Cormier² (1992), Primary structure of the *Aequorea victoria* green-fluorescent protein Douglas *Gene* Volume 111, Issue 2, 15 Pages 229–233
- Ramalho-Santos M, Verissimo P, Faro C, Pires E (1996) Action on bovine α 1-casein of cardosins A and B, aspartic proteinases from the flowers of the cardoon *Cynara cardunculus* L. *Biochim Biophys Acta* 1297: 83–89
- Ramalho-Santos M, Pissarra J, Verissimo P, Pereira S, Salema R, Pires E, Faro C (1997) Cardosin A, an abundant aspartic proteinase, accumulates in protein storage vacuoles in the stigmatic papillae of *Cynara cardunculus* L. *Planta* 203: 204–212
- Ramalho-Santos M, Pissarra J, Pires E, Faro C (1998a) Cardosinogen A. The precursor form of the major aspartic proteinase from cardoon. *Adv Exp Med Biol* 436: 253–258
- Ramalho-Santos M, Verissimo P, Cortes L, Samyn B, Van Beeumen J, Pires E (1998b) Identification and proteolytic processing of procardosin A. *Eur J Biochem* 255: 133–138
- Ramis C, Gomord V, Lerouge P, Loïc Faye. (2001) Deglycosylation is necessary but not sufficient for activation of proconcanavalin A. *Journal of Experimental Botany*, vol 52, No. 358, pp. 911-917
- Rayon, C., Lerouge, P. and Faye, L. (1998) The protein N-glycosylation in plants. *J. Exp. Botany*, 49, 1463–1472.
- Reyes C, Buono R and Otegui M (2011) Plant endosomal trafficking pathways. *Current Opinion in Plant Biology*, 14:666–673

- Rojo E & Denecke J (2008) What is moving in the secretory pathway of plants? *Plant Physiol* 147, 1493–1503
- Runeberg-Roos P, Kervinen J, Kovaleva V, Raikel NV, Gal S (1994) The aspartic proteinase of barley is a vacuolar enzyme that processes probarley lectin in vitro. *Plant Physiol* 105: 321–329
- Sparkes IA, Runions J, Kearns A, Hawes C (2006) Rapid, transient expression of fluorescent fusion proteins in tobacco plants and generation of stably transformed plants. *Nat Protoc* 1:2019–2025
- Sparkes I and Brandizzi F. (2012) Fluorescent protein-based technologies: shedding new light on the plant endomembrane system. *The Plant Journal* 70, 96–107
- Shaner, N.C., Campbell, R.E., Steinbach, P.A., Giepmans, B.N.G., Palmer, A.E. and Tsien, R.Y. (2004) Improved monomeric red, orange and yellow fluorescent proteins derived from *Discosoma* sp. red fluorescent protein. *Nature Biotech.* 22, 1567–1572
- Shaner NC, Patterson GH, Davidson MW (2007) Advances in fluorescent protein technology. *J Cell Sci* 120:4247–4260
- Shimada T., Shimada T and Hara-Nishimura I (2010) A rapid and non-destructive screenable marker, FAST, for identifying transformed seeds of *Arabidopsis thaliana* *The Plant Journal* 61, 519–528
- Simões, I. and Faro, C. (2004) Structure and function of plant aspartic proteinases. *Eur. J. Biochem.* 271, 2067–2075
- Staehelin LA, Moore I. (1995). The plant Golgi apparatus: structure, functional organization and trafficking mechanisms. *Annu. Rev. Plant Physiol. Plant Mol. Biol.* 46:261–88
- Staehelin LA. (1997). The plant ER: a dynamic organelle composed of a large number of discrete functional domains. *Plant J.* 11:1151–65
- Soares da Costa, D., Pereira, S., Moore, I. and Pissarra, J. (2010) Dissecting cardosin B trafficking pathways in heterologous systems. *Planta*, 232, pp. 1517–1530.
- Soares da Costa, D., Pereira, S. and Pissarra, J., (2011) The heterologous systems in the study of cardosin B trafficking pathways. *Plant Signaling & Behavior*, 6 (6), pp. 895-897.
- Surpin, M. and Raikhel, N. (2004) Traffic jams affect plant development and signal transduction. *Nat Rev Mol Cell Biol* 5, pp. 100–109.
- Terauchi, K., Asakura, T., Ueda, H., Tamura, T., Tamura, K., Matsumoto, I., Misaka, T., Hara-Nishimura, I. and Abe, K. (2006) Plant-specific insertions in the soybean aspartic proteinases, soyAP1 and soyAP2, perform different functions of vacuolar targeting. *Plant Physiol.* 163, pp. 856–862

- Tsien, R., Y. (1998) The green fluorescent protein. *Annu Rev Biochem* 67, pp. 509-44.
- Uemura, T., Nakano, A. (2013) Plant TGNs: dynamics and physiological functions. *Histochem Cell Biol* 140, pp. 341–345
- Uhlig, H. (1998) Plant proteases. *Industrial Enzymes and their Applications*. pp. 147-151
- Varki A. (1993) Biological roles of oligosaccharides: all of the theories are correct. *Glycobiology*, vol. 3, no. 2, pp. 97–130.
- Verissimo, P., Faro, C., Moir, A. J., Lin, Y., Tang, J. and Pires, E., (1996) Purification, characterization and partial amino acid sequencing of two new aspartic proteinases from fresh flowers of *Cynara cardunculus* L. *European journal of biochemistry / FEBS*, 235(3), pp.762-8.
- Vieira, M., Pissarra, J., Verissimo, P., Castanheira, P., Costa, Y., Pires, E. and Faro, C. (2001) Molecular cloning and characterization of cDNA encoding cardosin B, an aspartic proteinase accumulating extracellularly in the transmitting tissue of *Cynara cardunculus* L. *Plant Mol. Biol.*45, 529–539.
- Vitale, A., and Denecke, J., (1999) The endoplasmic reticulum-gateway of the secretory pathway. *The Plant cell*, 11(4), pp. 615-28.
- Xiang, L., Etxeberria, E. and Van den Ende, W. (2013) Vacuolar protein sorting mechanisms in plants. *FEBS Journal* 280, pp. 979–993.
- Wang Y., Shyy, J. Y.-J. and Chien, S. (2008) Fluorescence Proteins, Live-Cell Imaging, and Mechanobiology: Seeing Is Believing. *Annu. Rev. Biomed. Eng.* 10, pp. 1-38.
- White, P.C., Cordeiro, M.C., Arnold, D., Brodelius, P. E. and Kay, J. (1999) Processing, activity, and inhibition of recombinant cyprosin, an aspartic proteinase from cardoon (*Cynara cardunculus*). *J. Biol. Chem.* 274, pp. 16685–16693
- Wilkins, T., Bednarek, S. and Raikhel, N. (1990) Role of propeptide glycan in post-translational processing and transport of barley lectin to vacuoles in transgenic tobacco. *Plant Cell*, 2, pp. 301–313.